THE IMPACT OF RE-SURFACING GROINS ON HYDRODYNAMICS AND SEDIMENT TRANSPORT AT THE DELFLAND COAST

ANTOON HENDRIKS

DECEMBER 9TH 2011

TU Delft
Delft University of Technology

Deltares
Enabling Delta Life

MSC THESIS

THE IMPACT OF RE-SURFACING GROINS ON HYDRODYNAMICS AND SEDIMENT TRANSPORT AT THE DELFLAND COAST

AUTHOR: ANTOON HENDRIKS

STUDY NR: 1310607

EMAIL: ANTOON_JH@HOTMAIL.COM

MENTOR: STIVE, M.J.F.

INSTITUTION: DELTARES

KEYWORDS: GROINS, DELFLAND, RE-SURFACING, HYDRODYNAMICS, SEDIMENT TRANSPORT

DATE: 09-12-2011

COMMITTEE

Prof.dr.ir. M.J.F. Stive	TUDelft Hydraulic Engineering
Ir. P.K. Tonnon	Deltares
Ir. A.P. Luijendijk	TUDelft Hydraulic Engineering / Deltares
Ir. M.A. de Schipper	TUDelft Hydraulic Engineering
Ir. P.B. Smit	TUDelft Environmental Fluid Mechanics

ACKNOWLEDGEMENTS

At first I want to thank Deltares for giving me the opportunity to graduate, and for their support during the graduation. I want to thank the following persons in particular:

The committee members for their input in the graduation project. The discussions and critical views were very useful and inspiring. Special thanks to Pieter Koen Tonnon for his daily supervising at Deltares and for the enthousiasm in the guidance.

Further I want to thank Bert van der Valk for sharing his knowledge on the changes of the Holland coast. Also the interesting articles and books he showed me were very inspiring and informative.

I want to thank all Deltares graduate students for the help and the discussions during the graduation period, and for the nice times during the coffeebreaks and after office hours.

During my study I had a lot of good times and several inspiring talks with my friends, whom I want to thank for that. Special thanks go out to my parents and girlfriend who gave me unconditional support financially and emotionally.

CONTENTS

ABSTRACT

Due the coastal protection program along the Dutch coast, the groins that first defended the coast against erosion, are now covered under sediment. Due to erosion the covered groins will resurface however. The objective of this study is to investigate the effect of the resurfacing groins on the hydrodynamics and sediment transport. A schematized model is made to reduce effects due to a complex bathymetry and to get a clear view of the occurring processes. Three profiles are schematized at a suitable location based on the 1990, 2009 and 2010 Jarkus transects. Also a test case is modeled with a constant slope to get a view on the effect that groins have on several hydrodynamic properties and transports. The effects due to the bathymetry and the groin can now be separated. From this follows that the groins do not affect the alongshore current velocity significantly when the groins are relatively small, in the order of 50 meters or less. The offshore directed currents are considered more dangerous and are present and increasing with increasing groin length, although they are also small when groins are relatively small. When the groin length increases to 150 meters, both the longshore and the offshore currents become significantly larger. In the test case the increase in alongshore velocity is around 15% compared to small or no groins. The increase in current velocity depends largely on the bathymetry and the position of bars however. The sediment transports decrease quite constantly with increasing groin length when the foreshore has a constant slope, in case of a profile with bars the decrease of transport may not be constant anymore. In the schematized cases the sand transport in 1990 with groins of 140 meter is in the order of 50% smaller than in the 2010 situation without groins. Scour holes can increase the offshore directed transports and velocities, but further research is needed here.

SAMENVATTING

Door het kustversterkingsprogramma aan de Nederlandse kust zijn de strandhoofden, die eerst de kust verdedigden, nu bedolven onder zand. Door erosie zullen de strandhoofden echter weer tevoorschijn komen. Het doel van deze studie is onderzoek naar de effecten van de tevoorschijn komende strandhoofden op de hydrodynamica en het sediment transport. Er is een geschematiseerd model gemaakt om de effecten die een complex bodemprofiel kan veroorzaken te verminderen en te kijken naar de processen die zich afspelen. Drie profielen worden geschematiseerd gebaseerd op een geschikte locatie en op Jarkusraaien van 1990, 2009 en 2010. Er is ook een test model gemaakt met een constant hellend bodemprofiel om de effecten die strandhoofden hebben op hydrodynamische eigenschappen en transport. De effecten die optreden door het bodemprofiel kunnen nu gescheiden worden van de effecten door strandhoofden. Hier volgt uit dat de strandhoofden de kustlangse stroming niet significant verandert bij relatief korte strandhoofden, in de orde van 50 meter of korter. De zeewaarts gerichte stroming wordt als gevaarlijker beschouwd en nemen toe naarmate de strandhoofdlengte toe neemt, bij korte strandhoofden zijn ze echter ook klein. Als de lengte toeneemt naar 150 meter worden de kustlangse en zeewaarts gerichte stromingen significant groter. In het test model nemen de snelheden zo'n 15% toe vergeleken met korte of geen strandhoofden. De toename van stroomsnelheid is echter erg afhankelijk van het bodemprofiel en de positie van de banken. Sediment transport neemt vrij gelijkmatig af met toenemende strandhoofdlengte in het test model, als het profiel niet constant is en er banken op zitten is de afnamen van transport niet constant met afnemende strandhoofdlengte. In de geschematiseerde situaties blijkt dat het zandtransport in 1990 met strandhoofden van 140 meter in de orde van 50% lager is dan in de situatie in 2010 zonder strandhoofden. Erosiekuilen kunnen de zeewaarts gerichte transporten en stroomsnelheden versterken, maar op dit gebied is meer onderzoek nodig.

LIST OF FIGURES

LIST OF TABLES

1 INTRODUCTION

1.1 BACKGROUND

The Delfland coast (Figure 1) knows a long history of erosion and coastal protection. The first measures to defend the coast from eroding were taken two centuries ago. Groins that extended into the surf zone were built. These groins turned out to decrease the erosion rate and from then on they were used extensively to defend the coast of Delfland. The erosion of the coast was not stopped completely and the groins were modified and extended landwards and seawards several times since then.

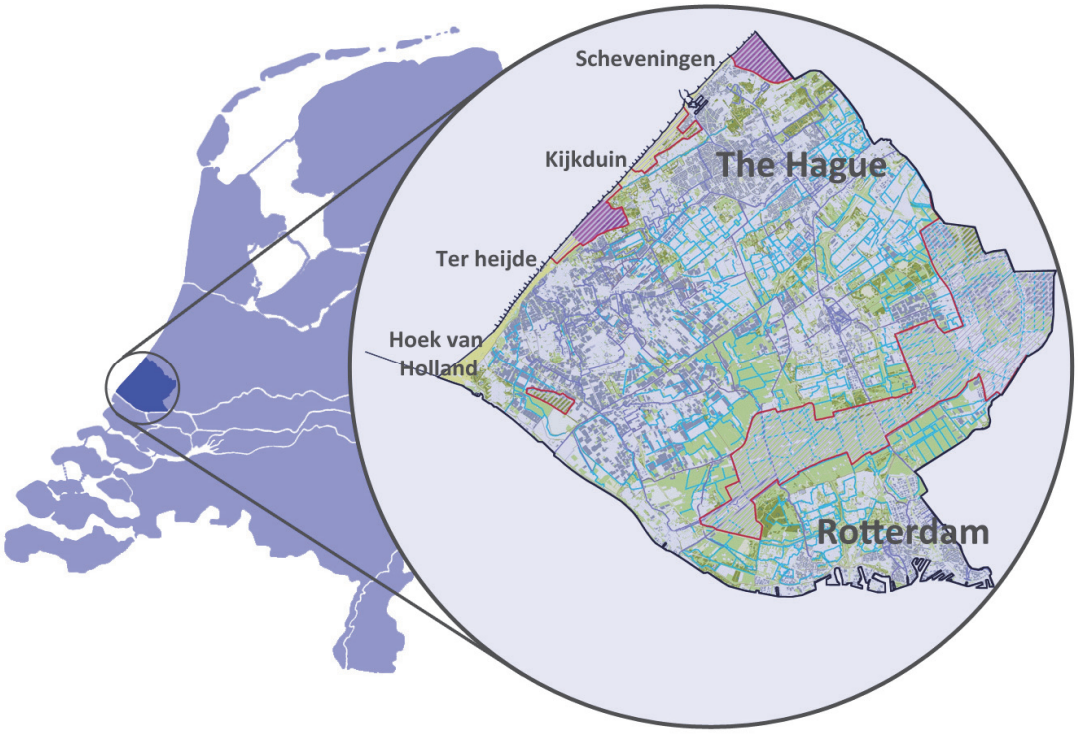

Figure 1 Location of Delfland in the Netherlands and a closer look on its coast

New developments in hydraulic engineering caused a change in coastal protection methods. After 1990 the coast was mainly protected with 'soft' coastal engineering methods, a suppletion program has been set up. Since then the coast is protected with nourishments that should counter erosion effects.

To make the coast safer and to improve natural areas, big coastal defense projects have been carried out in which a lot of sediment was nourished. The old groins were not removed during these projects, and therefore recently disappeared under the sediment. It is expected that the groins will resurface due to erosion.

It is unknown what the effects on currents and sediment transports are due to the re-surfacing groins. In this study the hydrodynamics and sediment transports are investigated.

1.2 PROBLEM DESCRIPTION

Due to changes in for instance water level and wave conditions, the shape and characteristics of coasts can change. At Delfland these changes caused the coast to become erosive, by making use of coastal structures the erosion was counteracted . Groins stop the coastal erosion by 'catching' sediment between them and nourishments complement the sediment that erodes away. Two types of nourishments are often used; foreshore and beach nourishments. In case of beach nourishments the sediment is directly placed on the beach, while in case of foreshore nourishments the 'feeder and berm' effects are used. This is the effect of the earlier breaking of waves by a shallower foreshore due to the nourishment. The nourishment acts like a berm that breaks the waves; the smaller waves generate an onshore directed sediment transport that accretes the beach.

The difference between the protection of the coast with groins or nourishments can induce a different sediment transport along the coast. The coast can therefore erode at a different speed. Some groins are now covered with sediment, but it is expected that these groins will resurface again because of erosion. The re-surfacing of groins has the consequence that currents and sediment transports can change. However, the exact impact is unsure and therefore can give rise to undesired situations.

In this study the impact of resurfacing groins at the Delfland coast on the hydrodynamics and sediment transports are investigated.

1.3 OBJECTIVE

The unknown hydrodynamics and sediment transports near re-surfacing groins are the main reasons for carrying out this research.

The two main objectives are:

- To study the impact on the hydrodynamics and the sediment transports of the re-surfacing groins at the Delfland coast.
- To improve the overall knowledge on re-surfacing groins or other hard structures.

These objectives can be summarized in the following research question:

'What is the impact of re-surfacing groins at the Delfland coast on the hydrodynamics and sediment transport?'

The research question can be answered by answering the following sub-questions:

- What are the physical effects near a groin in general?
  - What role do tidal currents have on the effectiveness of the groin?
- What are the hydrodynamic effects that occur in different stages of exposure of the groin and what are the differences between these effects?
  - How do the current patterns change when the groin gradually starts re-surfacing?

  - Under which wave conditions are the currents the strongest?
  - Where and at what stage of exposure are the currents the strongest?
  - When are strong currents formed and what are the current velocities?
  - How sensitive is the current related to the exposure of the groin?
- How does the sediment transport change in different stages of exposure of the groin?
  - How does the exposure of the groin affect the sediment transport?
  - At what locations is the sediment transport high?

1.4 RESEARCH APPROACH

First a literature review will be made. In the review it is examined why the coast is erosive, what measures have been taken against the erosion, what the characteristics of groin in general and in Delfland are, and what is known about the processes occurring in the vicinity of groins.

Then the model approach is determined. For this study it is chosen to make a schematized model which is based on the Delfland coast. Detailed area-specific situations are left out so the processes that occur will not be disturbed by irregularities due to the bathymetry. In this way the model shows what are the consequences due to resurfacing groins and leaves out additional effects. The schematizations will introduce uncertainties that have to be taken into account.
To understand the impact of the re-surfacing of groins on the coast, three model situations will be examined:

- A situation in which the groins are relatively large.
- A situation in which the groins are smaller, just before the nourishment.
- A situation after without groins, after the nourishment.

The profiles represent real situations which are then schematized alongshore uniform. The first situation with relatively large groins is used to get a good view on the differences between the situation before and after the nourishment. The differences can be scaled in this way. The three situations should give a clear view on the processes that are occurring around groins. The different situations will show how the coastal processes are affected when the groins resurface.

The problem with this approach is that the different situations have two variables; The bathymetry and the groin length. To deal with this problem a test case is set up in which the groin length changes and the bathymetry remains constant. The effect due to the groins can then be scaled and the effect of the bathymetry can be estimated.

1.5 READERS GUIDE

In chapter 2 a literature review is carried out. In this literature review first the coastal changes on a geological timescale are elaborated upon, as well as the changes on a decadal timescale. After that the functional design of groins is explained and the characteristics of the groins in front of Delfland are given. Then something is told about the interventions done on the Delfland coast.

In chapter 3 the modeling approach is described to understand the modeling process and the way in which the research is done. After that the input in the model is determined and the model set up is explained. The most important input parameters are the bathymetry, the groins and the wave conditions.

In chapter 4 the results are analyzed. First the results are compared to a drifter experiment to check if the model results can be compared to a real case. Then the hydrodynamics are analyzed, first the test case results are studied and then compared with the schematized situations. After that the sediment transports are analyzed in the same way, first the test case and then the comparison with the schematized cases. After this a sensitivity simulation is performed.

In chapter 5 the conclusions are given and in chapter 6 recommendations are done.

2 LITERATURE REVIEW

In this chapter an introduction is given to the problem of the re-surfacing groins on the Delfland coast. This problem has been described in *chapter 1.2 Problem description*. In the first two paragraphs of this chapter, an overview is presented on the historical changes of the Holland coast. This is done to show how the Delfland coast, which is a part of the Holland coast, is shaped and why it is erosive. Different measures were taken to prevent the coast from eroding. Groins were built and beach and foreshore nourishments were performed. A description of this measures and their impact on coastal processes, is given in the third, fourth and fifth paragraph of this chapter. Recent interventions are discussed in the final paragraph.

2.1 HISTORICAL CHANGES ON A GEOLOGICAL TIMESCALE

To understand the situation of the present Dutch coast we need to take a look at the Holocene evolution of it. This started 12000 years ago, when the last big ice age ended. This was the end of a period called 'Weichselian', which ended when the temperature on earth started to rise globally. The ice melted and caused a sea level rise of more than 100 meters. The newly started period is called the Holocene and it is this period in which the coast of the Netherlands, as it is known now, was formed.

Due to the high rate of sea level rise, the coast of the Netherlands retreated. The coast flooded and an open coast was formed, because the amount of sediment available to supply to the basins could not keep up with the increase of the storage capacity due to relative sea level rise (van der Spek and Beets 1992). This kind of coast is a so-called 'tide dominated' coast, which means that the coast consists of tidal basins behind barriers, this can be seen in Figure 2.

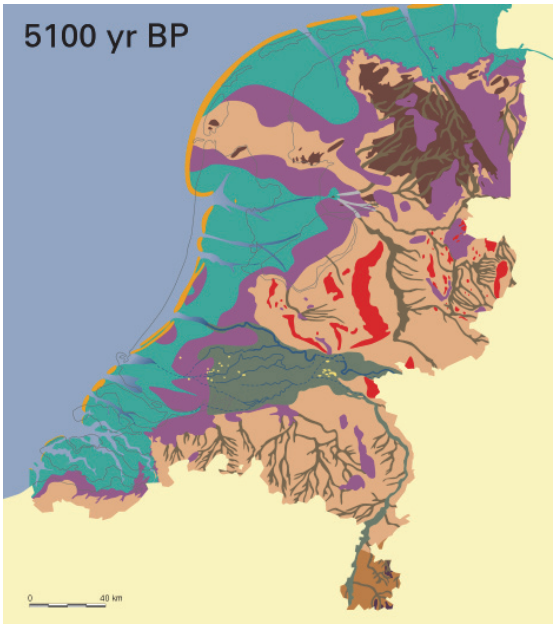

Figure 2 The Dutch coast 5100 years before present (from Berendsen, 2005)

During the last 5000 years, the relative sea level rise in the North Sea was not more than 4 meters (Bungenstock and Schäfer, 2009). During this period, the coastal area could develop into a 'wave dominated' coast as can be seen from reconstruction maps of the Holocene (Deeben, Drenth et al. 2005). The coast developed uninterrupted coastal stretches due to longshore sediment transport. Estuaries in the west were filled up with sediment, while in the north a stable tidal basin remained; the Wadden Sea. This transformation from an open 'tide dominated' to a closed 'wave dominated' coast, was one of the main events in coastal change until the Middle Ages (Beets, van der Valk et al. 1992), Figure 3.

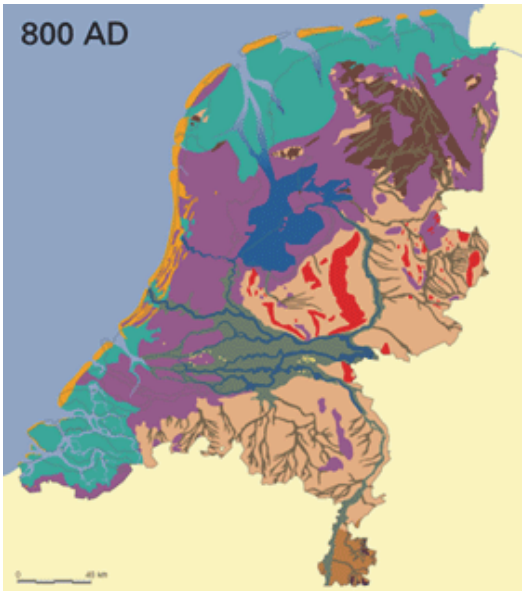

Figure 3 The Dutch coast 1200 years before present (from Berendsen, 2005)

The coast of Delfland was not erosive in the period in which the wave dominated coast was formed, from 3300 B.C. to 10 B.C. Due to longshore transport and the available sediment supply from the north (Old Rhine) and the south (Meuse) (Eisma 1968) this part of the coast even was accreting.

The Old Rhine began to silt up in the period around 500 A.D., which caused a decrease in sediment supply on the Holland coast. In addition, the river Lek started to discharge more water towards the old Meuse Outlet. In 1162, the Rhine was dammed and the Lek became the main discharge branch, which eventually lead to the silting up of the Old Rhine. A few centuries B.C., near Monster, a storm surge broke through the bank of the Meuse which caused the formation of a tidal inlet called the Gantel. The area behind the dunes consisted of peat in which a higher water level was present because of the spongy behavior of peat. Peat therefore also consists for a large part of water. The water level in the peat was a few meters higher than the mean sea level, which caused a strong gradient in the peat when the dunes were breached. The water flowed out of the peat causing it to dry out and made it vulnerable to wash away with a storm surge. This and the tidal motion caused the peat to wash away; the Gantel was formed and extended in the next centuries.

The increase of the discharge through the Lek and the formation of the Gantel were some of the causes that changed the characteristics of the Meuse estuary. They caused an increase of the tidal storage, which had the consequence that the estuary of the Meuse became sediment importing.

The sediment that was imported into the tidal basin was not available for the coastal stretches and therefore the surrounding coasts eroded (van Rijn 1997; Bosboom and Stive 2010a; Bosboom and Stive 2010b). A southern directed longshore transport, and the sediment importing behavior of the Meuse estuary, caused the sediment to erode from the coast and accrete in front of the Meuse estuary. This process caused the severe erosion in front of Delfland and the formation of a seaward spit called 'De Beer' (*Appendix A - Maps*, map 2).

2.2 HISTORICAL CHANGES ON A DECADAL TIMESCALE

For a long time the dunes in front of Delfland were wide. Because of the coastal erosion described above, the dunes narrowed. Eventually several excessive dune breaches occurred during a storm in 1564. Between 1600 and 1765 the coastline in front of Ter Heijde retreated with 1 kilometer according to the map of Johannes Bloteling (*Appendix A - maps*, map 2). In 1682, a sand dike was built to stop the erosion. In 1699, the dike breached and an expert was asked to design a coastal protection to stop the erosion. He advised to build three stone groins, but the water boards decided to postpone it because of financial reasons. In 1731 the first real measure was taken; a wooden groin. In the next year there were built two more. This measure was not very effective though. After a few storms the wooden groins were destroyed. The water board decided to renew them every year until 1791.

After a successful test with three stone groins in 1791 in front of Ter Heijde, the first 12 stone groins were built in the years thereafter. This measure was succeeding in its job to limit the coastal erosion, it was decreased to 0,5 -1 meter per year (van Rijn 1995). In 1807 three more groins were built and in the period from 1826 to 1827 six more were added. They were all built north of the first groins, because the groins partially stopped the longshore transport and therefore caused erosion on the lee side. In the period between 1846 and 1930 47 more groins were placed, mostly to the north (Elzelingen and Groothoff 1912; Dolk 1939). In total 68 stone groins were constructed. In *Appendix B - Groin data* the groins and their characteristics are given. Because of the building of the Noorderdam in 1874 the most southern groins were covered under sand. The coastline curved due to the dam, which is explained later in this report. The dam stopped a lot of the northwards longshore sediment transport, which caused more erosion near Delfland.

2.3 FUNCTIONAL DESIGN OF GROINS

2.3.1 FUNCTIONING OF GROINS

The idea behind a groin is the catching of longshore sediment transport. This transport is induced by wave breaking in the surf zone. When waves approach the coast under an angle differences in radiation stress (Longuet-Higgins and Stewart 1964) due to wave dissipation will cause an alongshore directed current in the direction of the breaking waves. This current is typically under 1 meter per second and depends on the cross-shore distance, but values have been measured of 3.5 meters per second (Basco 1983).

The catching of sediment leads to accretion on the updrift side of the groin. Because of the decrease in sediment transport, this must lead to erosion on another spot. This will happen behind a groin.

In case of a groin field the process described above will happen at every groin, this is shown in Figure 4. Because the sediment transport is not completely blocked, this will lead initially to erosion between the groins, but after a while, when a new equilibrium arises, accretion will occur.

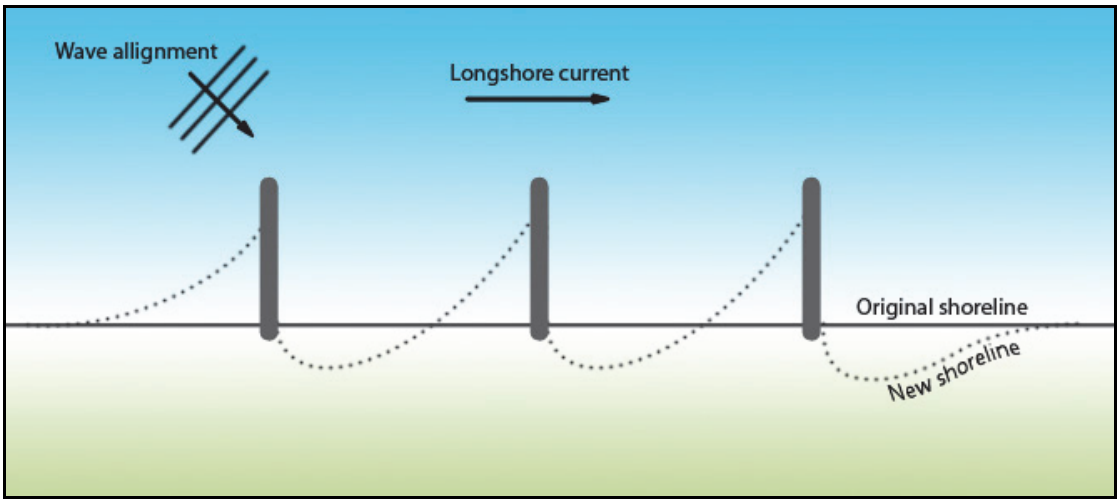

Figure 4 Groin field erosion behind groins in a groin field

2.3.2 GROIN DESIGN

Since wave induced longshore sediment transport takes place in the surf zone, the functioning of groins is dependent on the dimensions and characteristics of the surf zone. There are no generally applicable rules for the design of groins. There are some rules of thumb like the spacing, which is typically a few times the length of a groin. The groin length depends on the amount of sediment transport that has to be reduced. For a total blockage the groin has to extend at least beyond the surf zone (Bosboom and Stive 2010b).

2.3.3 CURRENTS BEHIND A GROIN

The exact current fields behind groins depend on the dimension of the groins and the longshore current velocity. Eddies and rip currents are likely to occur. The big eddy down drift of the groin is caused by the wave set-up effect in the 'shadow zone' behind a groin. According to model studies from Pattiaratchi et al. (Pattiaratchi, Olsson et al. 2009) the highest currents in this eddy are reached when the incoming wave angle is 45°. The eddy's center does not change position when only the wave height and period changes. Along the groin, a rip current occurs on both sides. When the conditions are right this rip current can extend out towards sea. With milder conditions, the rip current on the leeward side is attached to an eddy and will have a circulation pattern (Figure 5). The rip currents around groins are dangerous for swimmers and can cause sediment transport offshore.

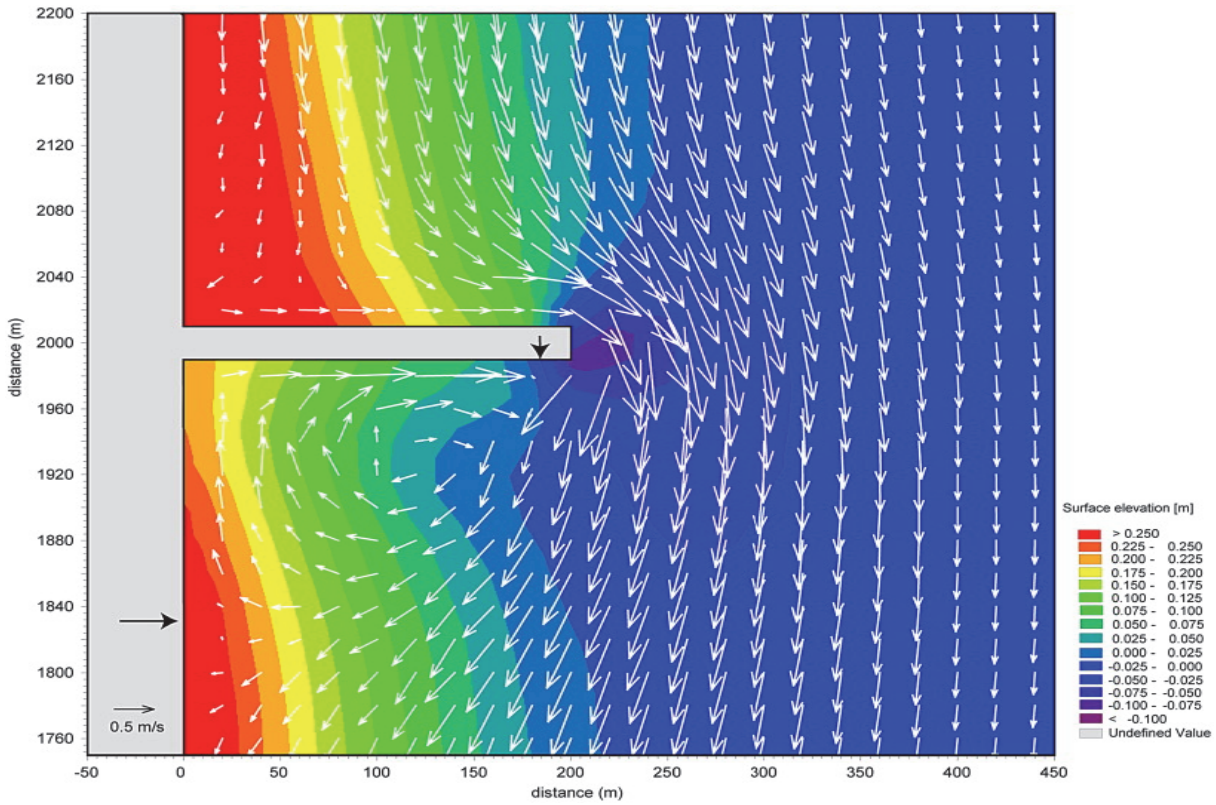

Figure 5 Vector plot showing the current vectors and the wave set-up behind a groin (Pattiaratchi, Olsson et al. 2009)

One way to reduce the rip currents is to make the groin more permeable. In this way the currents along a groin are reduced and therefore have a less negative effect for swimmers and the beach (Raudkivi and Dette 2002). Permeable pile groins however do not have as much effect as impermeable groins for the blockage of the longshore transport.

2.3.4 LOCATIONS OF THE HIGHEST CURRENT VELOCITIES

Current speeds are dependent on the wave conditions which determine the longshore current speed. High currents near a groin are located directly behind the groin as can be seen in Figure 5.

High currents do also occur on the tip of the groin. These higher currents are caused by the contraction of the flow because of the length of the groin.

The velocities near a groin are dependent on the exact wave conditions and the dimensions of the groin. Most rip currents are in the order of 0,3 meters per second, but the currents can get as high as 1 meter per second (MacMahan, Thornton et al. 2006).

2.3.5 MORPHODYNAMICS AROUND A GROIN

In case of a dominant wave direction climate, the beach line will be aligned with the incoming wave crests of the dominant wave direction. The beach level (height) near the groin can also be substantially higher updrift then downdrift of

the groin. This leads to a step-type difference in elevation across each groin. In a variable wave climate the beach will be curved between two groins. (van Rijn 2005)

The accretion zone in front of a groin is curved due to the decreasing sediment transport. The angle of the accretion zone with the original shoreline is at maximum equal to the angle of the incoming waves. At that location the longshore transport induced by the incoming waves is zero.

The point where the maximum erosion occurs is not directly behind the groin. A circulating current causes the sediment to flow back to the groin. This current is induced by the breaking of the waves, which causes a set-up near the shore. Directly behind the groin the waves, and thus the set-up are lower. The water level difference due to the reduced set-up triggers a current towards the groin. This current causes the specific curved shape behind the groin. In the case of variable waves the shape of the coastline is the same on both sides of the groin (Figure 6). (van Rijn 2005)

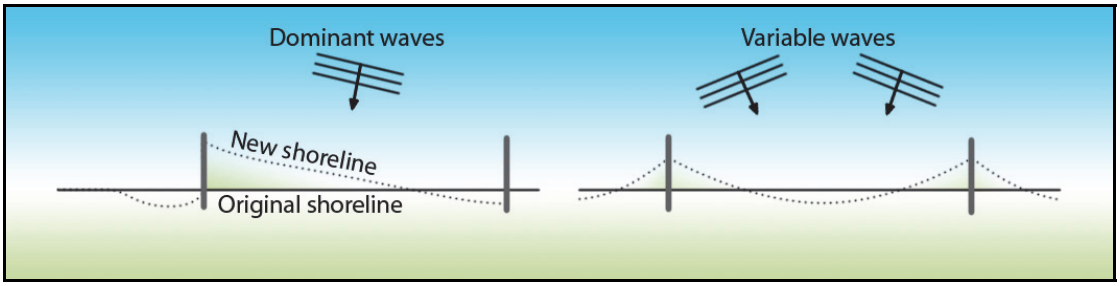

Figure 6 Coastline around groins in the case of a dominant wave direction (left) and of variable waves (right) (van Rijn 2005)

2.3.6 SCOUR

On the tip of a groin the flow gets contracted. This contraction leads to higher flow velocities which cause an erosion pit at the tip of the groin. Because of the eddy behind the groin and the relatively high current velocities, the erosion pit is located somewhat behind the groin as can be seen in Figure 7. A gully parallel to the groin can also be observed. The depth of the scour hole depends largely on the shape of the tip of the groin (round or sharp), the wave angle and the presence of a co-directional current (Sumer and Fredsøe 1997). Specific quantities of the erosion rate of scour holes with groins are not known for the Delfland coast.

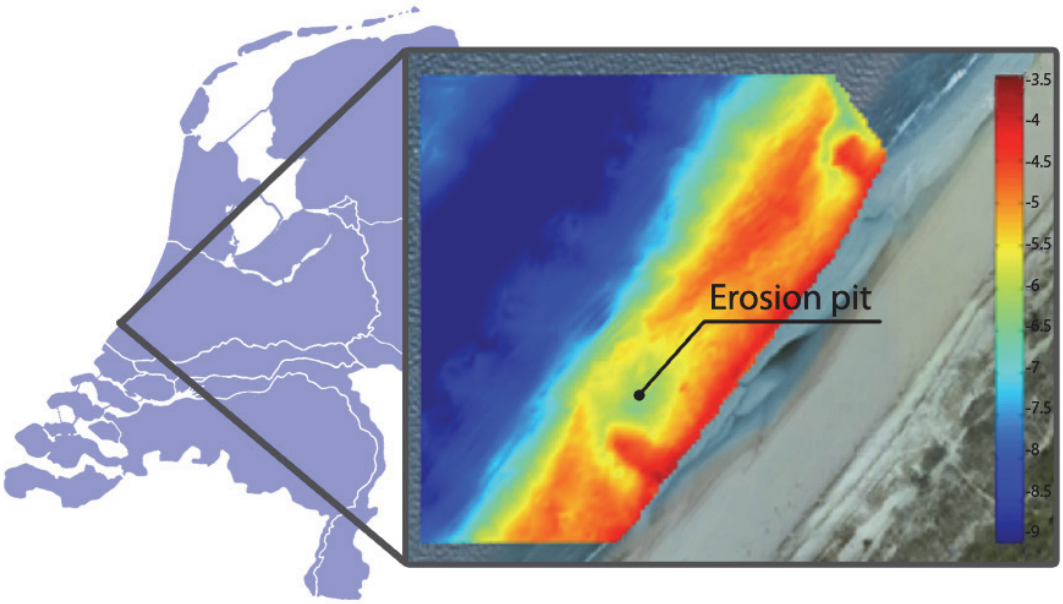

Figure 7 Erosion pit near a groin at Ter Heijde (Measurement from TUdelft/ Shore monitoring)

2.4 GROIN CHARACTERISTICS

2.4.1 LENGTH AND SPACING

The groins in front of the Delfland coast are not all of equal length. The length of the groins can be expressed in two ways; the length from the waterlevel=0 meter line, and the distance from the RSP=0 line. RSP stands for 'Rijksstrand-paal', this is the reference point for yearly Jarkus transect measurements. In Figure 8 the length and spacing of the Delfland groins is shown from the RSP = 0 line. The waterline is shown in the years 1990, 2009 and 2010. It is clear that the groins are not of equal length with respect to the waterline, this relative length also changes in time. From groin 11 and south the groins are alternating in length. The spacing between the groins is also not constant. From the harbor in Scheveningen to Kijkduin the spacing is 400 to 535 meters, then over 1 kilometer south of Kijkduin the spacing is 200 meters. The spacing between Kijkduin and Ter Heijde is 300 to 375 meters and from Ter Heijde to the Van Dixhoorn triangle the spacing is 200 to 250 meters. The groins south of that are all covered with sand by the Van Dixhoorn triangle (Hoogheemraadschap Delfland 1997). In *Appendix A - maps* map 1 the groins are shown In this map also the letters and numbers of the groins are given as well as a more detailed spacing table (van Langenhuysen and van Langenhuysen 1917).

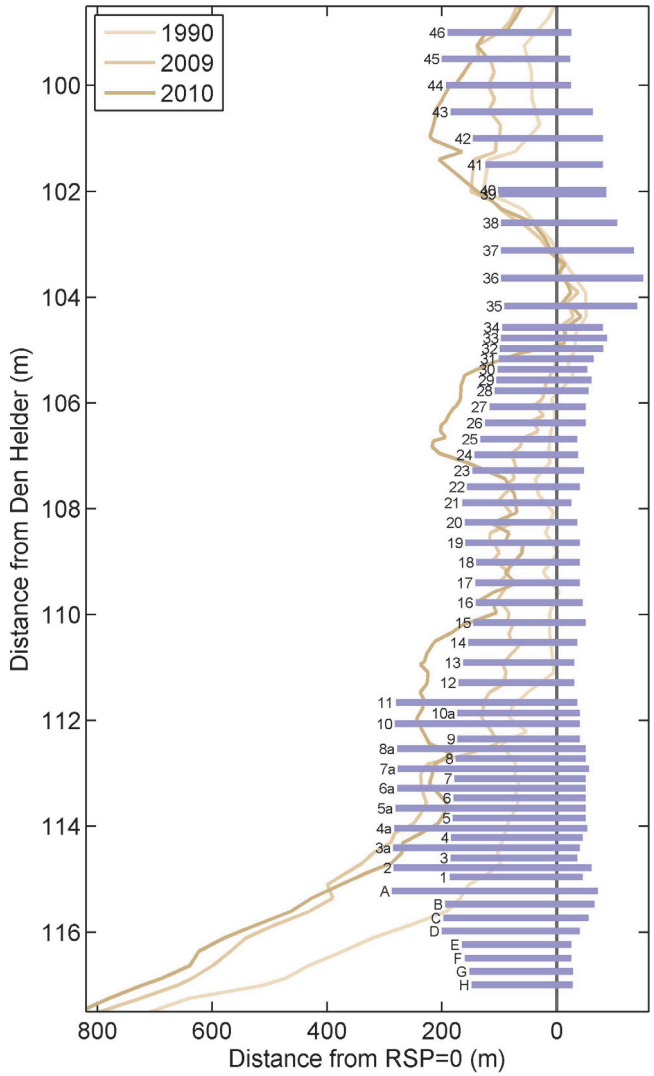

Figure 8 Overview of the groins in Delfland and the NAP = 0 m line in the years 1990, 2009 and 2010

2.4.2 HEIGHT

The height of the groins varies with the length. The long groins end around NAP -3 meters and the short groins around NAP -1,5 meters. This information is based on the interpolation of Jarkusraaien of 2005 (DHV, Alterra et al. 2007a). They of course change in time, but give a good presentation of the situation how it was before the coastal protection measures performed from 2008. The height of the groins varies between NAP 0 meter at the groin tip and NAP +3 meters on the dune foot. This is based on the design drawings from 1925 (DHV, Alterra et al. 2007a). In Figure 9 the depth at the tip of the groins are shown.

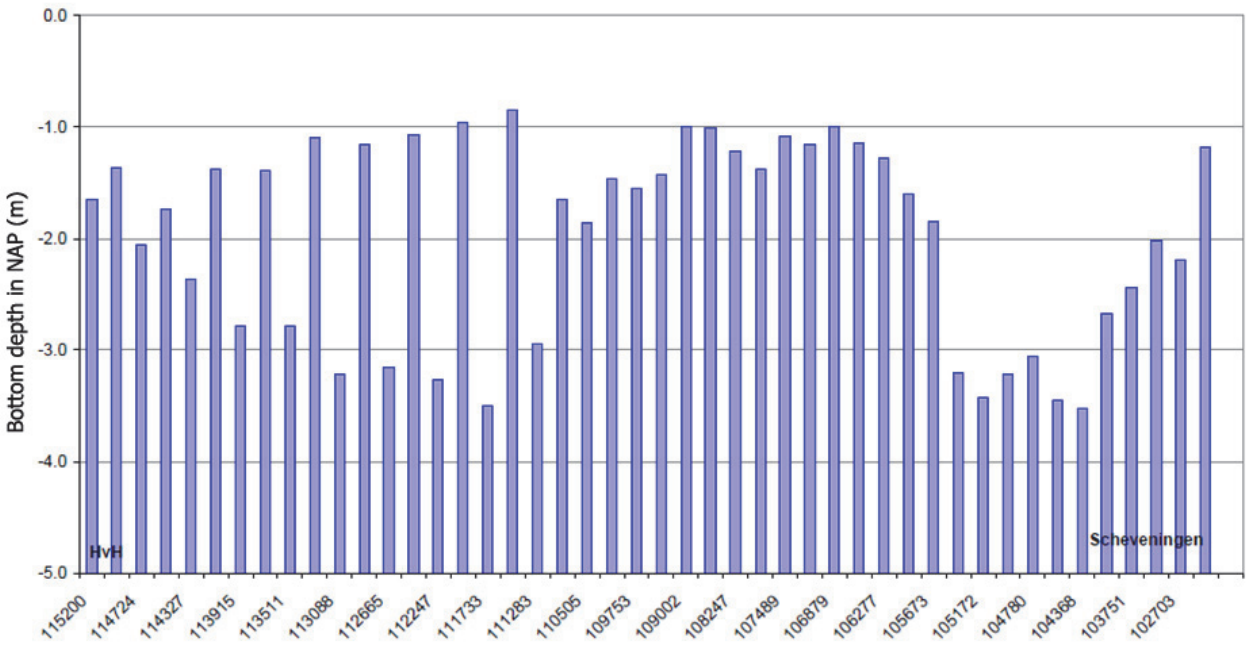

Figure 9 Bottom depth on the tips of the groins between Hoek van Holland and Scheveningen (DHV, Alterra et al. 2007a)

2.4.3 EFFECTIVENESS OF GROINS

The Delfland coast is maintained by nourishments. The effect of the groins on the maintenance demand is hard to distinguish, but because of the erosive character of the coast it can be concluded that the groins do not work optimal. Without the groins the maintenance demand is uncertain but it will probably be 0 – 100% higher than for a coast with groins (DHV, Alterra et al. 2007a).

2.5 BEACH AND SHOREFACE NOURISHMENTS

2.5.1 SEDIMENT TRANSPORTS

The sediment transports along the Dutch coast are computed and estimated in several studies. Van Rijn for example estimates the transport on the outcomes of models and data analysis of sediment budget analyzed with his expert opinion. In front of the coast of Delfland he estimates the net northward sediment transport to increase from 30.000 m^3/year in the south to 170.000 m^3/year in the north (van Rijn 1995). Stive and Eysink performed a study in 1989 which showed lower values. In Figure 10 the sediment transport along the Delfland coast is shown according to several different studies, the values are transports excluding pores. The exact value of the transport is hard to measure. That's why a large range of transports is found when different studies are compared.

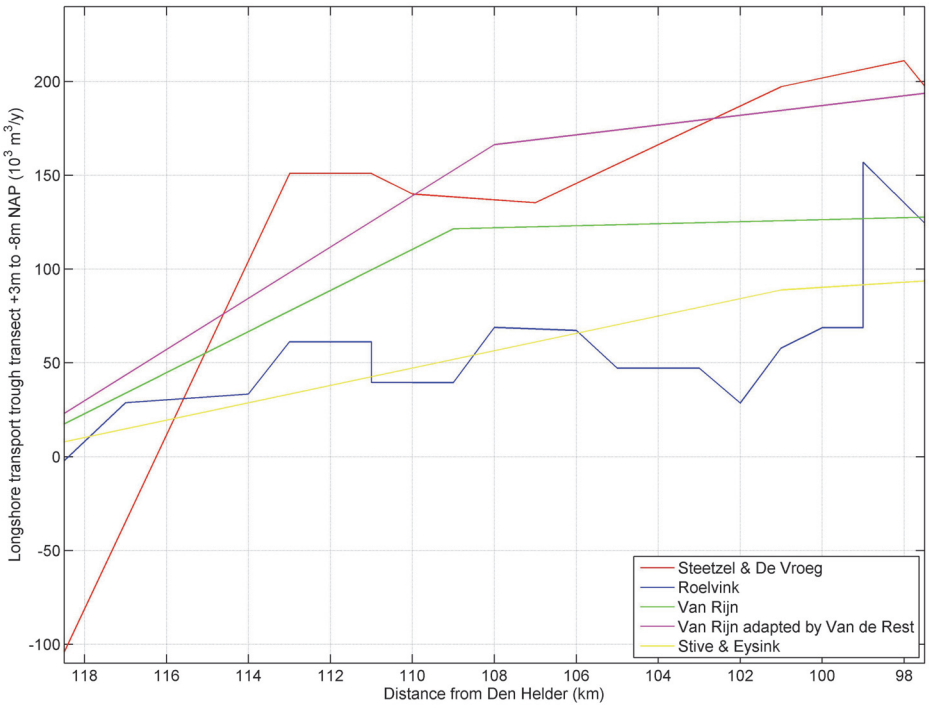

Figure 10 Annual average longshore transport in the surf zone along the Delfland coast. Red line: (Steetzel and de Vroeg 1999), blue line: (Roelvink 2001), green line: (van Rijn 1995), magenta line: (van Rijn 1995) adapted by (van de Rest 2004), yellow line: (Stive and Eysink 1989). See also (van de Rest 2004).

All the studies show a northerly directed sediment transport north of 116 km from Den Helder. Except Steetzel & De Vroeg all the studies show a small transport near the 118 km from Den Helder point. This is the location of the Noorderdam that protects the Nieuwe waterweg and blocks a great part of the longshore sediment transport.

2.5.2 NOURISHMENTS

As stated before, the Delfland coast is maintained by nourishments. The estimated maintenance demand for this part of the coast with groins is to supplement $400 \cdot 10^3$ Mm^3 sediment per year including pores which is somewhat higher than can be derived from Figure 10.This is an average with a bandwidth between $300 \cdot 10^3$ and $500 \cdot 10^3$ m^3/year. The erosion excluding pores in the area lays between $30 \cdot 10^3$ and $250 \cdot 10^3$ m^3/year, the average is around $125 \cdot 10^3$ m^3/year, which is approximately $200 \cdot 10^3$ m^3/year including pores. Extrapolations with autonomous increase because of climate change, show that the maintenance in 50 years will be $1200 \cdot 10^3$ m^3/year. (DHV, Alterra et al. 2007a)

The nourishments carried out are given in *Appendix C - Nourishments*.

2.5.3 RECENT INTERVENTIONS

NOURISHMENTS

New developments in hydraulic engineering caused a change in coastal protection methods. In 1990 the government decided to introduce the 'BasisKustLijn' (BKL), which implied that the coastline of 1990 should not shift more inland. To maintain this coastline an annual demand of $12 \cdot 10^6$ m^3 sand is needed along a distance of 340 km. These nourishments caused the effective length of the groins to shorten. The total coverage of the groins however was caused by large projects along the Delfland coast which are listed below.

VAN DIXHOORN TRIANGLE

The Noorderdam secures the entrance of the Rotterdam Waterway and was built between 1864 and 1874 (van Langenhuysen and van Langenhuysen 1917). This harbor mole was extended between 1968 and 1972 to reach a length of over 4 km long, thereby blocking a large part of the longshore sediment transport. Because of erosion on the coast, the Van Dixhoorn triangle was created in 1971. This was a big nourishment of 18,4Mm^3 that should compensate the erosion effects of the Noorderdam (DHV, Alterra et al. 2007a). The nourishment worked well, the coast initially accreted as intended, and because the regularly nourished amount of sediment is bigger than the erosion, the land is also accreting somewhat north of the area. The Van Dixhoorn triangle covered 10 groins under the sand (van Langenhuysen and van Langenhuysen 1917; Hoogheemraadschap Delfland 1997)

COASTAL REINFORCEMENT

In an analysis of the Dutch coast in 2003, several weak links were identified which did not meet the minimum requirements for a safe coast. The Delfland coast was one of these weak links and therefore needed reinforcement. The reinforcement works consisted of seawards widening of the dune row and the beach. The project was completed in 2011 and an amount of $12.5 \cdot 10^6$ m^3 of sediment is supplied in total. These reinforcement works are the main reason why the groins in front of Delfland were covered with sand.

DUNE COMPENSATION

Along with the reinforcing of the beach at the Delfland coast, the dunes are taken care of as well. The dune compensation has to counter the negative effects of the land reclamation project Maasvlakte 2. New dunes are made in front of the older ones with a valley of approximately 80 meters between them. In this valley, which will have a surface of 35 hectares, a new ecological system can develop. The coast is strengthened and new nature is realized. The new dunes cover the foot of the groins from groin 4a (*Appendix B - Groin data*) and south (see Figure 11). (DHV, Alterra et al. 2007b)

Figure 11 Dune compensation between the Rechtestraat in Hoek van Holland and Arendsduin in Ter Heijde (DHV, Alterra et al. 2007b)

SAND ENGINE

The sand engine is a pilot project in front of Ter Heijde. The project, whichis executed in 2011, consists of a nourishment of 21,5 Mm^3, which is placed in front of the coast in a certain shape. This shape gives room for nature to develop, and at the same time it protects the coast on the longer term. The longshore sediment transport will spread the shape out over the coast, which strengthens the coast. It is expected that the sand engine will change shape and protect the coast for 20 years.

Figure 12 Sand engine development after the nourishment, 5 years, 10 years and 20 years (http://www.dezandmotor.nl/nl-NL/de-zandmotor/ontwikkeling-van-de-zandmotor, 20-06-2011)

3 MODELING

3.1 MODELING APPROACH

The objective of the study is to determine what will happen to the hydrodynamics and sediment transport when groins resurface. To get insight in the processes occurring when groins resurface the problem is schematized and modeled. The following approach is used:

- The model domain is determined by choosing four consecutive groins that have roughly the same characteristics. Four groins are chosen to make sure the flow pattern is repeating after every groin.
- Three cases are considered; one after the nourishment when the groins are covered, one just before the nourishment with short groins and one case to scale the differences between the first two.
- The bathymetries in the three cases are smoothened and schematized to reduce effects that can disturb the observations. The groins are schematized because of the same reason.
- The conditions between the three cases should be the same, to have only two variables; the bathymetry and the groin length.
- A test case is set up with a simple profile with changing groin length to determine the effect of the groin length on hydrodynamics and sediment transport. The bathymetry can have many shapes; it is therefore difficult to determine the effect of the bathymetry on the hydrodynamics and sediment transports. There is no test case for the bathymetry therefore.

The model is then first compared to existing data from drifter experiments, model studies and sediment transport to check the reliability of the results. The differences between the three schematized cases are then compared by making use of the results of the test case.
First the hydrodynamics are studied. This is subdivided in the longshore currents and the offshore currents. After that the sediment transports are discussed.
The differences between the test case and the real schematized cases can be used to give a qualitative description about resurfacing groins.

3.2 MODEL SETUP

3.2.1 MODEL DOMAIN

For the modeling of the resurfacing groins, a uniform coastal stretch is implemented in a model domain. If the model domain can be chosen in such a way that the differences in the alongshore bathymetry are small, the model schematizations can be more easily determined and applied. To find the most optimal coastal stretch for the model domain, the

groin characteristics are compared. In *chapter 2.4 Groin characteristics* and in *Appendix B – Groin data* it is shown that the groins have a different spacing and length. It can be concluded that groin A to L and 1 to 11 do not have equal characteristics for a longer coastal stretch. The same accounts for the groins from groin 22 and northwards. Groins 12 to 21 do have more or less the same dimensions and are suitable to use in a schematized model. Groins 14, 15, 16 and 17 are used because good and consistent Jarkus data is available. An area of 2400 meters alongshore by 800 meters offshore around the groins is used as the model domain. The other groins in this area will be ignored to focus on the effects in the schematized part only. At the deepest point, the water depth is around 8.5 meters, which is a suitable depth to determine the model boundary conditions.

3.2.2 BOTTOM PROFILE

The approach of the study requires three different bathymetries that are determined with Jarkus transect data. The Jarkus profiles that are in between the groins are used to determine a uniform profile along the coast, because the transects that are close to the groin can be influenced by turbulent currents around the groin. The five Jarkus transects around the groins are transects 11072, 11034, 10996, 10958 and 10920, they are showed in Figure 13.

To make a good comparison between the three bathymetries the profiles on which the schematization is based should not change much in time. In this way it is assumed that the longshore sediment transport is more or less constant and something can be said about the differences between them. The profiles of 2009 and 2010 are used to compare, since this are the profiles before and after the nourishment that covered the groins. Since the groin in the 2009 profile is 'only' 60 meters long (this sounds long, but compared to the spacing and the position of surf zone this is relatively short), the profile of 1990 is used to get a better view on the scaling of hydrodynamic effects and sediment transport. It is checked that the profiles were not nourished in the near past so an equilibrium profile is formed. This does not account for the 2010 profile, since this is right after the nourishment. The profile will change further in time, which should be taken into account when analyzing the data.

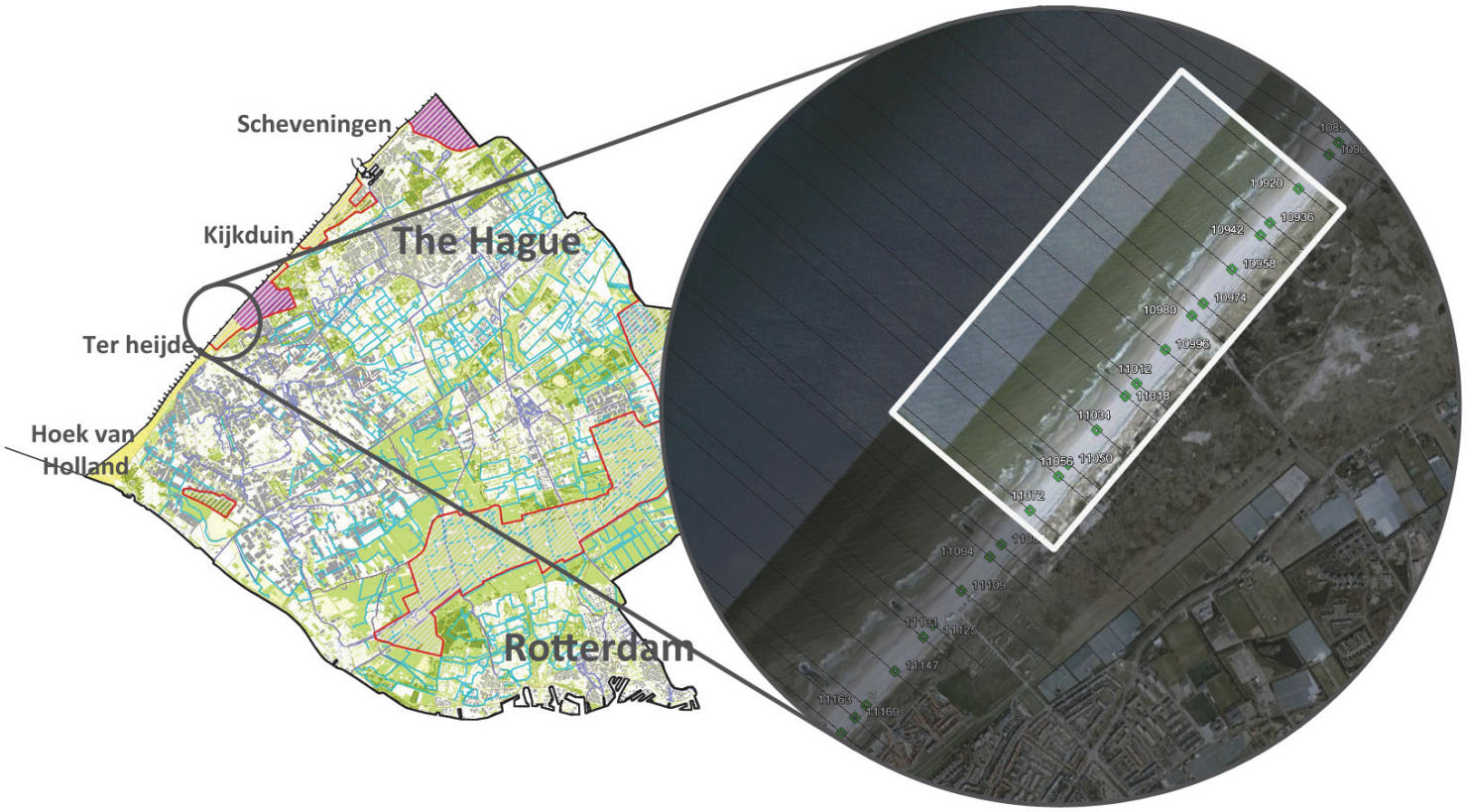

Figure 13 The four groins that are modeled and the transects along which the bottom is measured

3.2.3 PROFILE FITTING

The five transects have different profiles through which a mean profile should be fitted for the schematization. This is not done with determining the mean value at every cross-shore point, but with profile fitting by eye. Profile fitting with a standard slope profile and sinusoidal bars will result in a smoother profile, which is useful because a profile with irregularities can cause effects that can disturb the observations of the effect of the groin on the hydrodynamics.

The profiles are first normalized through the zero meter water level point to have a reference point in each profile. Now a uniform profile can be fitted through the five different profiles.

A Dean-Moore-Wiegel profile (DMW-profile) (Stive, de Vriend et al. 1992) is used for the fitting through the profiles that schematizes the mean coastal slope neglecting bars. Near the waterline, a constant slope is adopted to make the coast more realistic, if this is not done the slope would approach infinity near the waterline. The bars are schematized on this profile by adding sinusoidal functions multiplied by an amplification function so the sinus only has influence on a certain part of the slope. In this way a nice and smooth profile is required which gives a good representation of the actual foreshore.

1990

The profile of 1990 is determined with a DMW-profile with a constant slope of 1:35 near the waterline. Three sinus-functions and corresponding amplifier functions are added to represent the bars. To let the profile fit the Jarkus transects profile better, a single amplifier function is added. The resulting profile is shown in Figure 14.

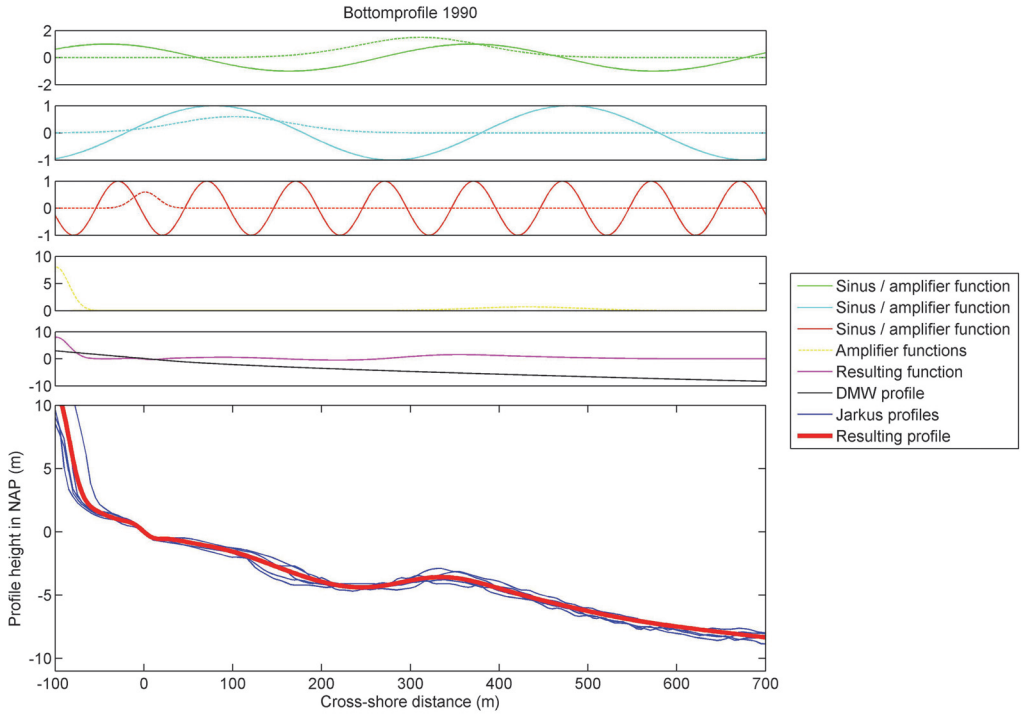

Figure 14 Profile schematization through the Jarkus transect for the 1990 bathymetry

2009

For the profile of 2009 three sinus functions are used to schematize the bars and one amplifier function to make the profile fit best. The DMW-profile is again used with the constant slope of 1:35 near the waterline. In Figure 15 the fitted profile is shown.

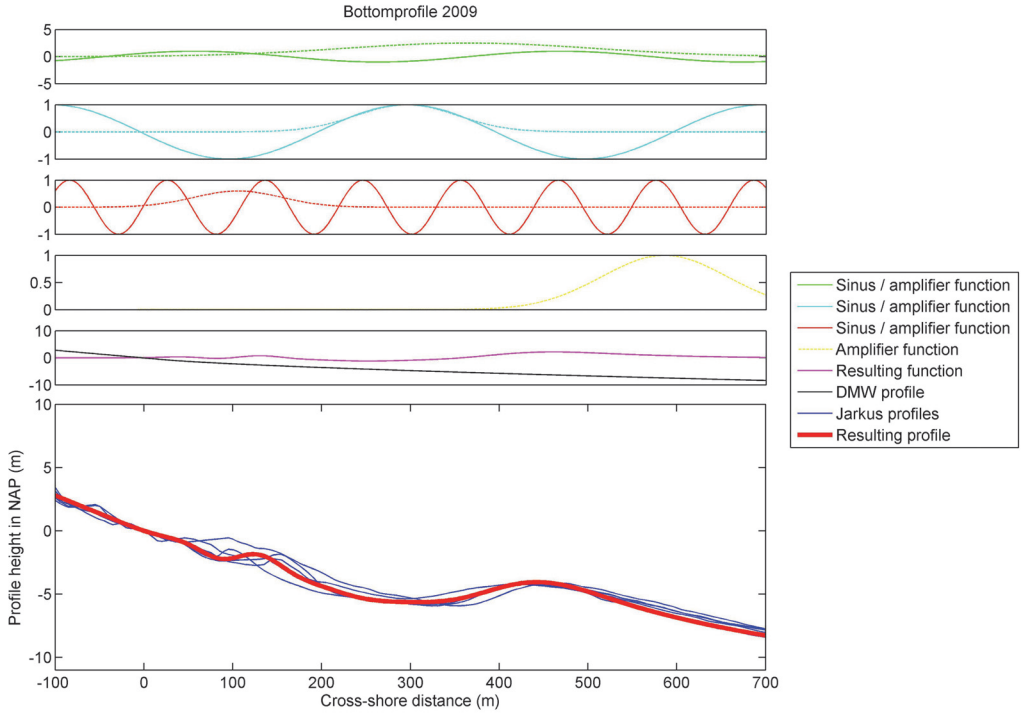

Figure 15 Profile schematization through the Jarkus profiles for the 2009 bathymetry

2010

In the 2010 Jarkus transects, the nourishment can clearly be seen, Figure 17. Because the nourishment is not yet fully placed in Jarkus transects 9010958 and 9010920, the 0 meter cross shore distance line is not taken in the normalized profile through the 0 meter water level line since this would induce a distorted reference between the Jarkus profiles. The 0 meter cross shore point is taken equal to the 0 meter cross shore point in the 2009 profile. The two Jarkus profiles are also neglected in the profile fitting left of 150 meters cross shore distance. The same DMW-profile as in the 2009 and 1990 profile is used. Sand bars do not have a fixed position and therefore the small inner bar in the 2009 profile is shifted a bit so it is in the right place. The deeper part of the foreshore is equal to that of the 2009 profile. The nourishment is schematized as a block profile with a linear descending thickness at the seaward side and a linearly increasing thickness at the dune side, Figure 16. The transitions between the straight lines are rounded off with a spline function to reduce the effect of a sudden jump in the bottom slope. Sudden changes in slope in the profile which are not realistic and can induce non-realistic currents and effects.

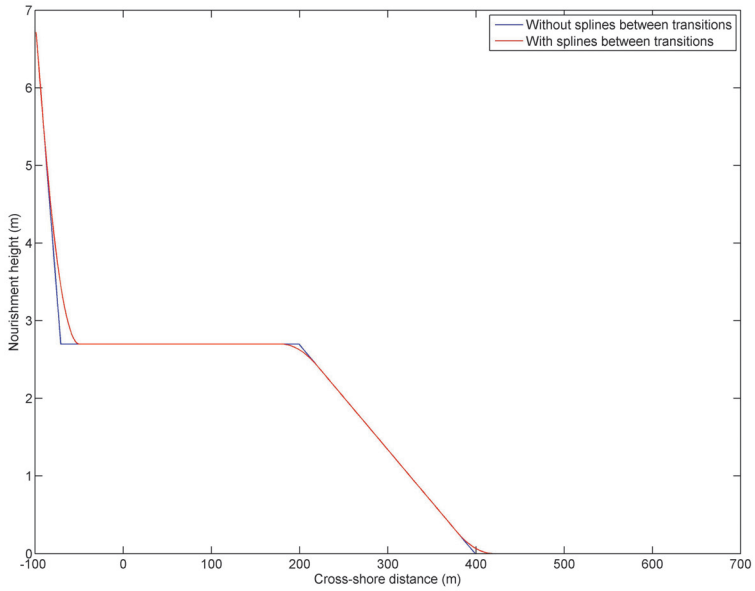

Figure 16 Nourishment thickness with and without splines between slope transitions

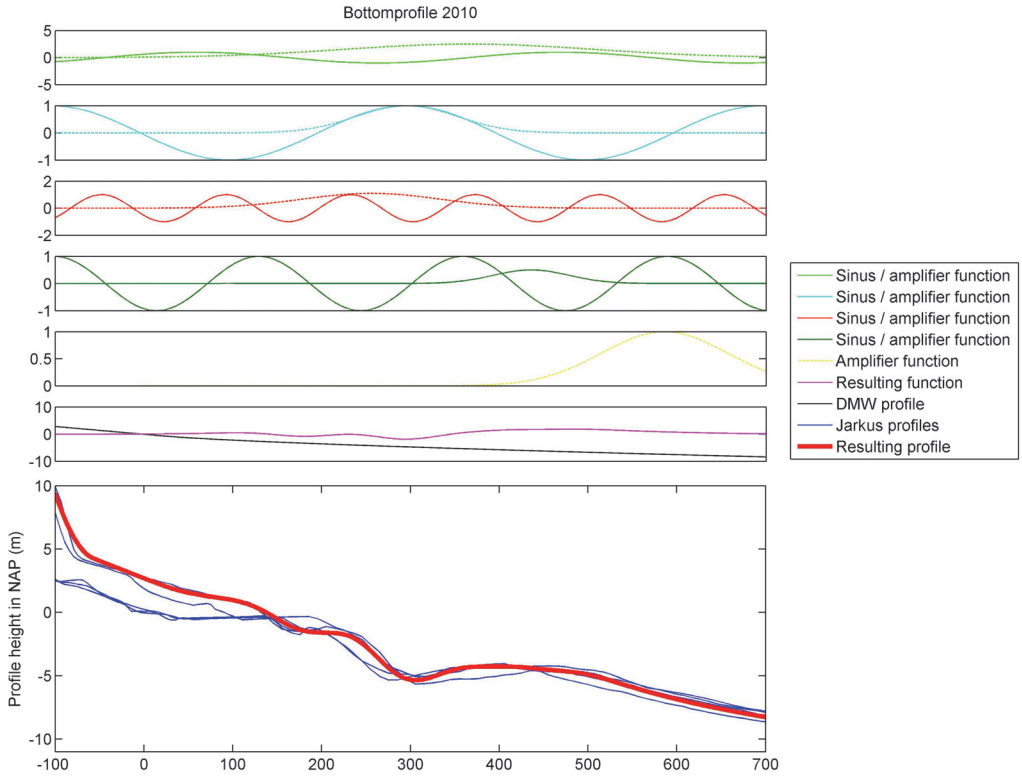

Figure 17 Profile schematization through the Jarkus transects for the 2010 bathymetry with nourishment

3.2.4 PROFILE COMPARISON

The profiles have a depth of 8.25 meters to 8.35 meters at a cross-shore distance of 700 meters. It is important to have approximately the same depth at the domain boundary because the wave conditions at the boundary are determined roughly on the -8 meter depth contour. To make a good comparison between the three situations it is also of importance that the offshore depth does not differ much.

For the 2009 and 2010 profiles the offshore part of the profile is equal except for a small difference in the bar profile. Therefore it is relatively easy to compare differences in hydrodynamics and sediment transport and express them in percentages at the offshore bar. In the 1990 profile the outer bar is located further onshore and therefore the water depth at the crest is slightly smaller. This should be taken into account when comparing the situations.

Unlike in the 1990 and 2010 profile the small bar is easily visible in the 2009 profile. Onshore of the bar the water depth increases which is not the case in the other profiles. In the 2010 profile the water depth nearshore remains constant for some distance and in the 1990 profile the water depth decreases more gradually. These differences in bathymetry have different effects on the wave energy dissipation. Due to bars the waves break over a short distance and dissipate more energy in a short time then when the bathymetry gradually changes and the waves break over a longer distance. The longshore current will therefore be different as this is related to the location of breaking and the amount of energy dissipated.

The comparison between the situations should be done with having the differences between the profiles in mind.

3.2.5 GROIN PROFILE

For the two approaches with groins in the bathymetry, the actual groin dimensions must be determined. For the determination of the slope and the width, use is made of old design drawings and LIDAR data. The groins in the model domain are groins 14, 15, 16 and 17. Groins 14 and 15 were constructed in the year 1807, groins 16 and 17 were built in the period from 1826 to 1827. Several data of groin 14 is shown to give an indication of the profile change in time.

In Figure 18 standard design drawings for groins are shown. According to these drawings, groins do not have a constant slope, but it changes with the distance offshore. The slopes that are mentioned are a slope of 24:1 for the upper part, 47:1 for the middle part and no slope for the head of the groin. It is assumed that these design rules were also applied to groin 14 when it was built in 1807.

In cross section A at the middle of the groin, it can be seen that the groin is built with two lines of poles with stones in between. Underneath the stones, a clay layer is placed. In cross section B at the head of the groin, the groin looks different. A bottom protection mat is placed underneath which consist of brushwood, this is held down with stones.

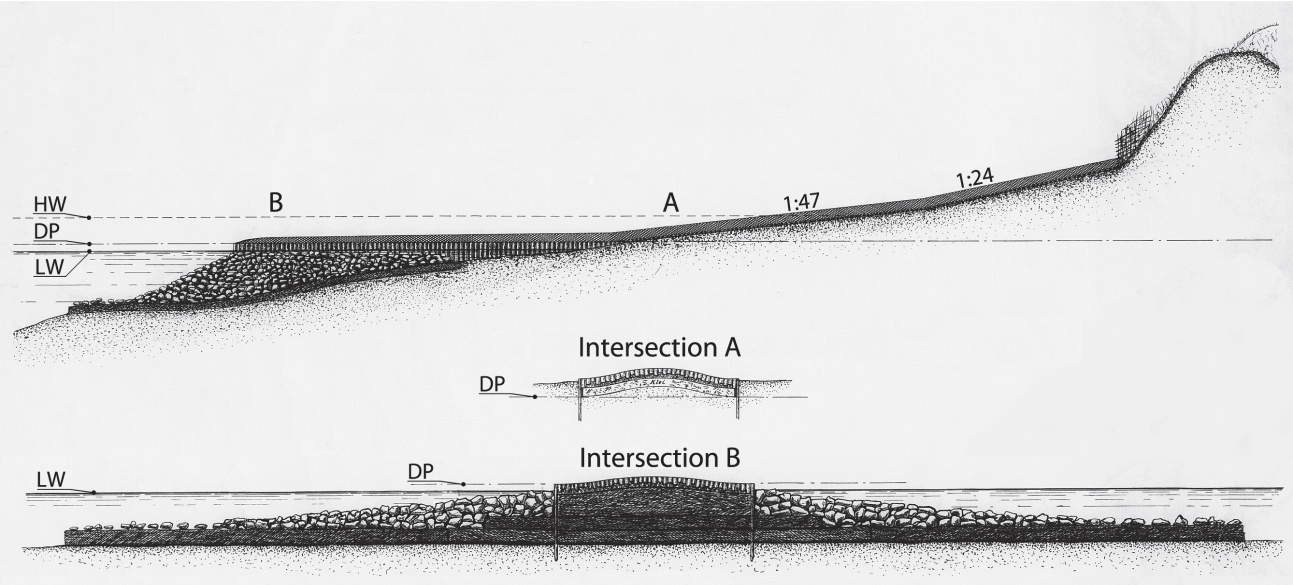

Figure 18 Standard groin design

In 1919 groin 14 was lowered. This was done after severe damaging during a storm in 1919, when the question raised if the groin should be restored in its old state. It was expected that the lowering of the groin would induce less damage in the future and therefore lead to a lowering of the annual maintenance costs. It was also thought that the lowering would have positive results regarding the beach, because it had a better connection to the beach. In 1922 the lowering was performed (Hoogheemraadschap Delfland 1922).

The present groin dimensions are determined with LIDAR data. With the LIDAR data the groins can be visualized, by specifying an angle under which the groin extends seawards, the height of the groin can be extracted across this line. This results in a graph that represents the height of the land from the groin tip up to the dune foot, this is shown in Figure 19. For the groins 15 and 16 these graphs can be found in *Appendix D - Groin profiles*.

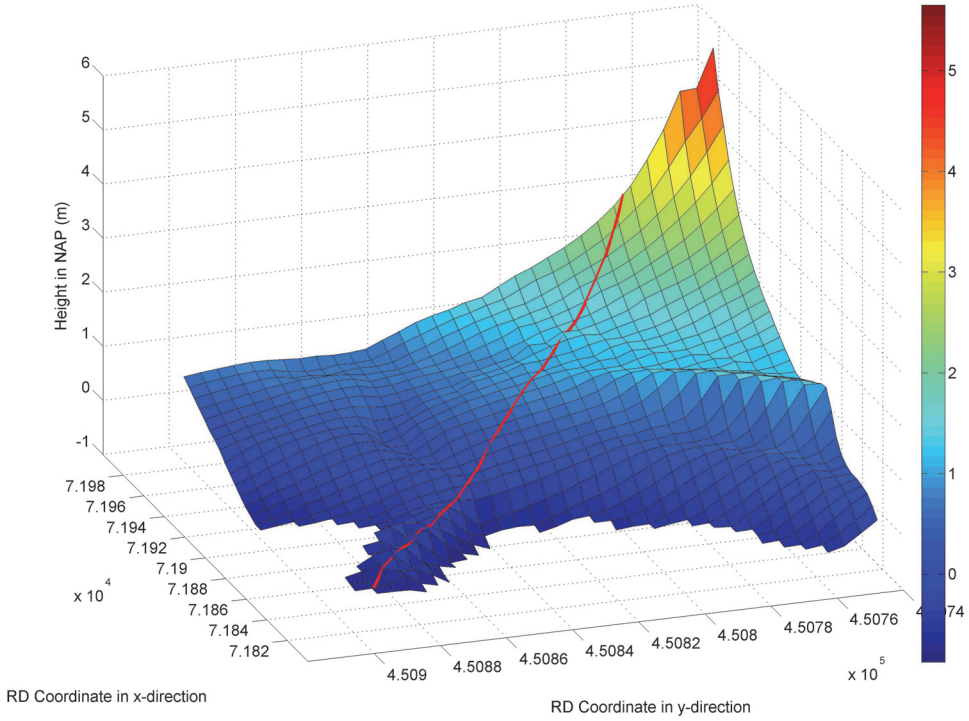

Figure 19 LIDAR data around groin 14. The red line is the line along which the heights are determined.

In this graph, only a part represents the height of the groin. It cannot clearly be seen where the groin is exposed and where it is submerged under the beach. By looking at a sudden change in the slope and making use of Google Earth, this point is determined. The red dots in Figure 20 represent the tip and the foot of the groin.

In *Figure 21* the height of groin 14 through time can be seen. In 2009 the groin is mostly covered with sediment. The profile of the groin under the beach is therefore not known. In this figure, it can be seen that the groin subsides gradually in time. At 120 meters from RSP =0, the groin height in 1922 is higher in 1911 (Hoogheemraadschap Delfland 1911). A reason for this could be that the groin tip was repaired and made somewhat higher, another reason could be the accuracy of the measurements. The big difference in groin height due to the lowering of the groin between 1911 and 1922 is clearly visible in the figure.

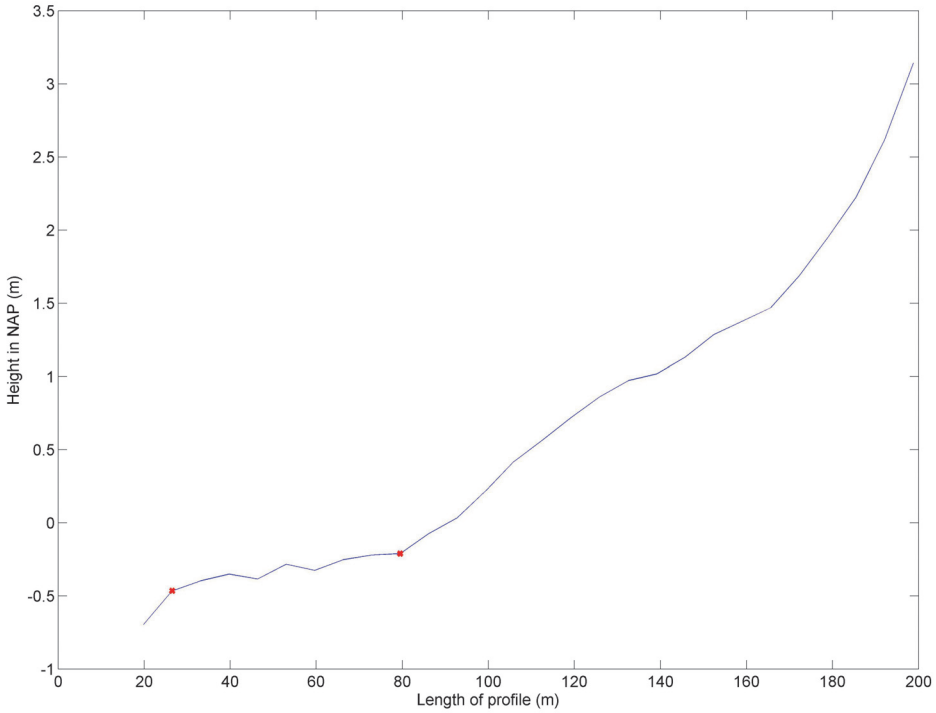

Figure 20 The height of groin 14 along the red line drawn in Figure 19. The red dots are the points from which the dimensions are determined.

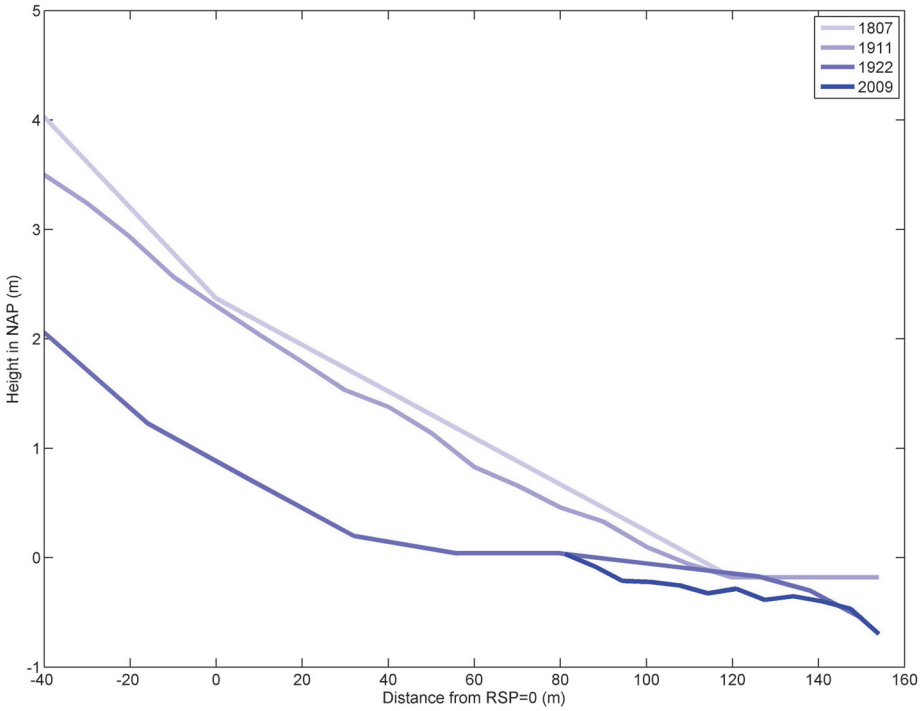

Figure 21 Height in NAP of groin 14 in time

As can be seen in Figure 21 the use of design drawings does not give satisfactory results regarding the height of the groins, therefore the LIDAR data is used in the model.

For groin 14, 15 and 16 the length and slope are determined with LIDAR data. Groin 17 is not clearly visible in the LIDAR data so the dimensions cannot be determined accurate enough. The length and slope are determined by choosing a point that represents the tip of the groin and a point that represents the location where the groin is submerged under the sand (the red dots in Figure 20). The slope is assumed constant between these points.

The data and graphs for groin 15 and 16 can be found in *Appendix D - Groin data*. A summary of the groin slopes and depths of the groin tips are shown in *Table 1*.

Groin	**Slope (1:a)**	**Tip groin depth (m)**	**Length (m)**
Groin 14	208.17	-0.465	53.0
Groin 15	168.53	-0.529	54.94
Groin 16	157.15	-0.48	42.43
Total mean	*177.95*	*-0.49*	*50.12*

Table 1 Groin depths and slopes

From this information, the mean slope is rounded off to 1 in 180 and the depth of the tip of the groin is set to -0.50 meters. The average length of the groin is rounded off to fit in the grid nicely to 50 meters; every grid cell is 3.33 meters so the groins in the 2009 profile are schematized as 15 grid cells.
In the 1990 profile it is assumed that the groins are in the same position as they are in 2009, have the same depth at the tip and have an equal slope. This means that the groin relatively will be longer because the 0 meter water level line is positioned further inland. The width of the groins can be approximated by making use of Google Earth and LIDAR data. It seems reasonable to assume a width of 20 meters for the groins.

3.2.6 BATHYMETRY AROUND THE GROINS

Nearby the groins the tidal and wave-induced currents are influenced and may be the cause of an erosion pit or a flow gully. If this is the case, the model does not give realistic results around the groins because the water depth differs from the schematized bathymetry and therefore the currents will be different. From mean Jarkus profiles in Figure 22, it can be seen that the groins do not play a major role on the bathymetry near the groin itself for the 2009 profile, this data is not available for the 1990 profile. In the figure the mean transects left and right of the four groins are separately shown so differences in the profile by erosion should be visible. The transects are measured roughly between 20 and 30 meters from the groin. The lines in the figure represent a mean profile through all the profiles on right, left and the middle of the four groins. It is clear that the groins do not create a tidal gully near the groin itself. The black line, which represents the bathymetry including the groin, does show a gully on the end of the groin. This is due to the position of the

bar, the bar is not visible in the mean profiles because the profiles show a large diffusion in the inner bar position, taking the mean profile cancels out the differences and shows a constant profile. This does not mean the bar should not be schematized however. The bar is present in each profile but differs in position, it does however influence the breaking of the waves and is therefore schematized. In the schematized profile, the bar is chosen in a mean position.

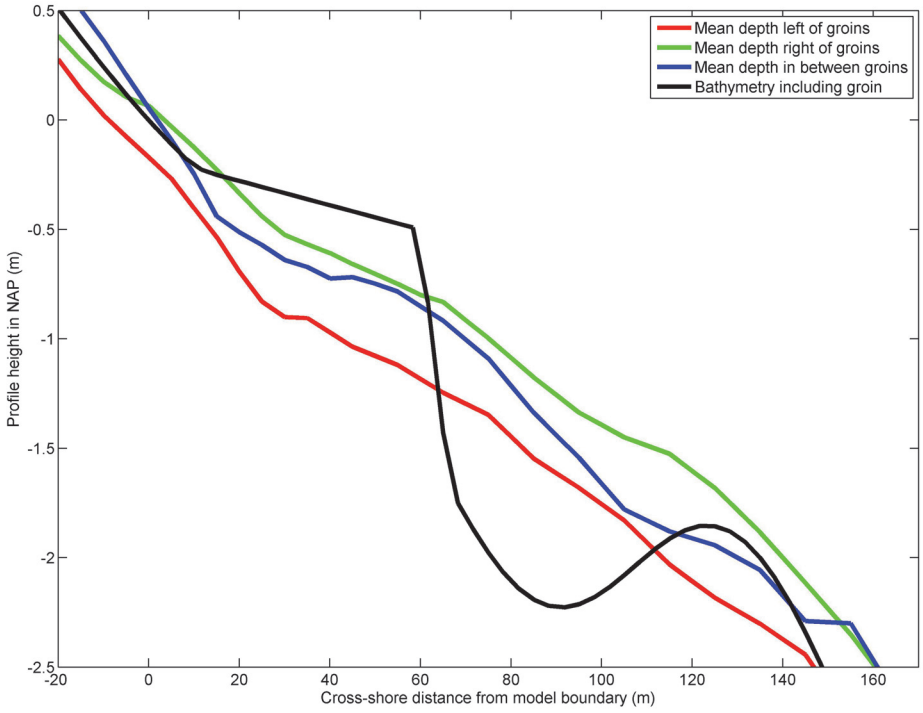

Figure 22 Mean Jarkus transects around the groin tip

3.2.7 BATHYMETRY

The bottom profiles of 1990, 2009 and 2010 are used for the bathymetries in the model. The position of the profiles 1990 and 2009 in the grid is chosen such that the water level = 0 meter NAP line is positioned 100 meters from the domain edge. In other words, if the water level is 0 meter NAP, a dry beach of 100 meters is visible in the model. For the 2010 profile the same reference is used as for the 2009 profile, to maintain the same boundary position and depth. In Figure 23 an overview of the profiles with respect to the groin position is shown.

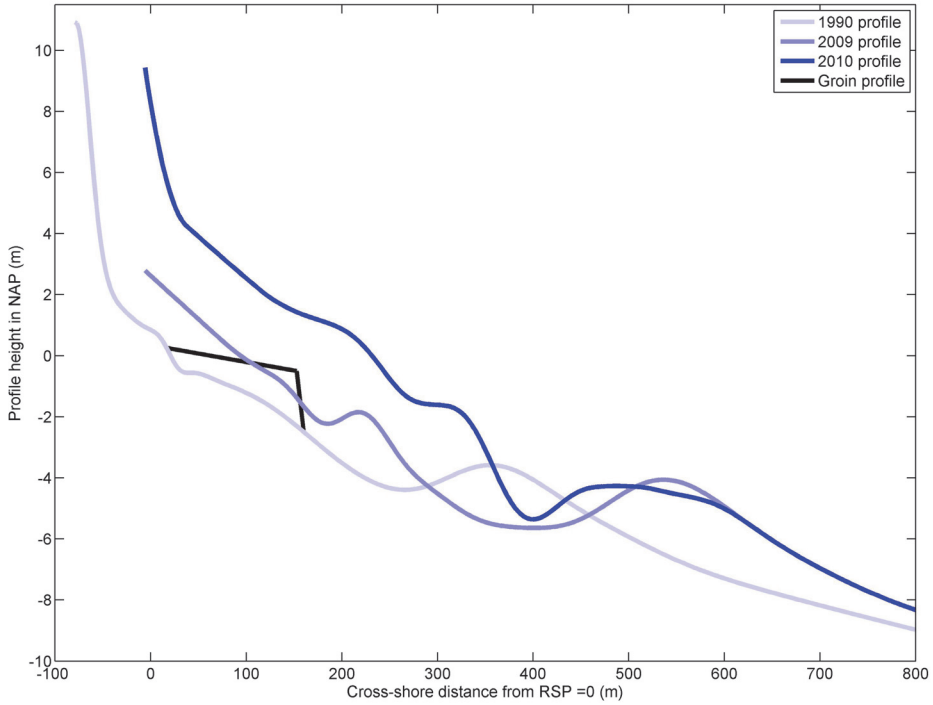

Figure 23 Profile overview with respect to the position of the groin

For the three profiles in 1990, 2009 and 2010 the bathymetries that are used in the model are shown. The used grid is plotted on top of the bathymetry.

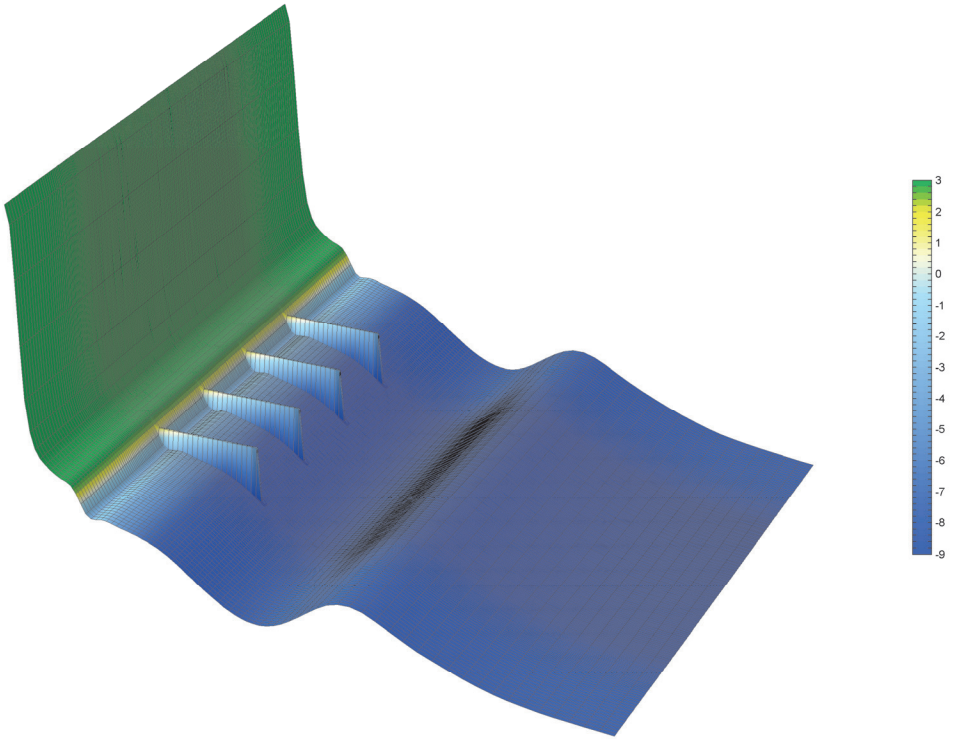

Figure 24 Bathymetry 1990

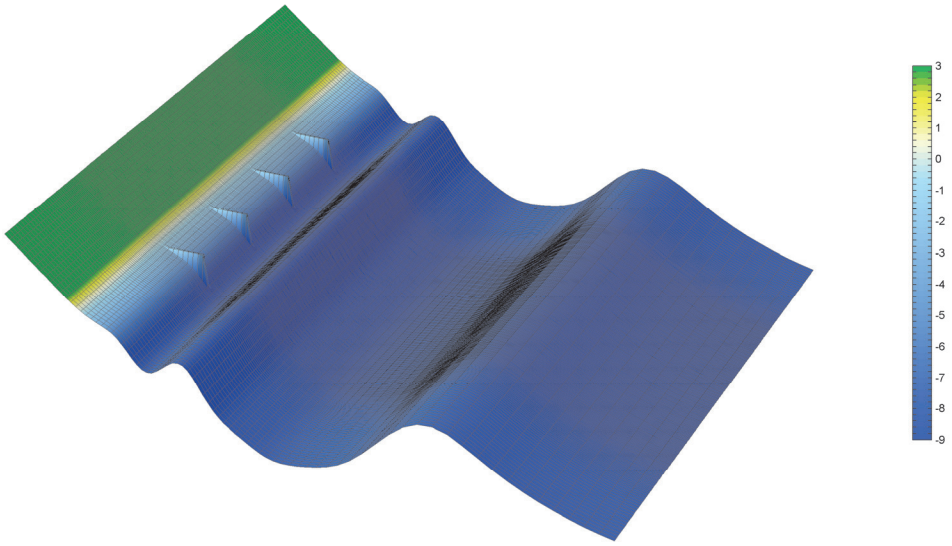

Figure 25 Bathymetry 2009

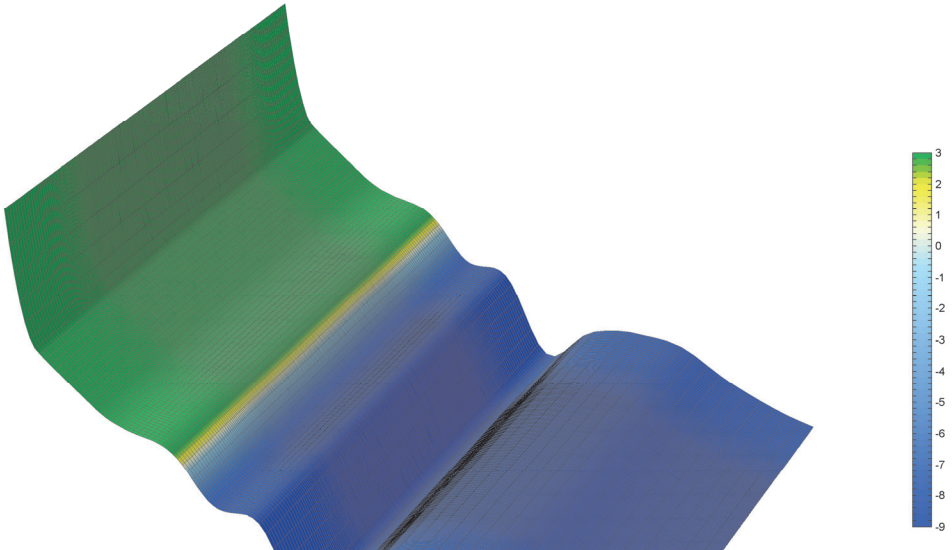

Figure 26 Bathymetry 2010

3.2.8 GRID

HORIZONTAL GRID

To obtain reliable results from the model calculations, the grid cell size should be as small as possible, smaller grid cells greatly increase the computation time however. To reduce the computation time it is therefore useful to only decrease the grid cell size at positions that require a higher accuracy. For the area around the groins, more accuracy is needed then for the area further away.

The groins itself needs at least three grid cells over the width to get a good representation of a real groin, this is due to the fact that Delft3D determines the depth in the grid cell centre. If three grid cells cover the width of the groin, the cell in the middle has the actual groin height and the two on the side have the mean height between the bottom and the groin. In this model, the groin will be modeled with 6 grid cells, giving the groin a smoother profile.

The grid cell size is therefore determined by the minimum size of the grid cells along the groin. In the groin area this cell size is taken constant. The width of the groins is around 20 meters, which means the grid cells cover at least 6.67 meters in x and y direction. To reduce errors the grid cell size is chosen at 3.33 meters in both x and y direction. Further away from the groins the grid cells can be bigger and are set on 10 meters. The transition from the larger to the smaller cells is gradually increasing for better results of the model. The resulting grid is shown in Figure 27.

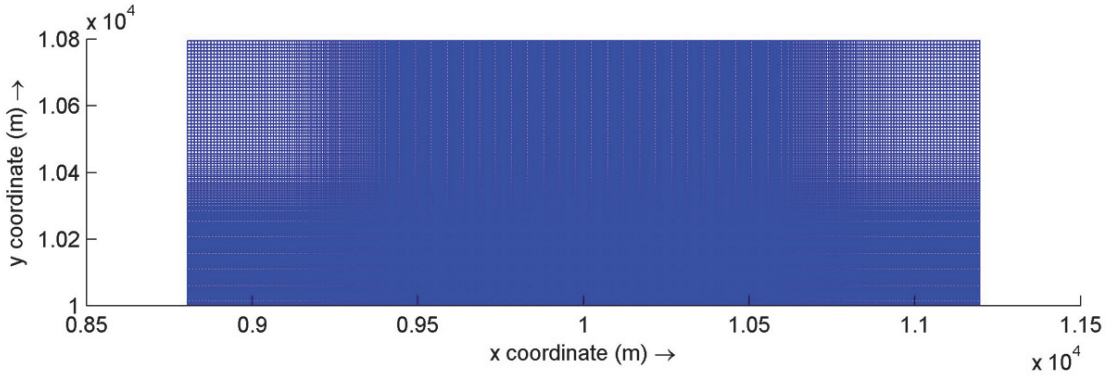

Figure 27 The grid used in Delft3D Flow computation

In this grid directions are specified for different properties. X and Y are the main directions to indicate position on the grid, X is directed positive offshore (upward in Figure 27), Y is directed alongshore and positive to the right. With the letters M and N grid cells are indicated, the direction is different than X and Y. M is directed positive onshore and N is directed alongshore to the right. U and V are used to indicate velocity components and have the same directions as M and N.

For the Delft3D Wave computation, another grid has to be made. This grid must be bigger to make sure the wave induced currents are triggered before entering the Flow domain. The Wave grid has the same basic grid as the Flow grid (as shown in Figure 27), but is extended. The width of the Flow grid is 2800 meter, the Wave grid is extended to 5400 meters with gradually increasing grid cell size in x direction. On the top of the grid, six cells are added so the grid becomes 860 meters high.

For the sake of simplicity the model is not aligned with the angle of shore normal at the Delfland coast. This shore normal is 310° in the nautical convention. The shore normal in the grid is in the direction of the positive X axis. Therefore the grid is rotated 50° clockwise from reality. Waves approaching from the left (southwesterlies in reality) then have an angle between 270° and 360°, waves approaching from the right (waves from the north in reality) have an angle between 0° and 90°. In this way it is easy to see the direction of the incoming waves.

The time step used in the model is 0.1 minute. The Courant number is then somewhat higher than the recommended value of 10 on some positions. Because the bathymetry changes only slightly on those positions the computation does not show errors due to the time step.

MODEL BOUNDARIES

On the offshore boundary condition a water level with a harmonic change in time is applied. The amplitude is 0.80 meter and the phase speed is 28.99 °/hour, which represents an M2 Tide, in *chapter 3.2.10 Tide* these values are derived. The phase of the wave shifts 1.6 degree over the offshore boundary from left to right. On the two lateral boundaries Neumann conditions are applied that represent a water level gradient. Also a phase difference of 1.6° between the left and the right boundary is present here, to take into account the propagation of the tidal wave. In the wave grid the wave conditions are only applied on the offshore boundary. The grid must therefore be large enough to get alongshore uniform wave conditions in the FLOW domain.

VERTICAL GRID

For the modeling of the three dimensional currents the vertical grid should have a good resolution. For this case, it is chosen to divide the water depth in 12 grid cells with a higher resolution near the bottom and the surface. The grid cells are defined as a percentage of the water depth, the grid is therefore dependent on the water level and changes in time. In Figure 28 an example of the grid in z direction is shown in the 2009 profile at time 12:25, at this time the water level is at its maximum. The resolution near the bottom and the surface is higher to have better results on locations where the interaction with the boundaries is high. For the vertical cells the main direction to indicate location is Z, which is directed positive upward. K is used to indicate the cell number, is directed positive downward, so K=1 indicates the surface layer. W, the vertical velocity component is directed equal as K.

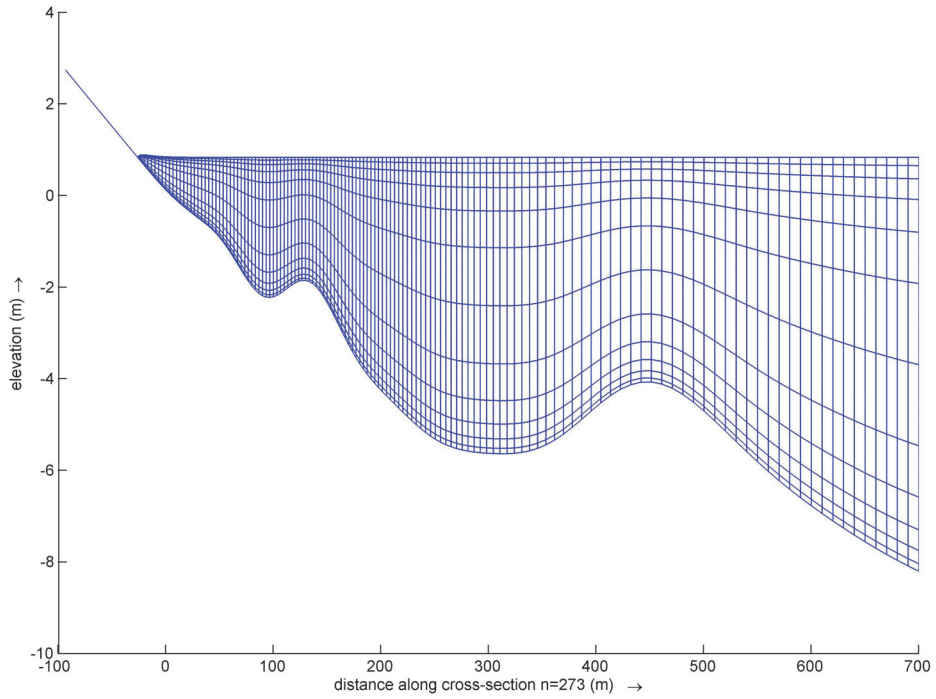

Figure 28 Grid in Z-direction during high water

The schematization of the groin in the grid is shown in Figure 29. The water depth is defined in the centers of the grid cell, in the picture the grid cell faces are shown as dotted lines. The groin height is defined in 6 grid cells.

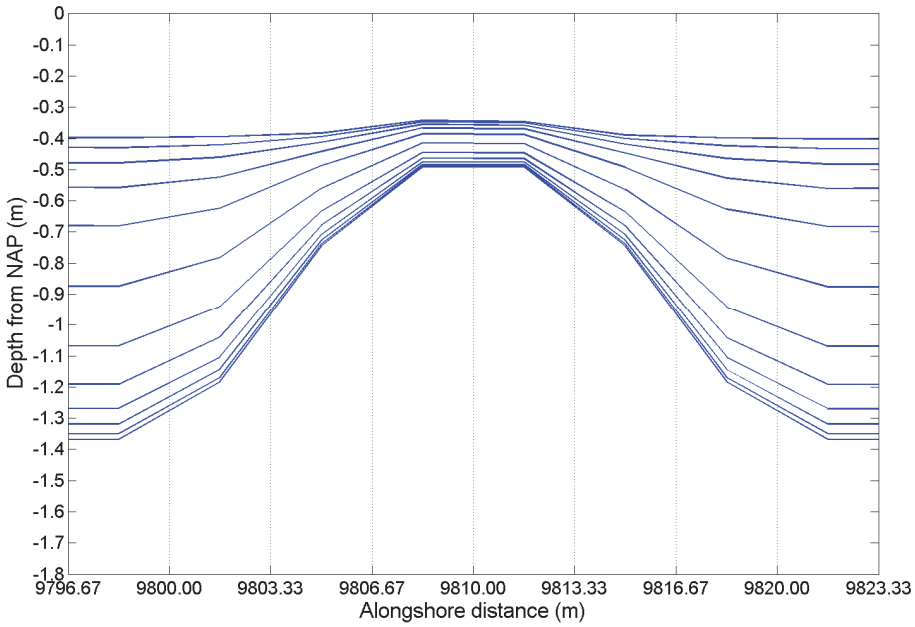

Figure 29 Hydrodynamic vertical grid for the 2009 bathymetry

3.2.9 WAVE CONDITIONS

Initially the wave conditions were derived with the Building with Nature tool that makes use of an interpolation matrix based on Delft3d calculations along the Dutch coast. After a few test runs it seemed that the wave climate derived from the BwN tool induced a southerly-directed sediment transport. Since many studies found a northerly-directed sediment transport, as can be seen in Figure 10 in *chapter 2.5.1 Sediment transports*, this result is highly doubtful. The wave climate is therefore not used. It is recommended that a closer look is taken at the wave climates derived with the BwN tool. The results from the BwN tool can be found in *Appendix E – BwN tool results*.

A new wave climate is needed, as the BwN tool did not lead to satisfactory results. In an earlier performed study concerning the Sand Engine a model of the North Sea is made to derive the nearshore wave climate. The wave conditions on the 8 meter depth line are used as boundary conditions. These wave conditions lead to a northerly-directed transport and are validated against sediment budget studies. The derivation of the wave climate is shown below and is translated from the Sand Engine report (Tonnon, van der Werf et al. 2009).

DERIVATION REDUCED WAVE CLIMATE

To reduce the computation time of simulations, we reduce the wave climate to a manageable number of wave climate conditions. Calculations with the reduced wave climate should give a similar morphological development as the whole number of wave conditions. This so-called morphological wave climate is derived using the OPTI program (Mol 2007). The purpose of the wave climate derivation with OPTI is to determine a smaller set of wave conditions that give a good representation of the average tidal sediment transport based on all 116 conditions. Since the area of interest in this study is the Delfland coast, we focus on the sediment transports between Hoek van Holland and the harbor of Scheveningen in the -20 to 3 meter depth contour line. The following steps are taken.

First, 116 different simulations are executed (one for each wave condition) without morphological bathymetry update. The influence of tide, wind and waves is included with the model settings described in section 2.3. For each simulation, the average tidal transport in the area of interest is determined. Then a weighted average based on the weighting factors (probability of occurrence) is determined, as is given in **Table 2**. The total transports are the target in the OPTI routine. After this the wave conditions are compared, of each wave condition the contribution to the transportation field is determined by the product of the weighting factor and the root of the quadratic mean transports. The wave condition with the smallest contribution is removed by setting the weight factor for this condition to 0. Then the weight factors of the remaining wave conditions arbitrarily changed by:

$$w_{\text{i,new}} = 2 * w_{\text{i,old}} * ran \quad (1)$$

With *ran* a random number between 0 and *scaleTo1* using a uniform probability distribution with *scaleTo1* a user defined value between 0.1-1.0. With these new weights (and calculated movements per condition), it is determined how

well the target, the transport field that follows from all wave conditions, is approached. The relative error is the indicator of this. Adjusting the weights and calculating the relative error associated with this set of weights is done *maxIter* times, with *maxIter* the user defined maximum number of iterations. Then the set of weighting factors chosen by the lowest relative error, i.e. the closest to the target, is selected as the new weighting factors. Then we check which of the remaining 115 conditions has the smallest contribution. This is then removed and the exercise is repeated until the desired number of wave conditions remain.

Based on a number of sensitivity sums the following parameter settings of OPTI are chosen: *scaleTo1* = 1.0 and *maxIter* =1000. These settings gave the lowest relative error and the 10 wave resulting conditions represented an equal wave direction distribution. The relative error of these 10 conditions is 7.9%, and the correlation coefficient is 1.00. *Table 2* shows the 10 wave conditions that represent the 116 wave conditions when looking at sediment transport in the region of interest.

Condition	$H_{1/3}$ (m)	$T_{1/3}$ (m)	Θ_{wave} (^{o}N)	V_{wind} (m/s)	θ_{wind} (^{o}N)	Surge (m)	Weight factor (-)
wc29	1.48	5.34	232	9.97	231	0.04	0.1224
wc31	2.46	6.34	232	13.37	227	0.12	0.0685
wc40	1.97	5.99	246	11.09	210	0.20	0.0118
wc49	1.48	5.45	261	8.24	197	0.16	0.0006
wc61	2.47	6.53	277	11.44	175	0.42	0.0460
wc62	2.97	7.00	277	13.30	171	0.59	0.0109
wc90	1.97	6.59	322	8.65	126	0.22	0.1206
wc92	2.96	7.71	322	11.93	127	0.53	0.0036
wc99	1.47	6.07	337	5.69	107	0.02	0.0652
wc108	0.96	5.63	352	3.62	73	-0.08	0.0823

Table 2 Reduced wave climate

The reduced wave climate contains six waves from the southwest sector and four from the northwestern sector. In terms of probability of occurrence two conditions are dominant, wc29 and wc90. The sum of the weight factors is 0.53 and therefore considerably smaller than 1. This is due to the fact that the reduced wave climate contains higher weighed average waves that need a lower weight factor to produce the same sediment transport (the relationship between sediment transport and wave height is nonlinear).

Figure 30 and Figure 31 show the (calculated) net annual sediment transport (excluding pores) through 34 transects cross shore and 16 transects parallel to the coast. The cross shore transects range from the -12 to -8 meter depth contour line and the -8 to 3 meter depth contour, respectively. The alongshore transects run roughly along the -8 meter depth contour line. These figures show that the transport field of 116 conditions is well represented with the 10 reduced wave conditions (with appropriate weight factors).

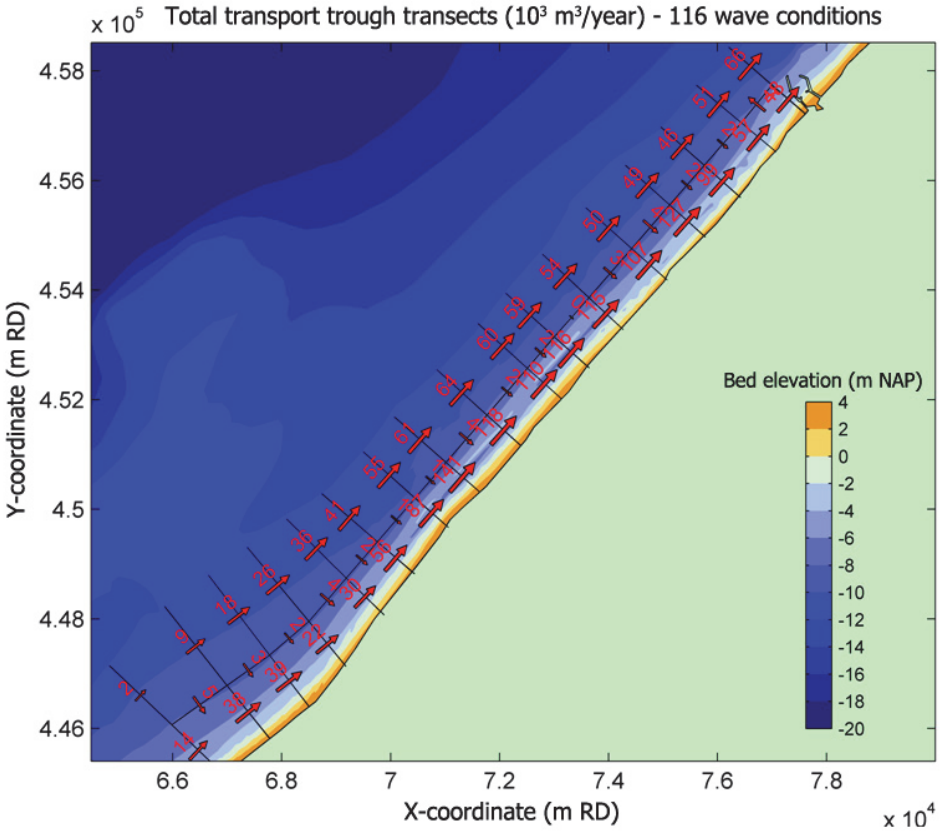

Figure 30 Tide mean total sediment transport through the transects (10^3 m^3/year) for all 116 wave conditions

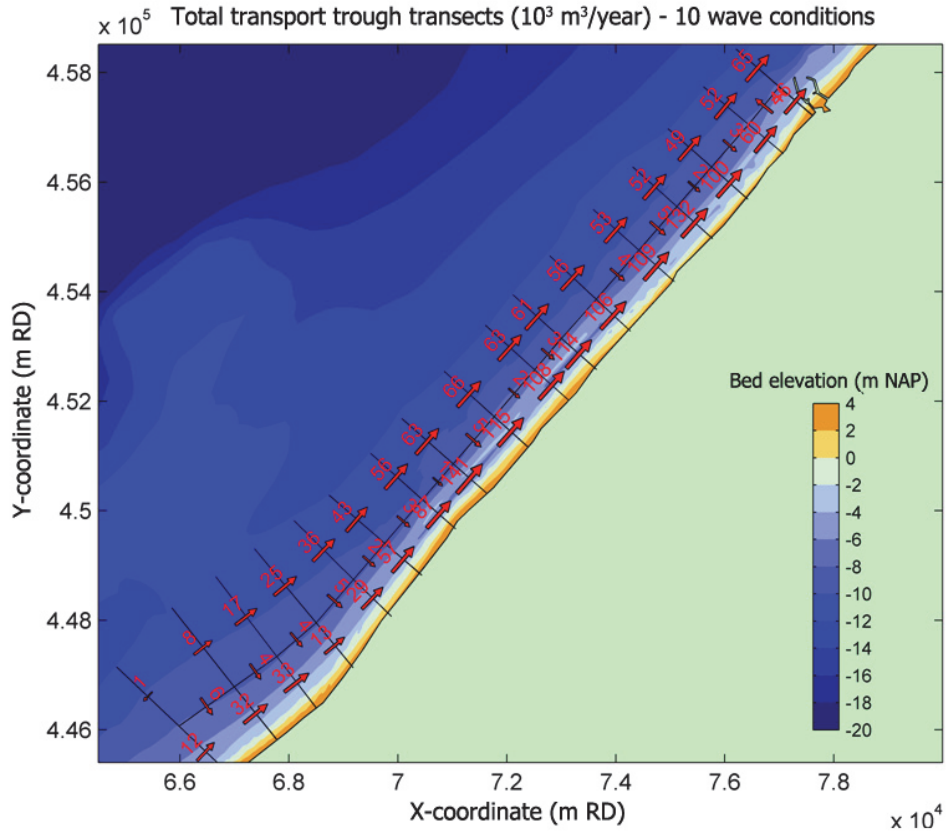

Figure 31 Tide mean total sediment transport through the transects (10^3 m^3/year) for reduced 10 wave conditions

Figure 32 confirms this. It shows the annual average transport time between -8 and -3 meter depth contour based on 116 and 10 wave conditions Hoek van Holland (118 km from Den Helder) to Scheveningen (102 km from Den Helder). Positive longshore transport is directed towards Den Helder. This figure includes the longshore transports in this area according to a number of other studies (see Van Rest, 2004). It follows that the long transport as calculated by the present model matches the values derived from previous studies.

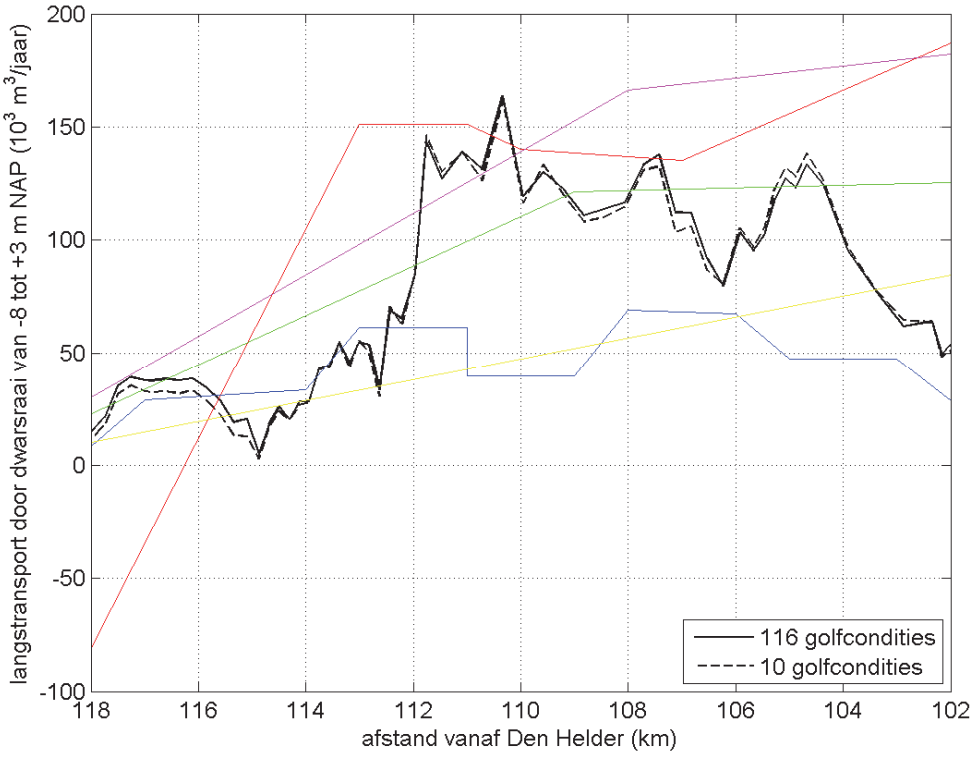

Figure 32 Annual average longshore transport in the surf zone along the Delfland coast as follows from the present study (black lines) and other studies. Red line: (Steetzel and de Vroeg 1999), blue line: (Roelvink 2001), green line: (van Rijn 1995), magenta line: (van Rijn 1995) adapted by (van de Rest 2004), yellow line: (Stive and Eysink 1989). See also (van de Rest 2004).

NEARSHORE WAVE CLIMATE

The wave conditions must now be known at the boundary of the model, roughly on the 8 meter depth line. The wave data is therefore extracted from the sand engine model at the 8 meter depth line at the model boundary. This leads to the wave conditions in Table 3 that are used in the model. Notice that the wave and wind directions are changed, a value of 50° is added. The model is turned 50° for the sake of simplicity, and therefore the angles must be changed as well. In the rest of the report the angles are given with respect to a shore normal of 0°, in this way it is easy to see from what angle the waves come with respect to the shoreline.

Condition	$H_{1/3}$ (m)	$T_{1/3}$ (m)	Θ_{wave} (^oN)	V_{wind} (m/s)	θ_{wind} (^oN)	Surge (m)	Weight factor (-)
01	6.6557300e-001	5.8682017e+000	3.1407376e+002	9.97	281	0.04	0.1224
02	1.0829979e+000	7.1776385e+000	3.1942419e+002	13.37	277	0.12	0.0685
03	1.0497481e+000	6.5879426e+000	3.2262445e+002	11.09	260	0.20	0.0118
04	9.6814799e-001	5.9086523e+000	3.2757452e+002	8.24	247	0.16	0.0006
05	1.7107484e+000	7.2007113e+000	3.3984991e+002	11.44	225	0.42	0.0460
06	1.9444991e+000	7.6208100e+000	3.4052509e+002	13.30	221	0.59	0.0109
07	1.4974996e+000	6.6532640e+000	8.9749146e+000	8.65	176	0.22	0.1206
08	2.2475009e+000	8.0720730e+000	8.2998047e+000	11.93	177	0.53	0.0036
09	1.1149989e+000	5.8388343e+000	1.9200073e+001	5.69	157	0.02	0.0652
10	7.1387392e-001	4.9482946e+000	2.8475403e+001	3.62	123	-0.08	0.0823

Table 3 Wave conditions at 8 meter depth at the model boundary

In the Sand Engine model the wind is taken uniform over the model domain. The wind conditions that belong to the wave conditions are used.

3.2.10 TIDE

The tide is represented in the model as an M2 semidiurnal tide. Two equal cycles are computed, one to let the computational errors leave the model domain and from the second cycle the flow results can be obtained. The amplitude of the tide is determined with nearby measuring stations and is taken at 80 cm. The M2 tide has a period of 12 hours and 25 minutes, so in total the model simulates 24 hours and 50 minutes.

3.2.11 DELFT3D REMARKS

During the modeling some errors came up, which were solved, but require extra investigation. It is recommended to have a closer look on the errors that occurred, because in more complex cases the introduced errors can be interpreted as being a physical occurrence.

WAVECON FILE

When the wavecon file, the file to specify the wave conditions, is used in Delft3D (extension .wav) the wave calculation shows errors. At some points, which were not completely random, the waves suddenly increased in height. This has the effect that the wave breaks and a lower wave travels further in the wave direction. When the wave conditions were defined in the main Wave calculation file (extension .mdw) the problem did not occur. It is thought that the problem has

something to do with the interaction of the wavecon file with the roller model, which is used, because this model can also make use of a wavecon file.

BOUNDARY CONDITIONS

In the model three open boundaries with conditions need to be specified. First this was done by using the same conditions for all three boundaries. For the offshore boundary these wave conditions are right, for the lateral boundaries this induces an error because the waves change when they approach the shoreline. Normally the introduced error is not inducing problems because the wave grid is chosen larger than the flow grid to let the waves adapt before they reach the flow grid. The problem that raises here is that the wave simulation shows a slowly changing wave height throughout the grid. This on its turn induces a changing sediment transport and causes a gradient in sediment transport along the straight coast. When the wave spreading on the lateral boundaries is small (order 10˚, instead of 30˚) the introduced error is less. When the wave conditions are not applied on the lateral boundaries the problem does not occur at all, the used wave grid must be extended somewhat to let the waves be more or less alongshore uniform. When the error occurs the differences in wave height are small and might not be seen in a more complex model.

SEDIMENT TRANSPORT

Often the sediment transport formula of van Rijn 2004 is used in Delft3D. In the model however this introduced large errors near the groins, which are implemented as a more shallow area with a locally non-erodible layer. The errors are in the order of a factor billion and therefore nowhere to realistic. The very large sediment transports occurred only near the groins in a few grid cells, which were changing at different time steps. Due to time constraints the source of the problem is not found, and therefore the sediment formula of van Rijn 1993 is used.

3.3 TEST CASE SET UP

In the model two variables are changed; the bottom profile and the groin length. This method is chosen to have a bathymetry that is in equilibrium and to give a good representation of a bar in the profile. The problem is that the situations are not very well comparable; the groin length and the bottom profile both influence the hydrodynamics and sediment transports. To test what the influence of the bathymetry is and what the influence of the groin length is, ideally two test cases should be made; one with varying groin length and one with a varying bathymetry. The test case with a varying bathymetry is hard to perform however; the bottom profile can have many shapes and bar heights and widths are changing in time. Therefore only the influence of the groin length is studied. The influence in hydrodynamics and sediment transport due to the bottom profile must be qualitatively determined from the differences in the test case and the three schematized situations.

The test case consists of an alongshore uniform profile with a constant slope. On this profile eight different groins are placed, each with a different effective length, as can be seen in Figure 33. By comparing hydrodynamic effects at different groin length a relation can be found between the groin length and other quantities.

The calculations that are performed are equal to the ones performed before, only the bathymetry and the groin length are adapted. The bathymetry is schematized with a constant sloping foreshore starting at -8.05 meters at the model boundary (10800 meters in y direction) gradually decreasing to 0 meter NAP in 700 meters. 100 meters of dry cells, at mean water level, will remain in this way.

In Figure 33 the different groin lengths in the bathymetry are shown. The groin effective lengths are defined as the length from the tip at -0.5 meters NAP to the foot of the groin (the point where the groin disappears under the beach). It should be noticed that the foot of the groin has less influence as it lies higher on the beach, until a point is reached where the water does not reach the foot of the groin anymore. From this point, the definition of the effective length should change. As can be seen in the figure this point is not reached since the water level due to the tide is +0.8 meters NAP.

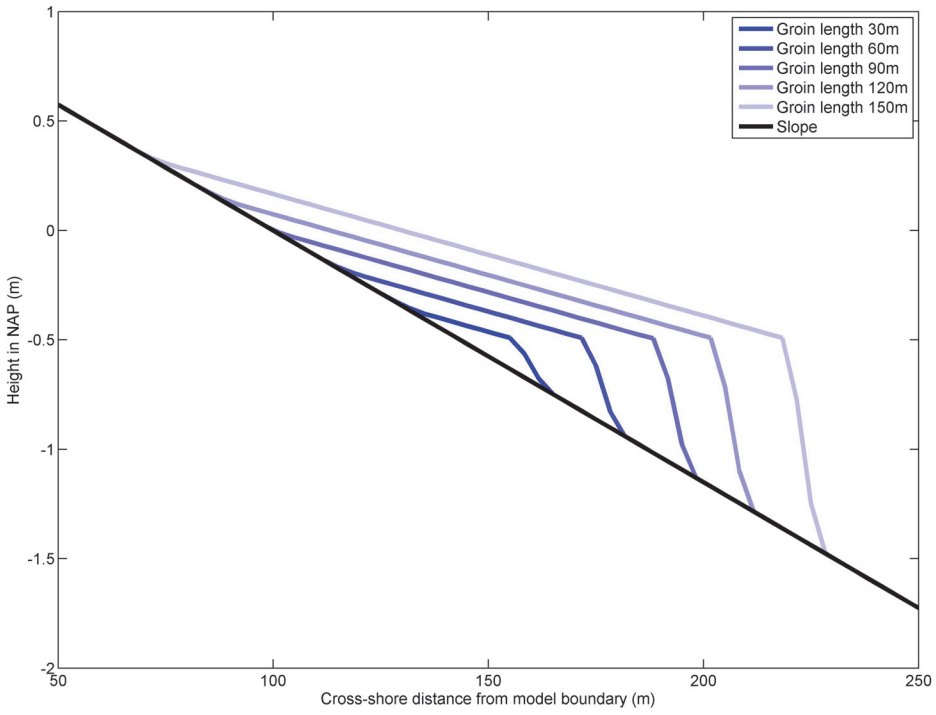

Figure 33 Different groin lengths in the test case

4 RESULTS

In this chapter the model results are analyzed. First the results are qualitatively compared to drifter experiments to check if the model reproduces the flow characteristics around groins.
Then the hydrodynamics are analyzed, first the test case results are studied. This is done to get a good view on the effect of the groin length on the hydrodynamics. After this the schematized situations from 1990, 2009 and 2010 are elaborated upon. The test case results are used to compare the differences and indicate the effect of the bathymetry on the hydrodynamics.
After that the sediment transports are treated in the same way. First the test case is studied which is then compared to the schematized cases to indicate the effect of the bathymetry on the sediment transports.
After this a sensitivity simulation is performed to show the influence of a scour hole at the tip of a groin.

4.1 MODEL COMPARISON

To estimate how the model can reproduce the flow characteristics around groins, the model needs to be compared to other studies and data from measurements in reality. First a quick comparison is made with an earlier model study by Pattiaratchi. Then the hydrodynamics are discussed. In this case not a lot of data is available that meets the situation in the model. Because of the schematization and the lack of data the validity of the model is hard to determine. Because of this it is decided to make a qualitative validation of the model in which the current patterns are compared. Current velocity data is carefully compared to data calculated by the model.
Finally the yearly averaged transport rates in the situation of 1990 calculated by the model are compared to the yearly averaged transport rates found in other studies. These values should roughly match the calculated values in the model.

4.1.1 MODEL STUDY BY PATTIARATCHI

Pattiaratchi et al. showed how wave-driven circulation patterns in the lee of groins look like in an experiment with drifters, he compared the data to model results. The drifter experiment was performed at a location with a curved coast, which might have had a big influence on the results. Therefore only the model is dealt with. In the model the bathymetry around the groin was taken longshore uniform. In Figure 34 one of the results of this model is shown. The black arrows indicate the position of the divergence and convergence points of eddy's in the lee of groins. The positions are dependent on the current speed, which is of course dependent on the wave conditions. When the longshore current is higher the convergence point is located closer to the tip of the groin, the divergence point is located further away from the groin. (Pattiaratchi, Olsson et al. 2009)

This convergence and divergence point are clearly visible in the present model at certain time steps when the groin is not submerged. The convergence and divergence points are also affected by the current flowing over the groin, which is not present in the study of Pattiaratchi et al. The models can be compared because the bathymetry is longshore uniform in both the study of Pattiaratchi and in the model in the present study. The models also have the same limitations with representing reality however.

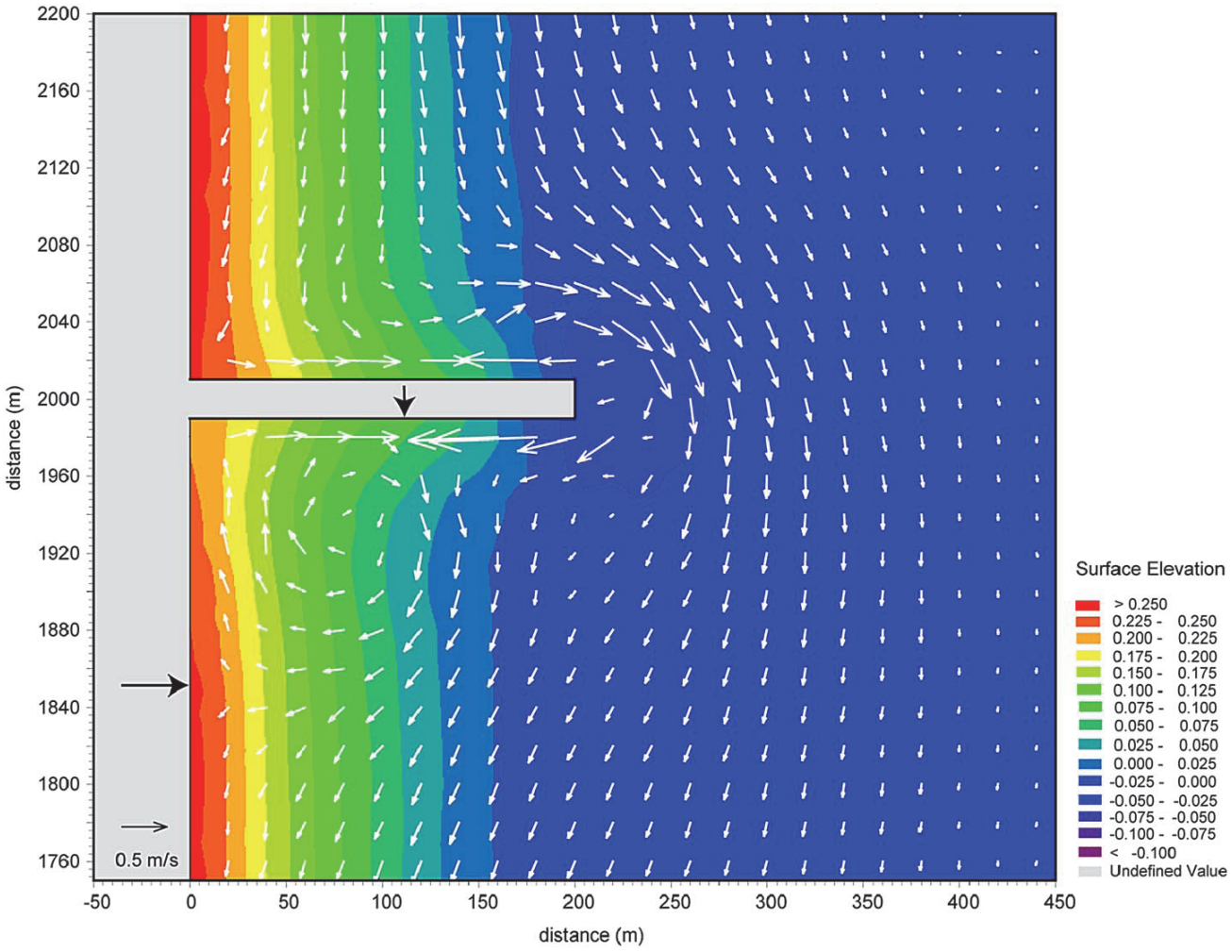

Figure 34 Currents in the lee of groins by Pattiaratchi (Pattiaratchi, Olsson et al. 2009)

4.1.2 SCHEVENINGEN DRIFTER EXPERIMENT

TU Delft and Shore Monitoring performed a drifter experiment at the coast of Scheveningen. Several drifter deployments were carried out in different locations and conditions. The drifters are followed with a GPS-device which results in a flow pattern. With the data, the velocities are calculated which can be used to compare to the model outcomes. Most of the deployments are not useful in this case because the locations are too specific, or the groins almost disappeared under the sediment. On July 16th 2010 a deployment is performed between 11:00 and 14:00 that can be used for a qualitative comparison with the model. During the measuring time the tide falls from 0 cm NAP to -50 cm NAP as can be seen in Figure 35. The drifter paths are shown in Figure 36 (Van Ettinger & De Zeeuw, 2010).

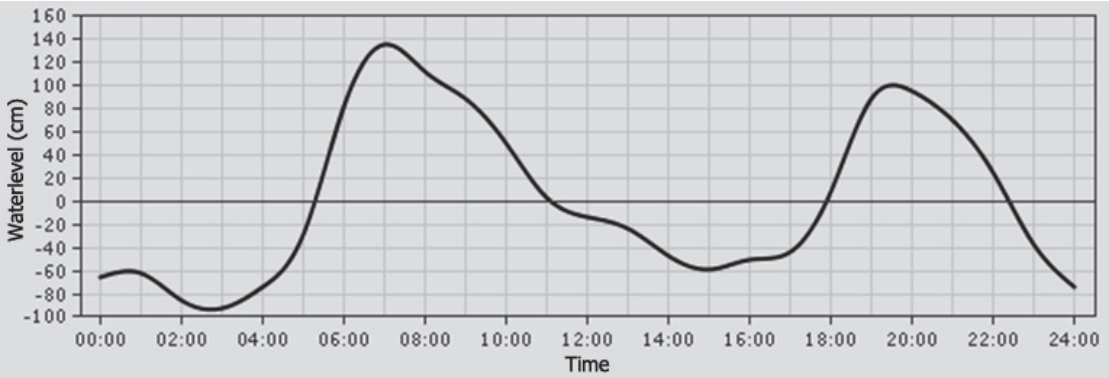

Figure 35 Water level in Scheveningen on July 16th 2010

Figure 36 Drifter movement on July 16th 2010

The Scheveningen pier crosses the measuring site and can thus have an effect on the wave conditions behind the pier. The effect of the pier is assumed to be small because the poles on which the pier is build have a relatively large spacing as can be seen in Figure 37.

Figure 37 Scheveningen pier foundation

The bathymetry at the measuring site is not measured because the drifters floated outside the area of interest. To make a good comparison between the measured values and the model outcome, the bathymetry in the model should be equal to the bathymetry on the 16th of July 2010. In Figure 38 the difference between the 2009 profile as used in the model and the profile of transect 9009925, located 100 meters north of the pier, is shown. This profile is measured on June 4th 2010 and is therefore assumed to be accurate enough to use. The outer bar which is clearly visible in the 2009 profile is not seen in the Scheveningen profile. Therefore the bathymetry is assumed with the Jarkus profile 9009925. It is assumed that the groins have the same properties as the 2009 groins, an extension of 50 meters from the beach and a slope of 1:180.

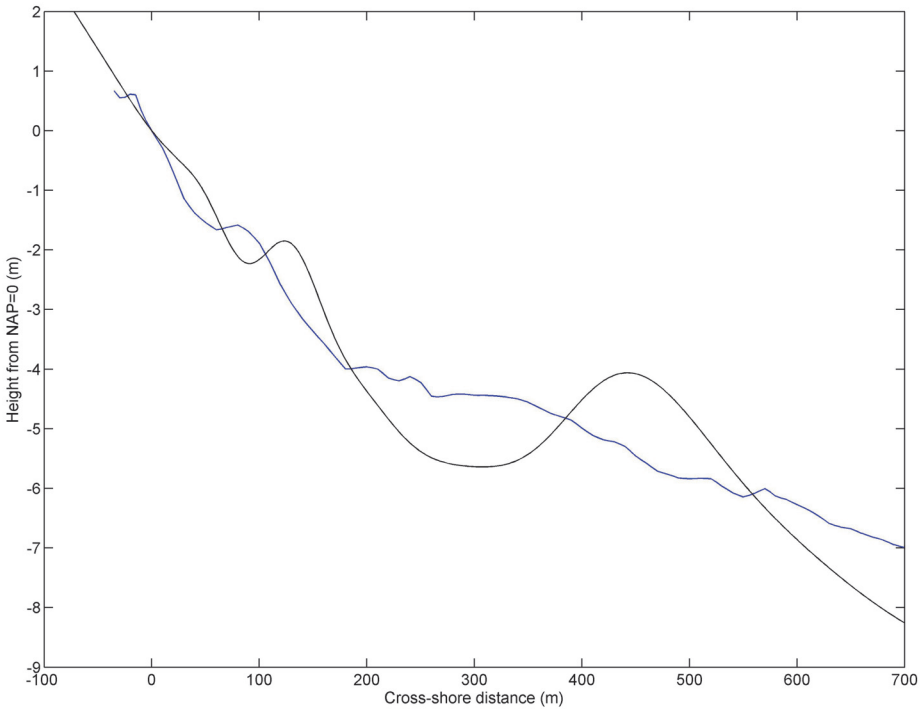

Figure 38 Bottom profile 2009 (black) and bottom profile in Scheveningen transect 9009925 on June 4th 2010 (blue)

The model boundary conditions for the validation are determined with the BwN Tool. As was found earlier, see *chapter 3.2.9 Wave Conditions*, the BwN tool did not lead to satisfactory results, it is assumed that the errors are not very large and therefore are usable to determine the wave climate. The resulting wave conditions are:

- Hs = 1 meter
- Tp = 4.5 s
- Dir = 305 °

Only the wave conditions and bathymetry are put in the model to make the qualitative validation with the drifter experiment.

For the validation, two situations discussed. The difference between the situations is the water level. In the first situation the water level is sufficiently high to flow over the groin, in the second situation the water level dropped so the current is forced to flow around the groin. This can be seen in Figure 40 and Figure 41, compared to Figure 39

Figure 39 Drifter measurements comparison locations

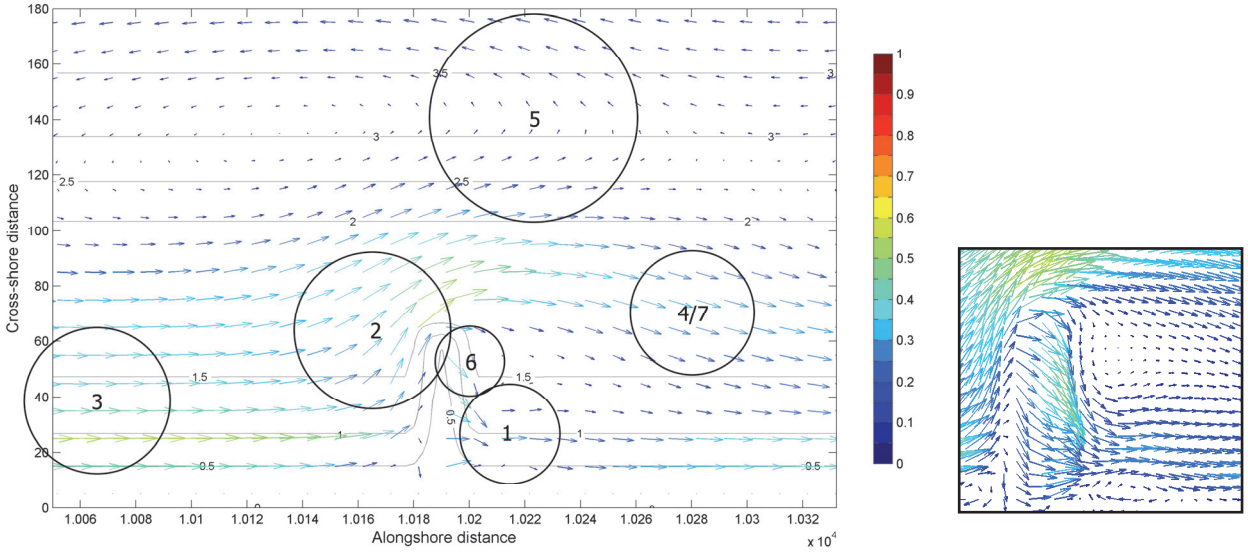

Figure 40 Current pattern around the groin with a high water level, flow over the groin

Near the groin, the bathymetry in the schematized model will differ from the bathymetry in reality. Due to shadow zones and rip currents near the groins the bathymetry will change. Often gullies on the side of the groins are formed because of the strong currents. The changes in bathymetry are likely to cause different flow patterns around the groin. These effects should be taken into account when comparing the current patterns around the groin.

In the situation with a high water level and flow over the groin, Figure 40, the following conclusions can be drawn:

1. The eddy near the foot of the groin is visible although it is small and the velocities are lower than in the drifter experiment. This is probably due to the water flowing over the groin that is affecting the eddies position.
2. The flow velocities when passing the groin are smaller than in the experiment. Only at the tip of the groin the velocities are comparable. This can well be caused by a different bathymetry around the groin, which is adjusting to the wave conditions. In *chapter 2.3.6 Scour* a more likely bathymetry around the groin is shown.
3. The current velocities are comparable; the width of the stronger flow might be somewhat underestimated.
4. The flow returning to the coast is clearly visible in the model, in the drifter experiment the drifter is flowing more straight to the coast.
5. The path of the drifter that gets caught in the ebb tidal current experiment is well recognizable in the model. Also the paths position is fairly the same.
6. The flow parallel to the groin is visible in the model results, although this current is located on the lower parts of the groin. This current is induced by wave breaking over the groin.
7. The current velocities just behind the first groin are higher than calculated in the model. This can be due to a different bathymetry as stated at point 2. The drifter in point 4 does have a much lower speed at the same position relative to the groin.

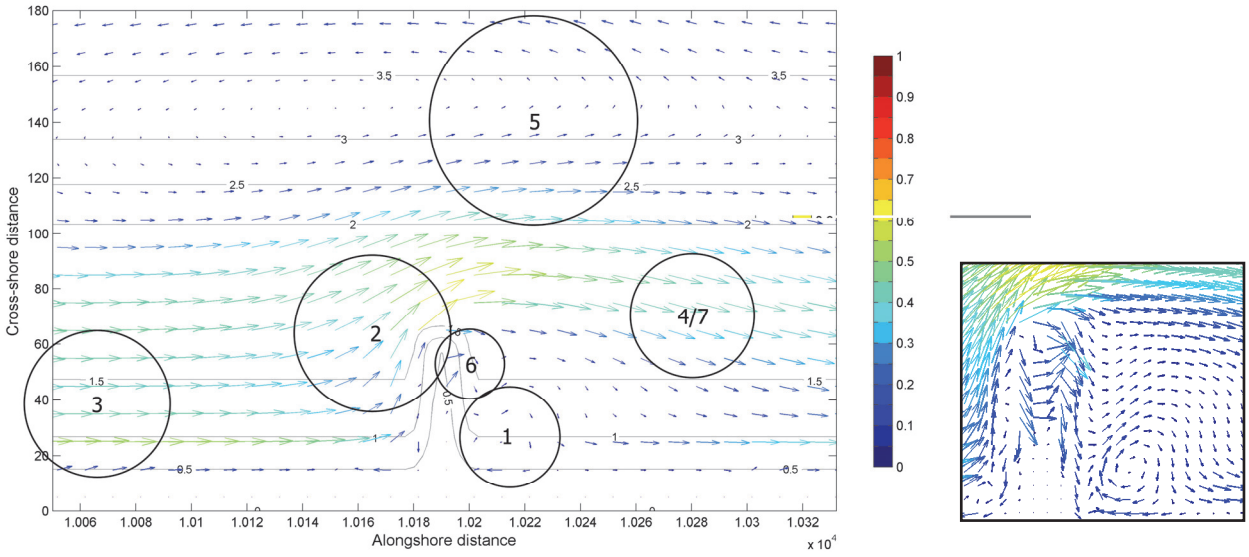

Figure 41 Current pattern around the groin with a lower water level, flow around the groin.

In the situation where the water level is lower and the water has to flow more around the groin as showed in Figure 41, the following conclusions can be drawn that differ from the conclusions in the high water situation:

1. The eddy is clearer and extends further offshore. This eddy looks roughly the same as in the drifter experiment.
2. The velocities are a little higher and more like the velocities in the experiment.
3. The current is a bit wider and better comparable to the measurements.
4. The current is stronger, the angle remains the same, the higher water level situation gives a better representation at this location.
5. This looks the same as in the situation with a higher water level but the location of the 'turning point' is shifted a bit to the right due to the higher velocities at the tip of the groin.
6. The return current velocity is not as high and wide. But can still well be compared to the measurements, also the offshore directed curve is visible in this situation.
7. The velocities are somewhat higher in the lower water level situation, but the differences between the locations of the velocities in the measurements and the model are still quite big.

4.1.3 SEDIMENT TRANSPORT

The transports calculated in the model should match the best estimates of the sediment transports found in other studies. The goal of this study is not to determine the exact transports, but showing what the differences will be when the groins resurface. The sediment transports must therefore be in the same order rather than to be equal. Sediment transport studies also have a big uncertainty, which is another reason to compare the data on the order of magnitude.

As is shown in *chapter 2.5.1 Sediment transports* in Figure 10 the sediment transport at 110 km from Den Helder lies between approximately 40.000 m^3/ year and 140.000 m^3/ year excluding pores, depending on the different studies. The

transport in the 1990 situation in the model gives a transport of around 115.000 m^3/year. This value represents the sediment transports from the studies well.

CONCLUSIONS

The model reproduces the observed flow patterns in the measurements near Scheveningen at most locations. The differences between the hydrodynamics are most likely to be caused by a difference in the bathymetry near the groins. The schematized straight coast is not realistic in the vicinity of groins. The overall picture is that the model does give a reasonable representation of the currents occurring near a groin, however the differences between the schematizations and reality and its effects must not be forgotten.

4.2 HYDRODYNAMICS TEST CASE

In this section the hydrodynamics in the test case are analyzed. The test case consists of several simulations in which the groin length varies in a bathymetry with a constant slope. In this way the effect of the length of the groins on the hydrodynamics is determined. First the alongshore velocities are analyzed, then the offshore directed velocities are investigated. For the test case simulations the conditions 01 (Hs = 0.7m, Tp = 5.9s, Dir = 314°), 06 (Hs = 1.9m, Tp = 7.6s, Dir = 340°) and 09 (Hs = 1.1m, Tp = 5.8s, Dir = 19°) are used.

4.2.1 ALONGSHORE CURRENTS

The maximum current velocities are an important indication for swimmer safety. Along the transects N=273 and N=330, the maximum wave induced current in alongshore direction in the upper layer of the model (K=1) is compared. These transects are in between two groins and over the groins, the definitions are given in Figure 42.

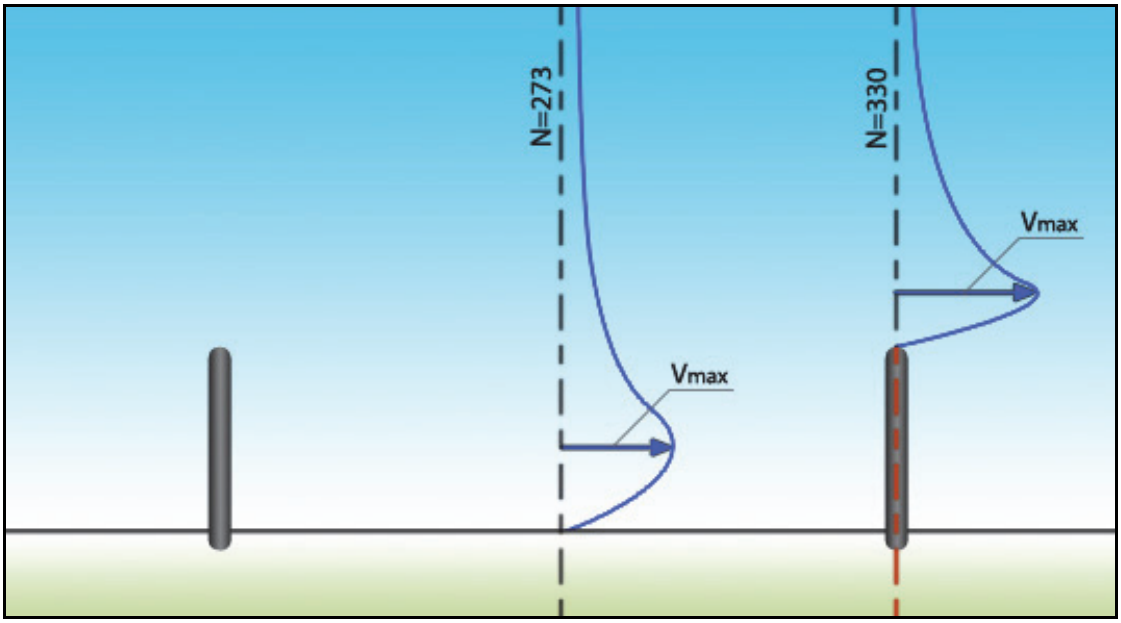

Figure 42 Definitions of the transects in between the groins (N=273) and over the groins (N=330)

The results are shown in Figure 44 for condition 01. In Figure 43 the dissipation due to breaking waves and the groins is shown to indicate the position of the surf zone with respect to the groin length. This is important to indicate where the longshore current is positioned and how far the groins extend into that current. The width of the surf zone during condition 01 is approximately 130 meter. During flood the surf zone is directed more onshore due to the high water level. The groins are then located in the centre of the surf zone, the water can flow over the groins. At low water the surf zone is located further offshore, the water must now flow around the groins.

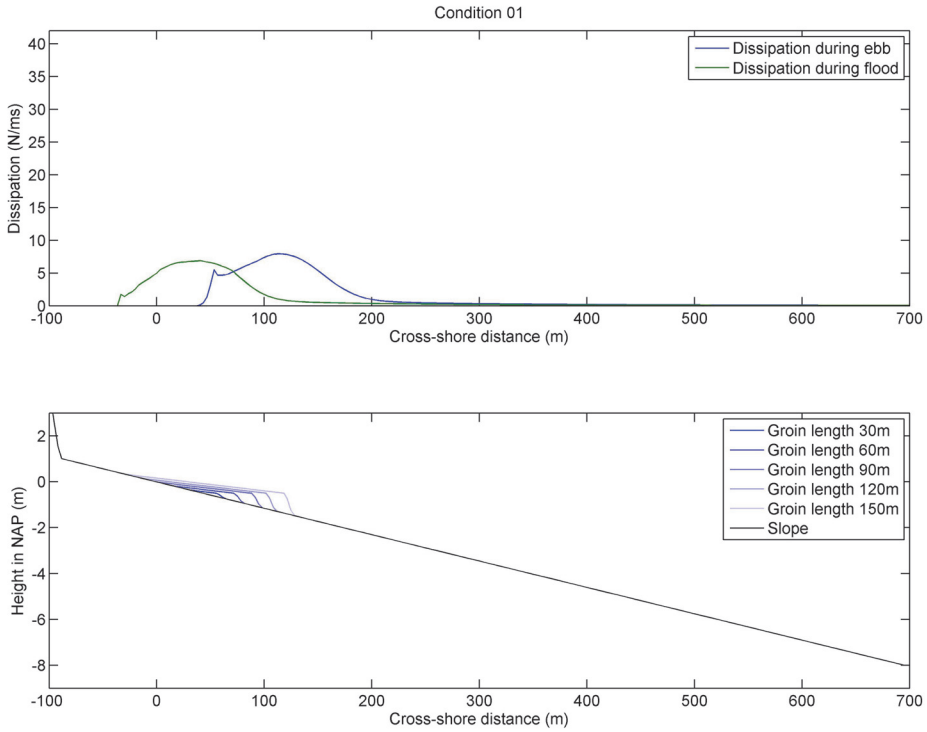

Figure 43 Location of dissipation of waves with respect to groin length, condition 01 (Hs = 0.7m, Tp = 5.9s, Dir = 314°)

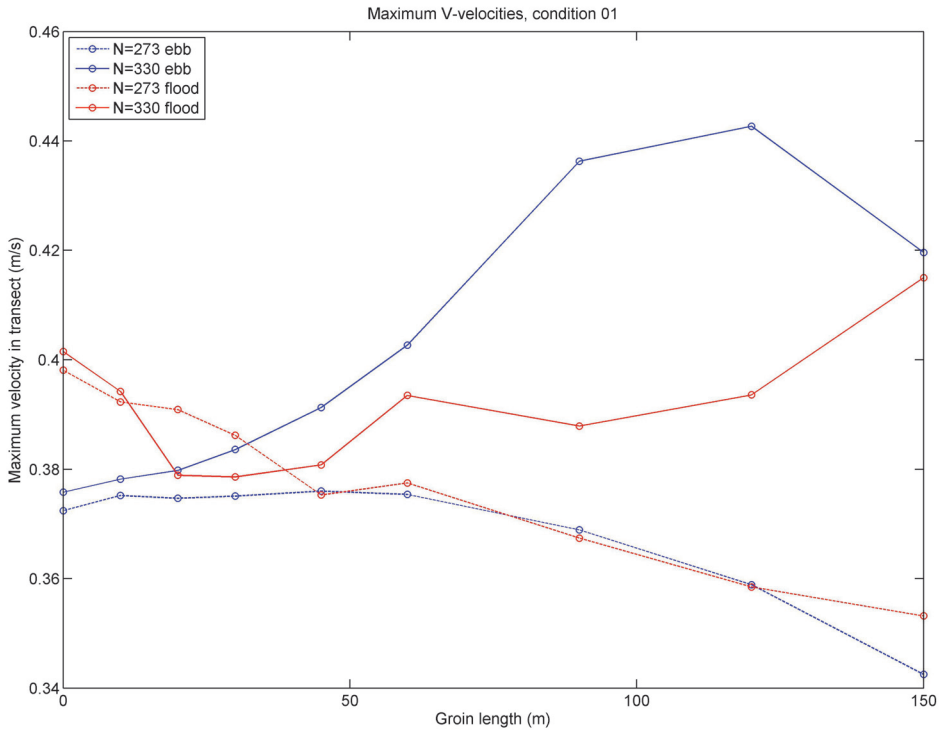

Figure 44 Maximum alongshore velocity along transects, condition 01 (Hs = 0.7m, Tp = 5.9s, Dir = 314°)

The solid lines in the graph represent the transects over the groins at N=330, the dotted lines represent the transects in between the groins at N=273. The blue and red lines respectively represent the velocities on these transects during ebb and flood tide. From the graph it can be seen that the maximum V-velocities along the transects at N=330 get higher

with increasing groin lengths. This can be explained by the contraction of the current due to the groin; the same amount of water has to flow through a smaller area when passing a groin. When looking at the maximum velocity in transect N=330 during ebb, it can be observed that, when the groins are larger than 90m, the maximum velocities decrease again. This is due to the ebb current which is opposite directed to the wave driven current; when the groin is long the flow is pushed offshore where the tidal current velocity is larger. When considering the same transect during flood the first thing that can be observed is that the maximum velocities are not as high as during ebb. This sounds contradictory; the tide is now in the same direction as the wave driven current but the maximum velocities are lower. At flood tide however, the water flows over the groin and the contraction is therefore less. Over the groin the current velocities may be higher, but these are left out of the analysis for the sake of consistency. The relatively fast increase of the velocity with groin lengths larger than 90 meters can again be explained by the tidal current which has now the same direction as the wave driven current.

The maximum alongshore velocity on the transect in between the groins does the opposite; the velocities decrease with increasing groin length. This indicates that the groins slow down the longshore current. The tidal current does not have much effect on this velocity because the maximum currents occur near the coast.

Figure 46 shows the maximum alongshore velocity graph for condition 06 (Hs = 1.9m, Tp = 7.6s, Dir = 340°). Condition 06 induces, just as condition 01, a longshore transport with the same direction as the flood current, the figure should therefore have the same characteristics. In condition 06 the difference in the maximum current velocity between flood and ebb is larger than in condition 01. This can be explained by the higher waves of condition 06, the waves break in deeper water as can be seen in Figure 45, the surf zone is now approximately 400 meters wide. The maximum velocity occurs therefore more offshore where the tidal currents are larger, which means a larger difference between the maxima.

During ebb the difference between the maximum current velocities over the transects is small. Due to the high waves the maximum velocity along the transect occurs further offshore and the groins do not have much effect on this current.

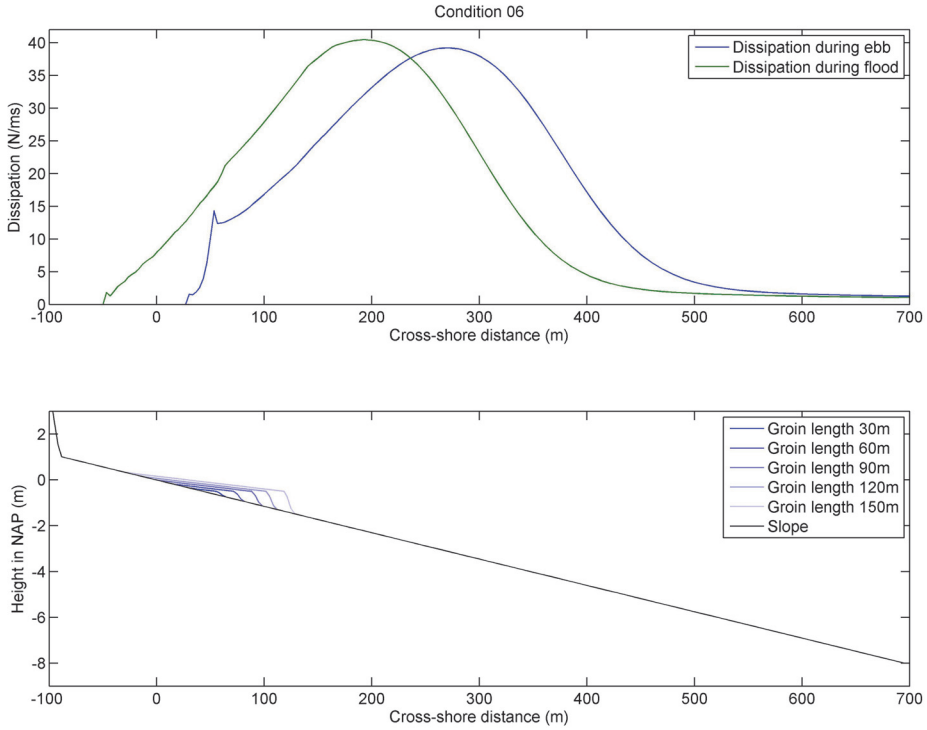

Figure 45 Location of dissipation of waves, condition 06 (Hs = 1.9m, Tp = 7.6s, Dir = 340°)

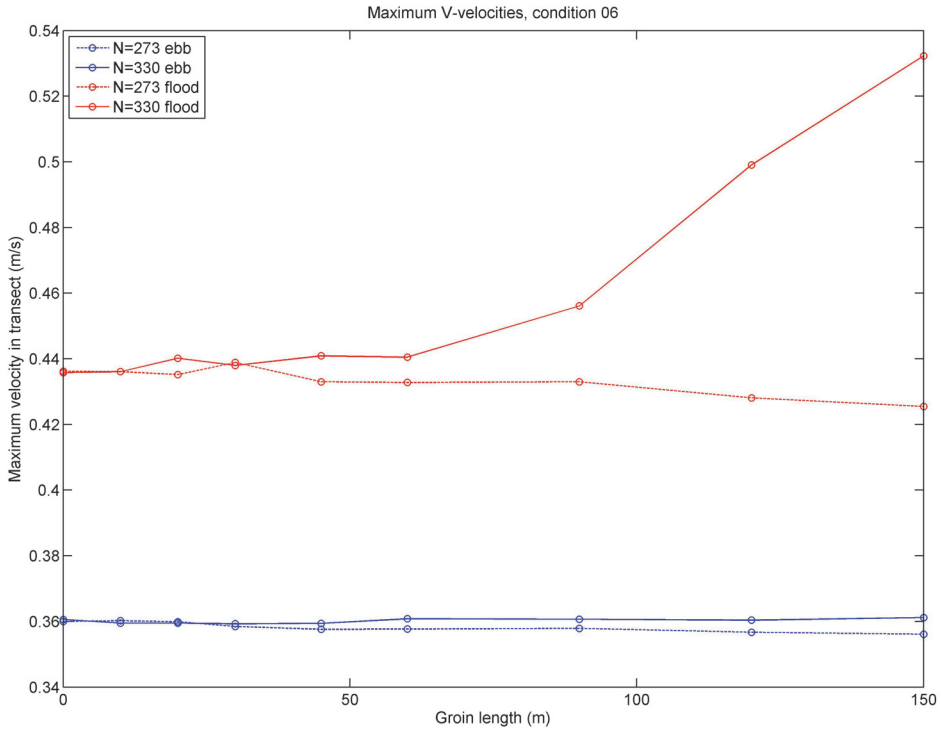

Figure 46 Maximum alongshore velocity along transects, condition 06 (Hs = 1.9m, Tp = 7.6s, Dir = 340°)

In Figure 48 the maximum current velocities during condition 09 (Hs = 1.1m, Tp = 5.8s, Dir = 19°) are shown, notice the higher maximum velocities during ebb due to the southerly directed wave induced current (notice that the vertical axis

is negative). The waves are higher than during condition 01, but the angle of incidence is smaller and therefore the current speeds are smaller. During flood the current speeds are so small that the scatter is relatively large. The surf zone is not as wide as during condition 06, approximately 250 meters wide as can be seen in Figure 47, therefore the maximum velocities during ebb are influenced by the length of the groins.

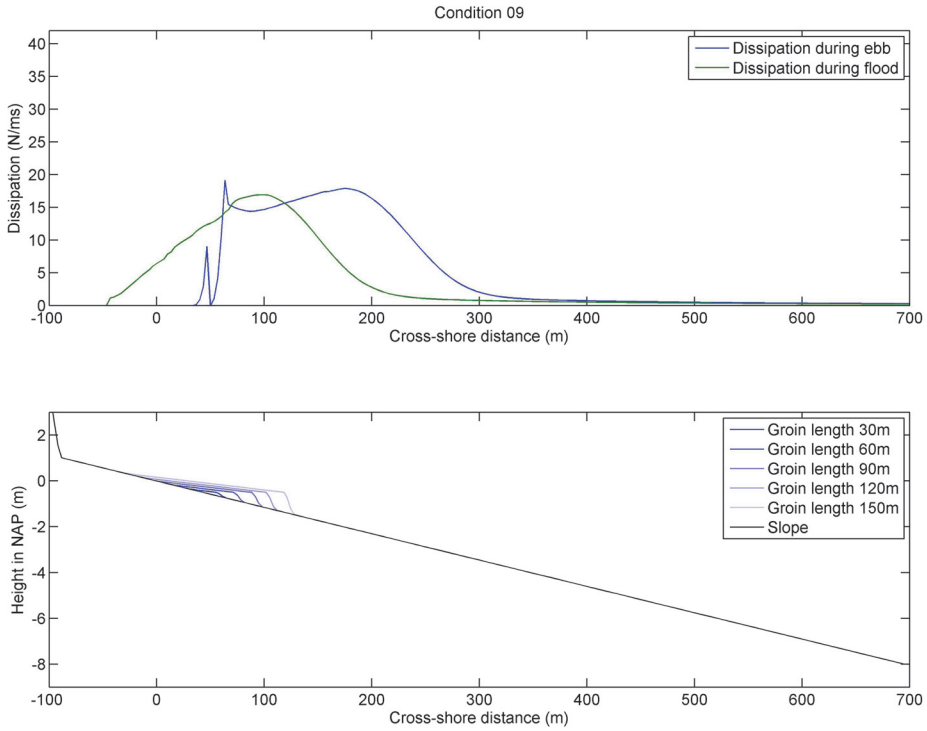

Figure 47 Location of dissipation of waves, condition 09 (Hs = 1.1m, Tp = 5.8s, Dir = 19°)

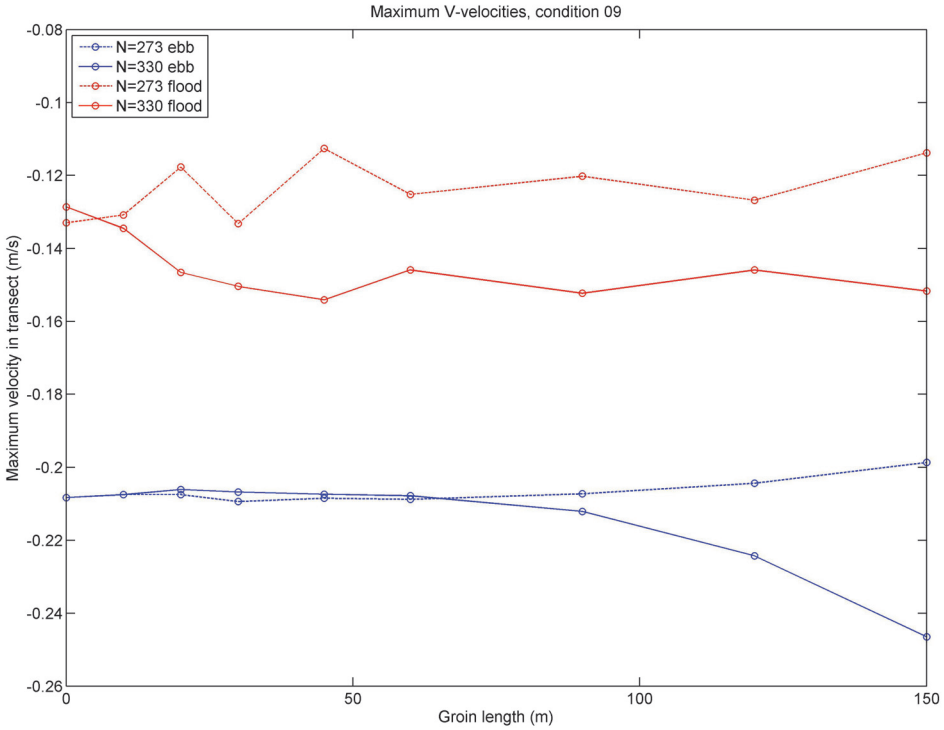

Figure 48 Maximum alongshore velocity along transects, condition 09 (Hs = 1.1m, Tp = 5.8s, Dir = 19°)

The differences between the maximum current velocities are thus dependent on the wave conditions and the phase of the tide. The increase in maximum alongshore current velocity through transect the transect over the groins (N=330) with groins of 150 meter compared to the situation without groins, is during all three conditions around 15% to 20% when the tidal current has the same direction as the longshore current. The width of the surf zone and the location of the strongest current in the surf zone are important parameters for the increase in maximum velocity. The velocities begin to increase significantly when the groin lengths are larger than 60 meters. The maximum velocities do not increase much when groins are shorter than 60 meter.

4.2.2 OFFSHORE DIRECTED CURRENTS

Offshore directed currents are the most dangerous considering swimmer safety. In Figure 49 the maximum offshore directed currents over a whole tidal cycle are shown in the test case simulation with groins of 60 meter during condition 01 (Hs = 0.7m, Tp = 5.9s, Dir = 314°). These offshore directed currents are most severe during ebb when the current has to flow around the groin. Offshore currents in the order of 0.15 m/s can be found in front of the groins. On the lee side no offshore current is found. In the upper layer the offshore velocities are lower.

In Figure 50 the groins are 150 meter. The offshore directed current is larger, in the order of 0.3 m/s, and on the lee side of the groin the current is now much more pronounced and reaches current velocities in the same order of magnitude. The current in the lee side does not extend beyond the groin because the current is part of an eddy that is triggered by the high alongshore current velocities at the tip of the groin during low water. If the current would extend be-

yond the surf zone the mechanism that produces the eddy would disappear and therefore the current would disappear, therefore this does not happen.

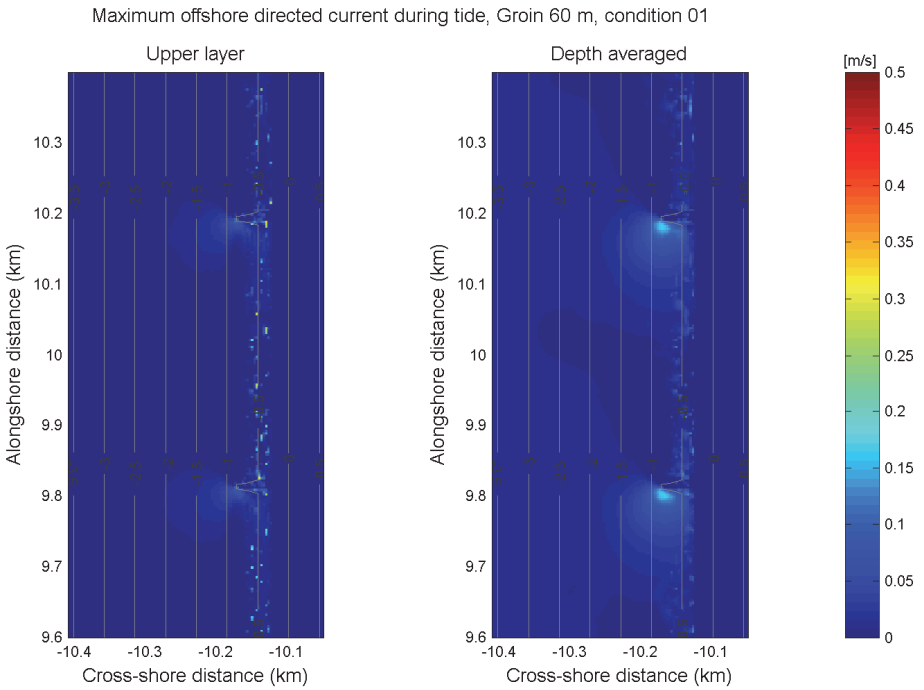

Figure 49 Maximum offshore directed current with groins of 60 meter, condition 01 (Hs = 0.7m, Tp = 5.9s, Dir = 314°)

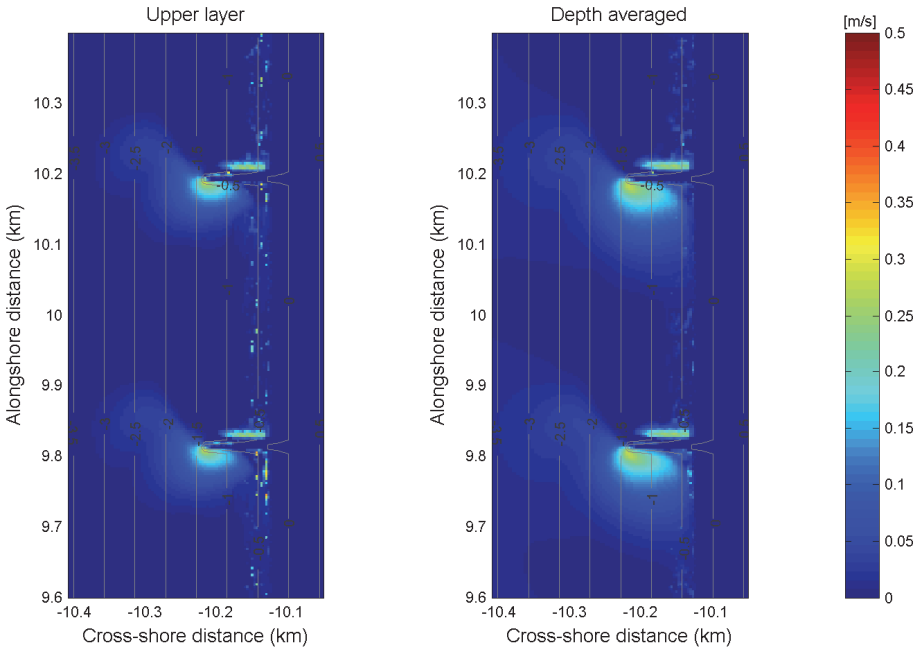

Figure 50 Maximum offshore current speeds with groins of 150 meter, condition 01 (Hs = 0.7m, Tp = 5.9s, Dir = 314°)

CONCLUSIONS TEST CASE

The following conclusions can be drawn from the above:

- In an alongshore uniform profile with a constant slope, the maximum alongshore velocities due to the groins begin to change significantly at a groin length of approximately 60 meters.
- The maximum current speeds due to the groin in this situation are 15 to 20 % higher with a groin of 150 meter, compared to the situation without groin.
- The tide influences the maximum current speeds when the groin reaches far enough offshore. In this case the maximum current speeds are affected when the groin has a length of approximately 90 meter.
- The offshore directed currents increase with increasing groin length and the offshore directed current on the lee side of the groin does not extend beyond the surf zone.

4.3 HYDRODYNAMICS

The hydrodynamics of the three schematized situations derived from the 1990, 2009 and 2010 bathymetry are analyzed in this section. First an overview of the current patterns is given, then the alongshore and the offshore directed currents are looked at. The results from the test case are used to analyze the hydrodynamics. Conditions 01 (Hs = 0.7m, Tp = 5.9s, Dir = 314°), 06 (Hs = 1.9m, Tp = 7.6s, Dir = 340°) and 09 (Hs = 1.1m, Tp = 5.8s, Dir = 19°) are used. For the current patterns the condition 06 is changed for condition 07 (Hs = 1.5m, Tp = 0.7s, Dir = 9°) because in this condition the waves are perpendicular to the coast.

4.3.1 CURRENT PATTERNS

The currents around the groins in the different situations are dependent on the water level and the tidal currents. To give an indication of how the currents behave in a tidal cycle, the current patterns and velocities are shown when the maximum ebb-current and the maximum flood-current are present, for all three situations. A distinction is made between the currents in the upper layer and depth averaged currents because the upper layer is more important for swimmer safety. Only condition 01 is shown (Figure 51 to Figure 56). In *Appendix H - Dissipation in profiles* the dissipation due to breaking waves is shown to indicate the location of the surf zone. The wave patterns and offshore currents for condition 07 and 09 can be found in *Appendix J - Current patterns*.

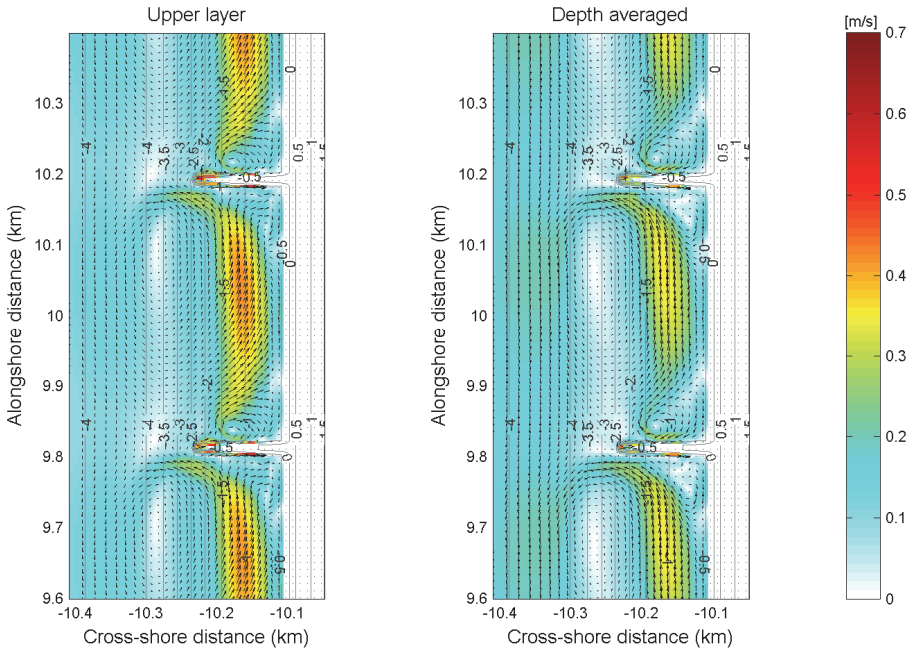

Figure 51 Depth averaged current velocity and direction during maximum ebb-current, 1990 condition 01 (Hs = 0.7m, Tp = 5.9s, Dir = 314°)

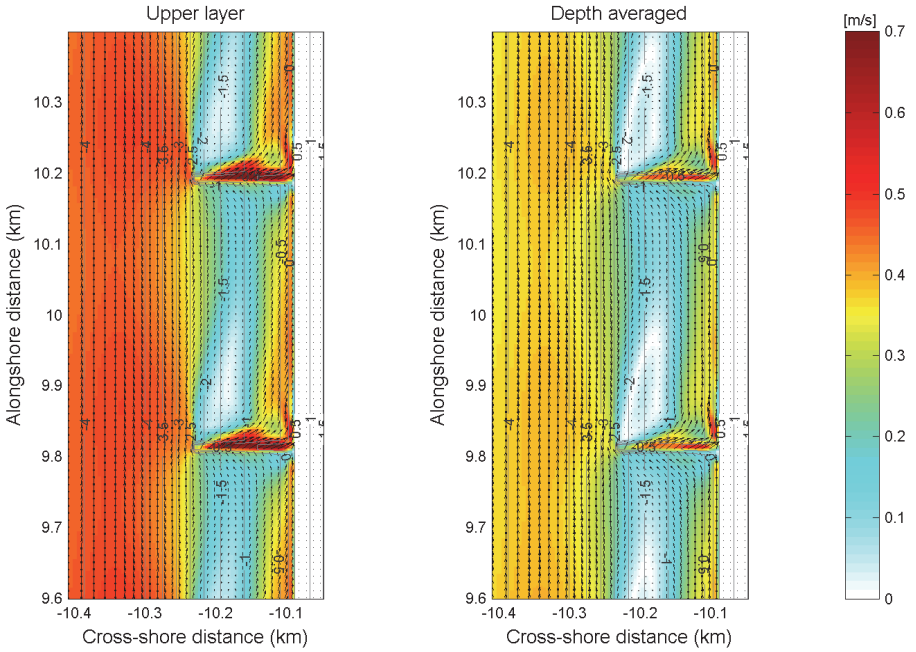

Figure 52 Depth averaged current velocity and direction during maximum flood-current, 1990 condition 01 (Hs = 0.7m, Tp = 5.9s, Dir = 314°)

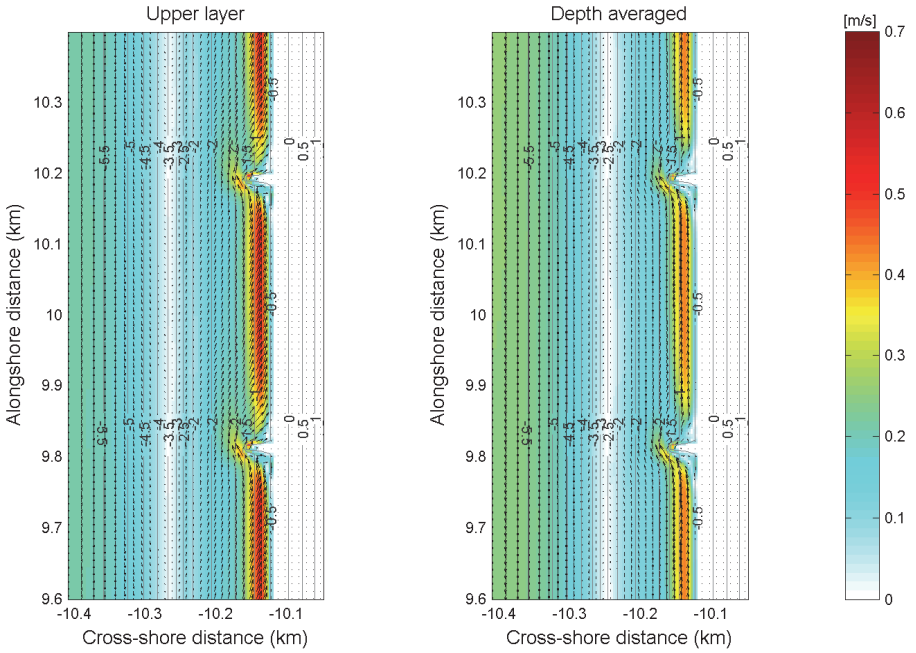

Figure 53 Depth averaged current velocity and direction during maximum ebb-current, 2009 condition 01 (Hs = 0.7m, Tp = 5.9s, Dir = 314°)

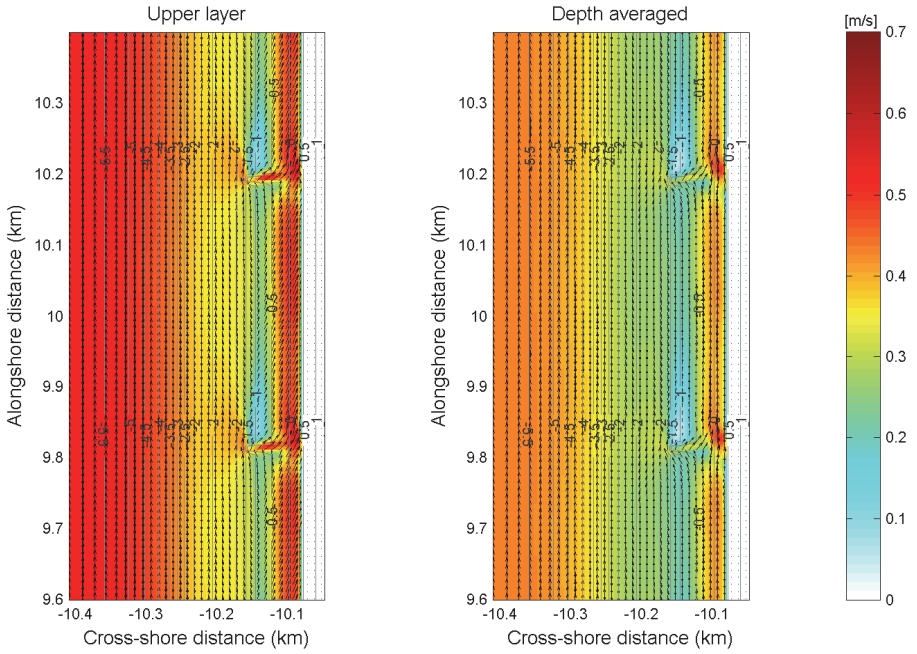

Figure 54 Depth averaged current velocity and direction during maximum flood-current, 2009 condition 01 (Hs = 0.7m, Tp = 5.9s, Dir = 314°)

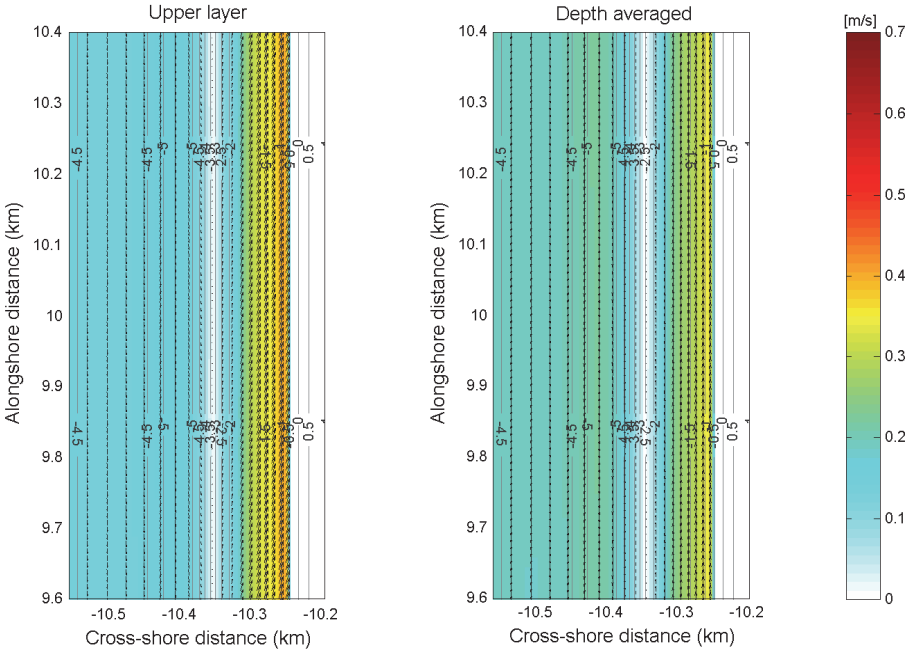

Figure 55 Depth averaged current velocity and direction during maximum ebb-current, 2010 condition 01 (Hs = 0.7m, Tp = 5.9s, Dir = 314°)

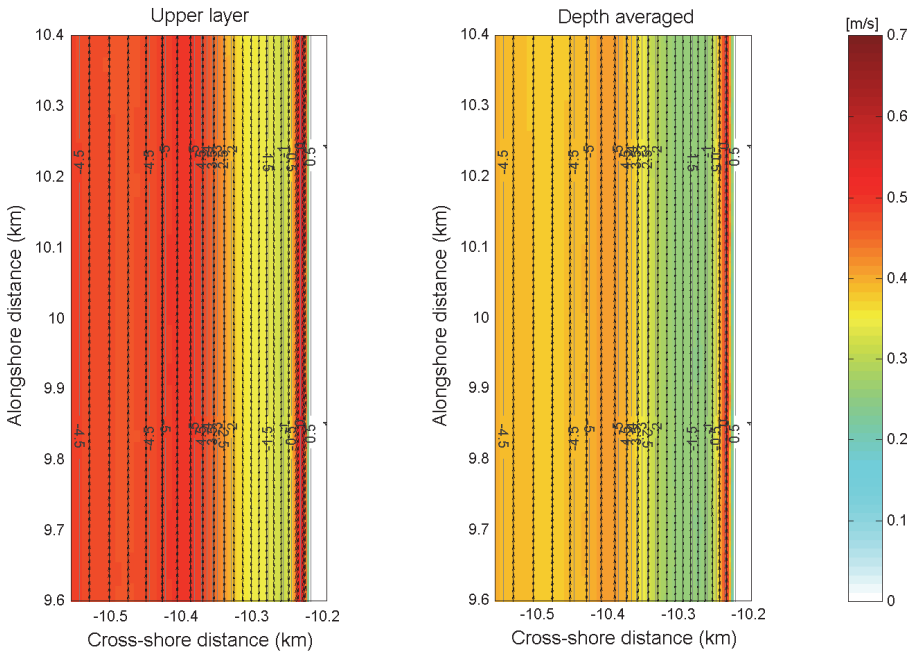

Figure 56 Depth averaged current velocity and direction during maximum flood-current, 2010 condition 01 (Hs = 0.7m, Tp = 5.9s, Dir = 314°)

Figure 51 to Figure 56 show that the long groins in the 1990 situation affect the longshore current the most. During low tide, a strong offshore directed current is present which reaches the ebb-current and gets deflected in the opposite direction. A relatively strong eddy is present behind the groin. At high tide, the water can flow over the groin. This reduces the offshore directed current velocity and prevents the eddy on the lee side of the groin from forming. In the 2009 situation, the offshore directed current is smaller and the groin is too small for a proper eddy to occur. During flood the water flows over the groin and both effects are even smaller. In the 2010 situation, the currents are not interfered by coastal structures and can propagate freely along the coast.

4.3.2 ALONGSHORE CURRENTS

The graphs in which the maximum velocity is related to the groin length are made for the three cases. For condition 01 (Hs = 0.7m, Tp = 5.9s, Dir = 314°) this is showed in Figure 57. Notice that on the x-axis the groin lengths of the situations are given and not the year in which the profile is determined.

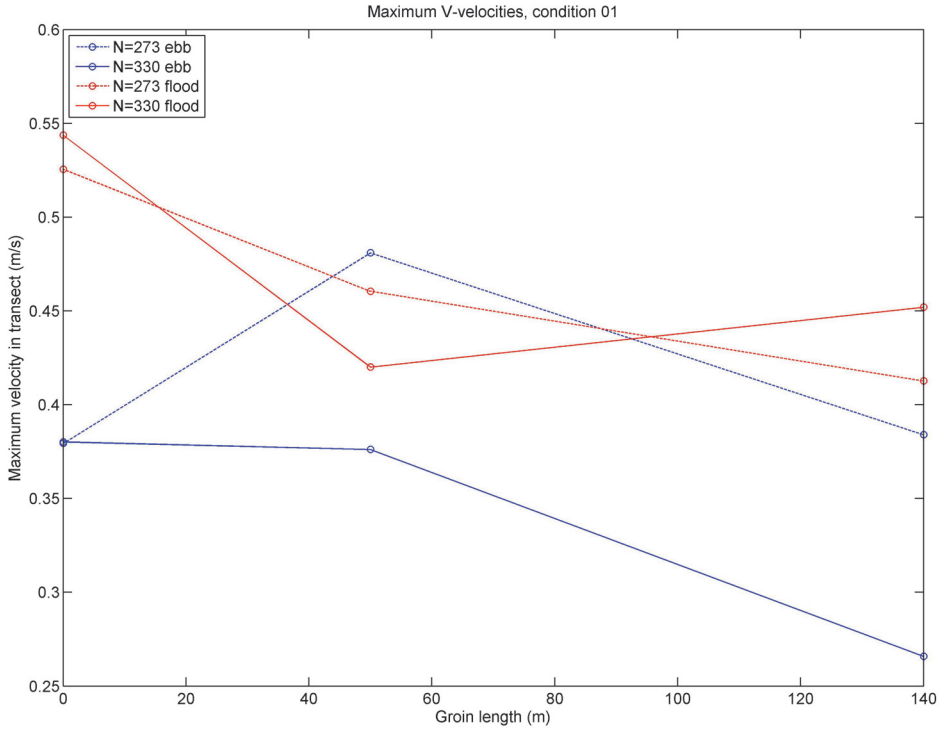

Figure 57 Maximum alongshore velocity along transects, condition 01 (Hs = 0.7m, Tp = 5.9s, Dir = 314°)

The findings on the changing maximum velocity in the test case are not recognized in the schematized situations. In transect N=330 along the groin the maximum current velocity does not increase, it is even decreasing both during maximum ebb and maximum flood tide. Since the maximum current speeds are affected differently with the groin length as shown in the test case, this significant difference must be caused by the bathymetry. The same results are found for conditions 06 and 09, shown in *Appendix F - Maximum alongshore velocities condition 06 and 09*. In Figure 58 the profiles are shown to give an explanation for the differences due to the bathymetry.

The 2010 profile, which is shown as 0 meter groin length in the graph, is relatively steep compared to the other two and the outer bar is somewhat lower. The waves will therefore break more onshore and cause a high current velocity peak in the cross-shore velocity distribution. This is the reason for the high maximum current velocity in the 2010 profile.

In the 2009 profile a bar is positioned just in front of the groin, which causes higher current velocities in front of the groin. After the bar the profile is quite steep regarding the profile of 1990. This causes just as in the 2010 profile a short dissipation period which induces higher current velocities further onshore.

In the 1990 profile the early foreshore is shallow and gentle; waves will break over a longer distance, causing low maximum velocities in between the groins. On the tip of the groins the velocity will be partly dependent on the water depth. The depth at the tip of the groin is larger in the 1990 profile than in the 2009 profile, which causes lower current velocities in the 1990 profile.

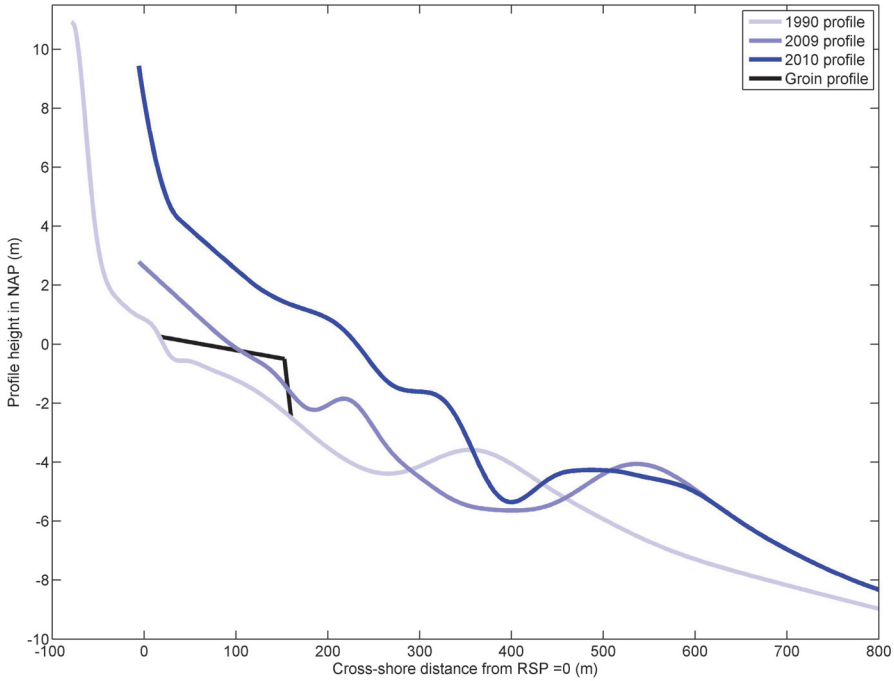

Figure 58 Model profiles

4.3.3 OFFSHORE DIRECTED CURRENTS

To give an indication of the swimmer safety in the schematized situations, the maximum offshore current velocity over a tidal cycle is shown in Figure 59 and Figure 60. These offshore directed currents are the most severe during low water when the water has to flow around the groin, this can be seen in *Appendix J - Current patterns* and in Figure 51 to Figure 56 for condition 01 (Hs = 0.7m, Tp = 5.9s, Dir = 314°). The 2010 situation is left out of this analysis because the coast is straight and the offshore currents are small.

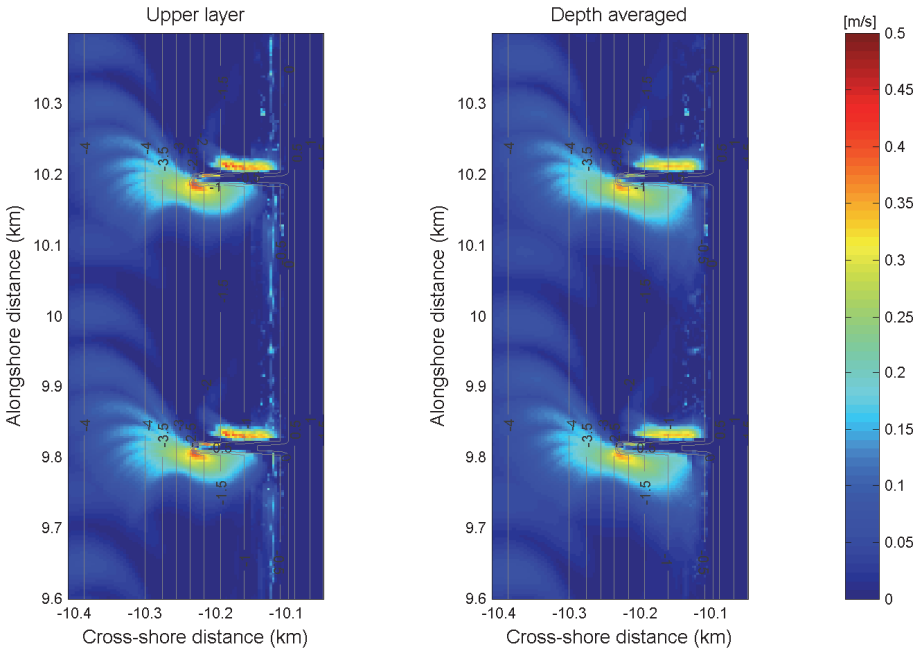

Figure 59 Maximum offshore directed current over a tidal cycle, 1990 condition 01 (Hs = 0.7m, Tp = 5.9s, Dir = 314°)

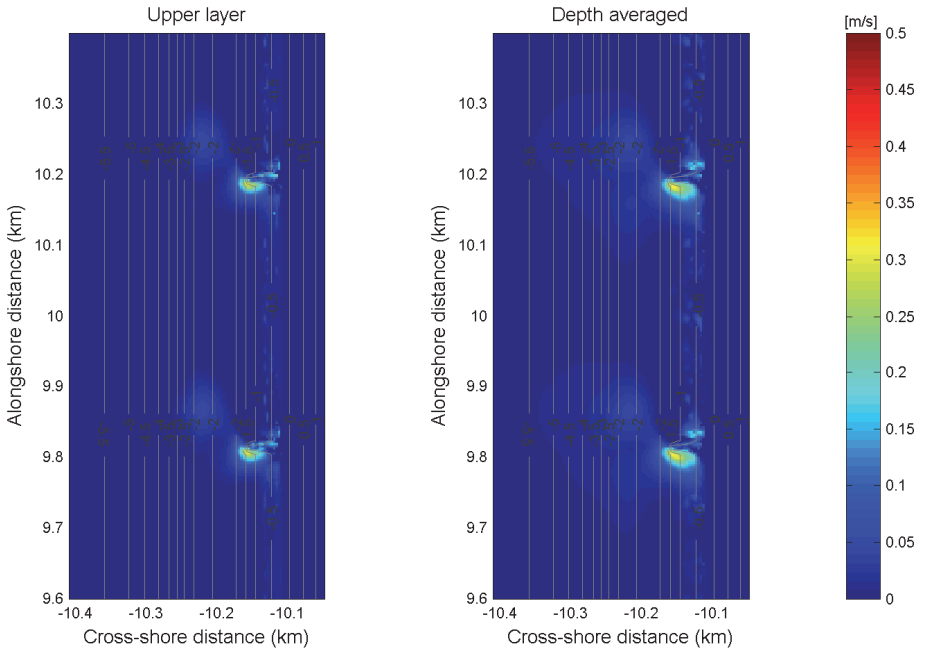

Figure 60 Maximum offshore directed current over a tidal cycle, 2009 condition 01 (Hs = 0.7m, Tp = 5.9s, Dir = 314°)

As can be seen, the differences between the situations are large. A concentrated offshore directed rip current is clearly recognizable in the 1990 situation. Notice that the 'steps' in the flow are due to the data saving interval of 20 minutes, and is not physical. In the test case the offshore directed flow was much less powerful. The maximum current speeds are in the order of 0.4 m/s. The groins are approximately the same length, the bathymetry must therefore play a role in the occurrence of this rip current. In this study it is not further investigated why and when such a strong concentrated rip current occurs, but because it can be the cause of severe erosion (offshore transport) and dangerous situations it is recommended that this effect is further analyzed. Also a concentrated flow directly behind the groin is visible with current speeds of around 0.3 m/s. The offshore directed current does, just as in the test case, not extend beyond the tip of the groin.

In the 2009 situation the offshore directed current south of the groin is present, although much smaller in size and velocity. Due to the small length, the formation of an eddy that feeds the rip current near the groin is not possible. In front of the groin, a minor offshore current can be observed.

In the 2010 profile no high offshore currents are presents because the current can flow uninterruptedly along the coast. It must again be noticed that the profile might not be realistic in the vicinity of a groin. The current speeds and profiles might therefore be somewhat different, it is believed however that the overall view does give a good representation of the occurring processes and current speeds.

CONCLUSIONS

The following conclusions can be drawn from the above:

- The bathymetry plays a major role in maximum alongshore and offshore current speeds near the coast and near groins.

- The magnitude of the offshore directed currents is dependent on the groin length, and increases significantly with longer groins.
- The eddy on the lee side of the groin can induce strong rip currents that do not extend beyond the tip of the groin. The length of the groin plays a major role in the occurrence and the velocity of the eddy.

4.4 SEDIMENT TRANSPORT TEST CASE

The sediment transports are scaled with the test case. First the alongshore sediment transport is elaborated upon, then the offshore transports are analyzed. Conditions 01 (Hs = 0.7m, Tp = 5.9s, Dir = 314°), 06 (Hs = 1.9m, Tp = 7.6s, Dir = 340°) and 09 (Hs = 1.1m, Tp = 5.8s, Dir = 19°) are used.

4.4.1 ALONGSHORE SEDIMENT TRANSPORT

In Figure 61 the sediment transports are shown related to the groin length. This is done for three conditions and in the two transects N=273 and N=330, in between the groins and over the groins respectively. The sediment transports show a more or less constant decrease with the lengthening of the groins. The factor of the total sediment transport that is blocked by the groin is dependent on the wave conditions; during condition 06 the percentage of the sediment that is blocked is substantially lower than during the other two conditions. The significant wave height is large during condition 06, the waves will break early and the surf zone will be wide; the sediment transport concentration will be positioned more offshore. In Figure 45 in *chapter 4.2.1 Alongshore currents* the surf zone is indicated with respect to the groins. The groins thus have much less effect on the total transport.

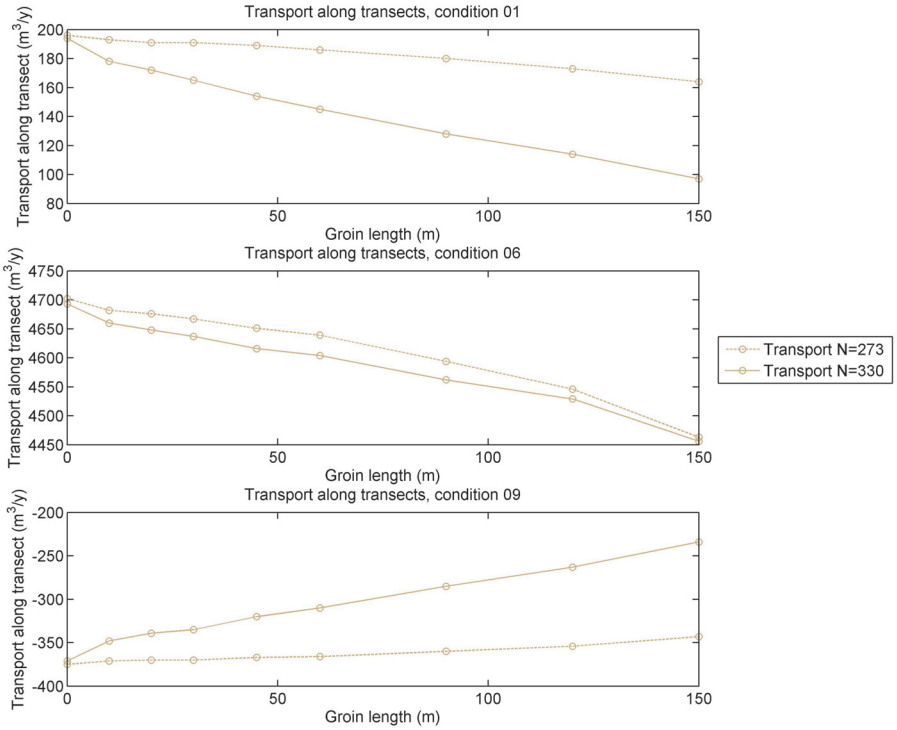

Figure 61 Sediment transports related to groin length during the different conditions 01, 06 and 09

It can be observed that the transports in transect N=330 over the groins, and in transect N=273 in between are different. This is the effect of the alongshore uniform profile which is not in equilibrium near the groins. The difference in transports causes a morphological change of the profile, which changes the transports again. In Figure 62 the sediment transport distribution between two groins is given. The groins stop a part of the longshore sediment transport, but in between the groins the transport is much higher. Due to the large transport gradients the profile will adapt in time and get a more constant longshore transport. The magnitude of the final sediment transport is hard to estimate. The transport in between the groins will lower due to the adaptation of the shoreline; the profile will curve in between the groins as shown in Figure 6 in *chapter 2.3.5 Morphodynamics around a groin*. The transports over the groin will increase due to this adaptation; the effective length of the groins will decrease. The formation of scour gullies where the current velocities are high can also induce a higher transport along the groins. It is hard to give a quantitative description of what will happen to the transports in a groin field. It is expected that the sediment transport will be in between the transports through transect N=273 and N=330. To find out what will happen to the sediment transport the effect of the groins on the transport distribution is analyzed.

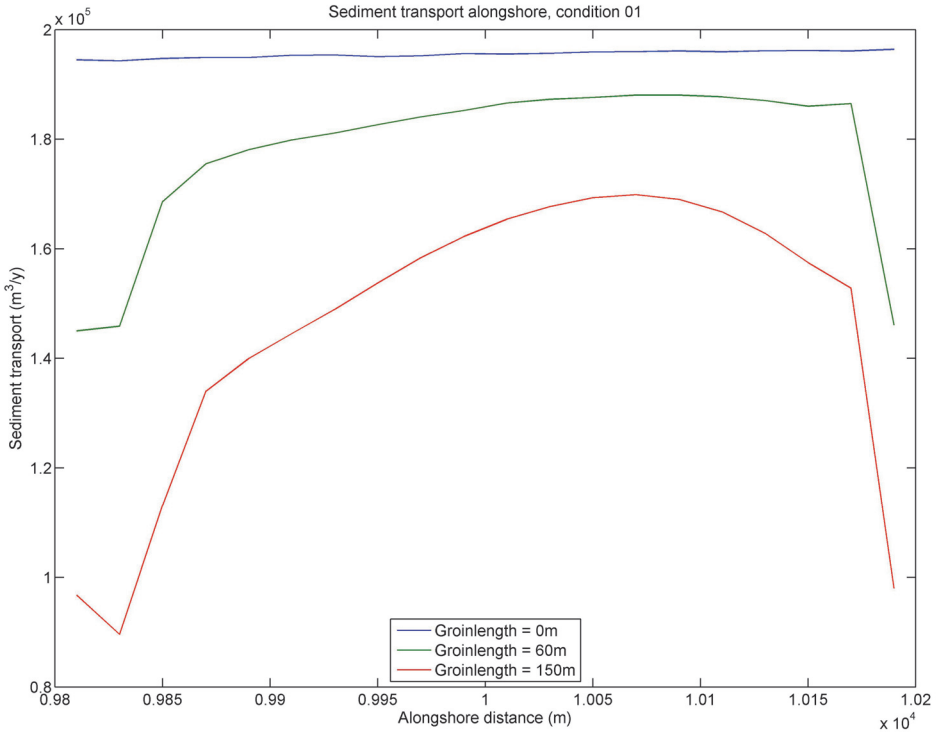

Figure 62 Sediment transport distribution between two groins, condition 01 (Hs = 0.7m, Tp = 5.9s, Dir = 314°)

The sudden drop in sediment transport in front of the groin indicates that the groin catches a lot of sediment. The cross-shore sediment transport distribution during flood in Figure 63 shows that the groin stops most of the transport over it, even a very small groin stops a large part of the sediment transport. With long groins a small transport peak at the tip of the groin can be seen; the sediment concentration flow is pushed out a bit. The sediment transport distribution in between the groins at N=273 does get smaller but the location does not change.

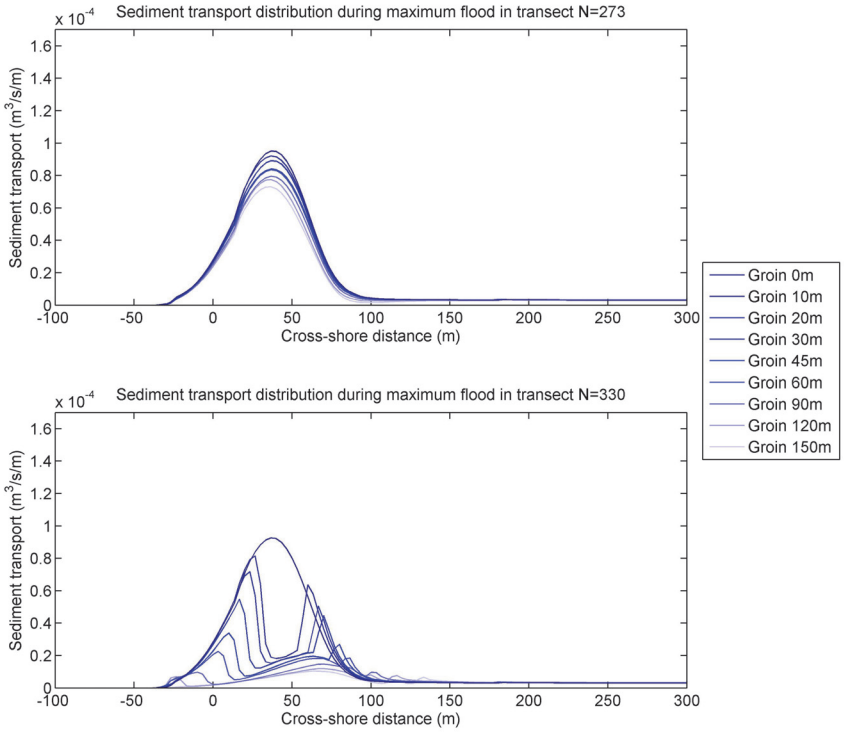

Figure 63 Cross-shore sediment transport distribution during flood

The mean transport at the tip of the groin increases with increasing groin length, but the sediment transport distribution is not pushed seawards, Figure 64.

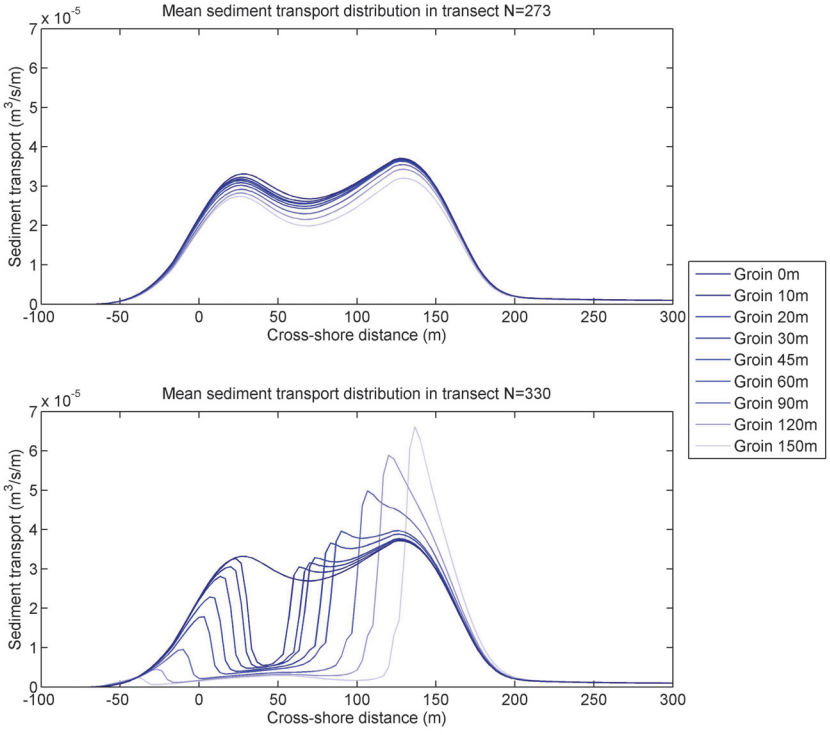

Figure 64 Mean cross-shore sediment transport distribution

The capturing of most of the sediment that is transported over the groin by even the small groins is not realistic, the bathymetry will adapt fast and therefore the transports will increase. The average value of the transports in the groin field will therefore tend to be closer to the transport over the transect in between the groins, N=273.

4.4.2 OFFSHORE SEDIMENT TRANSPORT

To test the effect of groins on the offshore transport the test case is used. To determine the effect of the groins on this transport the effect of the offshore transport due to the wave conditions must be determined first. The offshore transport is determined in the cross-section in between the tips of two groins, and therefore the offshore location of the cross-section changes with the length of the groin. In Figure 65 the offshore transport due to the groin, due to the waves and the total offshore transport is shown. The transport due to the groin is determined by taking the total offshore transport through the cross-section, and subtract the offshore transport through this cross-section in the situation without groins. In this way the offshore transport due to the groins remains. This method can induce an error because the groins affect the waves and therefore the transport due to the waves only, determined without groins, is an estimation.

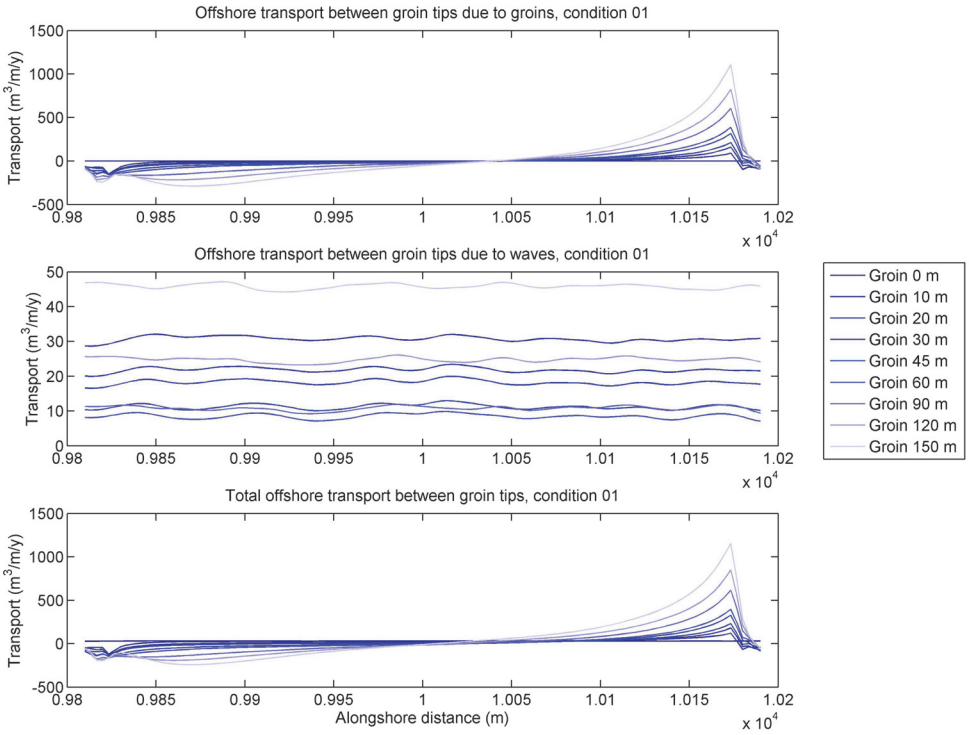

Figure 65 Offshore transport due to groins, due to waves and total

It is clear that the groins change the offshore transport at certain locations. The transport just in front of the groin, seen from the longshore current direction, is directed offshore. In the transport due to the groins in Figure 65 can be seen that the majority of this transport returns over a larger area behind the groin.

The net onshore and offshore transport due to the groins is given in *Table 4*. For the conditions 06 and 09 the transport graphs are given in *Appendix G - Test case offshore transport condition 06 and 09*. The values for the onshore transport due to the groins can be larger than the total onshore transport, because the waves induce an offshore directed transport which is included in the total transport.

	Onshore transport through cross-section (10^3 m^3/year)	Offshore transport through cross-section (10^3 m^3/year)	Total offshore transport through cross-section (10^3 m^3/year)
Condition 01 total	27	49	22
Condition 01 due to groins	37	42	5
Condition 06 total	48	834	786
Condition 06 due to groins	262	220	-42
Condition 09 total	30	390	360
Condition 09 due to groins	95	117	22

Table 4 Offshore transport

As can be seen in the table the groins do not account for a large part of the offshore transport and in the case of condition 06 the groins even induce an onshore directed transport. It is thought that this onshore transport is an effect of the assumption that the transport due to the groins can be assumed by taking the total offshore transport minus the transport when the groins are absent. The groins also affect the waves and therefore this assumption might induce errors, the error is relatively small compared to the total offshore and onshore transports.

CONCLUSIONS TEST CASE

The following conclusions can be drawn from the above:

- The sediment transport decreases quite constantly with increasing groin length up to 150 meter.
- An alongshore uniform profile around a groin is not realistic and will change due to longshore sediment transport gradients.
- In the alongshore uniform profile with a constant slope, the groin catches the majority of the sediment from the cross-shore sediment transport distribution at the same cross-shore distance as the groin.
- The offshore directed sediment transport due to groins is relatively small.

4.5 SEDIMENT TRANSPORT

For the three schematized situations, the total transports over a year are calculated with the weighted wave conditions. To make the comparison with the test case conditions 01 (Hs = 0.7m, Tp = 5.9s, Dir = 314°), 06 (Hs = 1.9m, Tp = 7.6s, Dir

= 340°) and 09 (Hs = 1.1m, Tp = 5.8s, Dir = 19°) are used. Condition 06 is chosen here because of the high significant wave height and because condition 07 is not very interesting for longshore sediment transport since the waves are almost perpendicular to the coast.

4.5.1 ALONGSHORE SEDIMENT TRANSPORT

The sediment transports for the three different situations are shown in Figure 66 to Figure 68, notice this are the yearly averaged transports excluding pores, all the 10 conditions are taken into account with the appropriate weight factors. The sediment transports in the figures are given in 10^3 m^3/year.

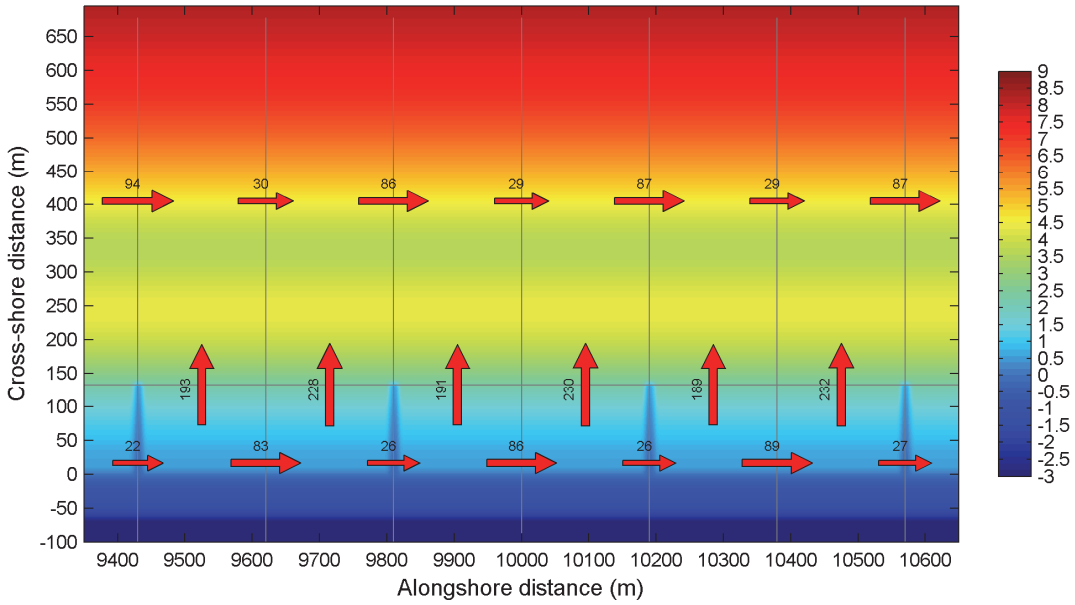

Figure 66 Sediment transport through cross sections 1990 (10^3 m^3/year)

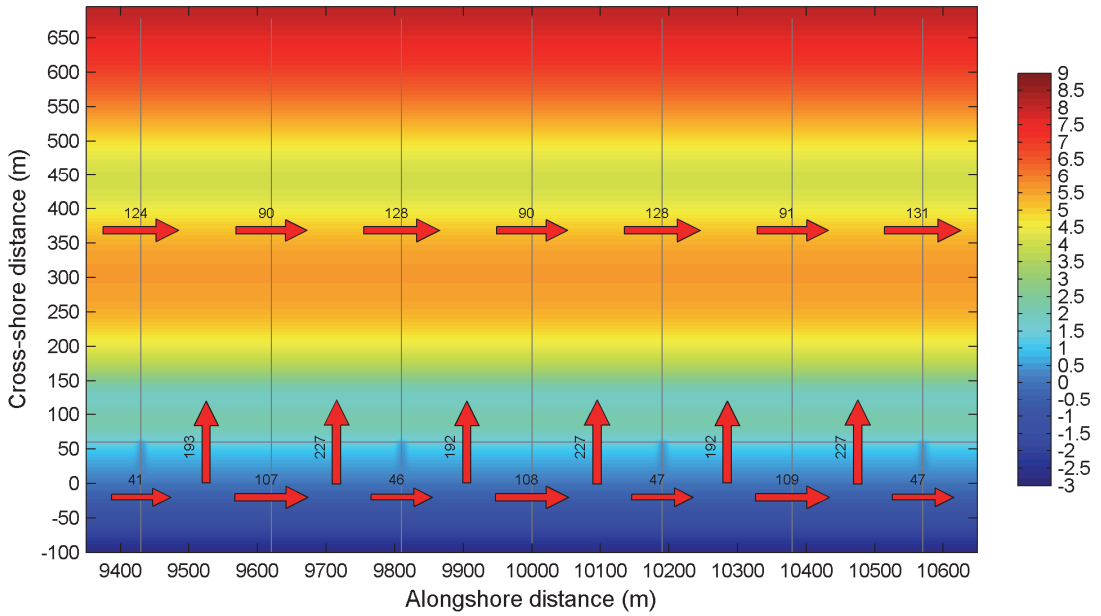

Figure 67 Sediment transport through cross sections 2009 (10^3 m^3/year)

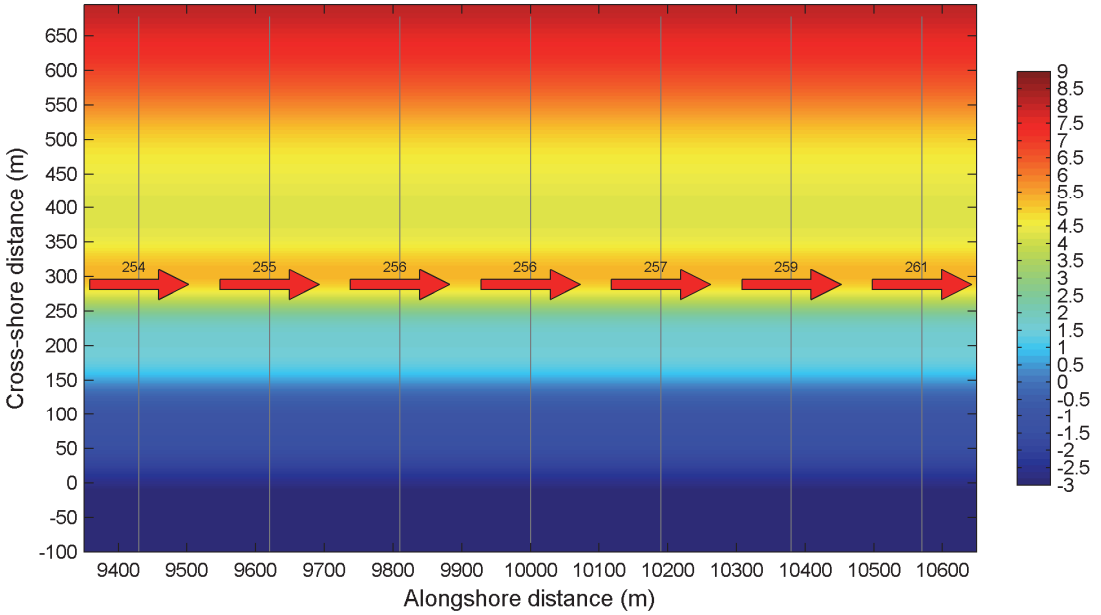

Figure 68 Sediment transport through cross sections 2010 (10^3 m^3/year)

In Table 5 below, the longshore sediment transports are given through the transects in between the groins at N=273, and over the groins at N=330.

Model run	Transport cross-section	On groins N=330 (10^3 m^3/year)	In between groins N=273 (10^3 m^3/year)
1990	Tip groin - 8 meter depth line	86	29
	Beach - Tip groin	26	86
	Beach - 8 meter depth line	**112**	**115**
2009	Tip groin - 8 meter depth line	128	90
	Beach - Tip groin	46	108
	Beach - 8 meter depth line	**174**	**198**
2010	**Beach - 8 meter depth line**	**256**	**256**

Table 5 Sediment transports through cross-sections

The sediment transports in the model run of 1990 are around 115.000 m^3/y between the +3 meter and the -8 meter depth line as can be seen in Table 5. In the 2009 model the transports through the cross-sections over the groin show a smaller transport than the transports through the cross-section in between the groins. This indicates that the profile is not in equilibrium as is explained before. The transports will tend to be closer to $198 \cdot 10^3$ m^3/year as explained in *chapter 4.4.1 Alongshore sediment transport*.

The transports through the cross-sections in the 2010 model are more or less equal, which is logical because nothing disturbs the current along the coast. The difference between no groins in 2010 and the long groins in 1990 is in the order of 50% less. This decrease does affect the nourishment demand for the Delfland coast, which depends on the alongshore sediment transport gradient. From Figure 10 in *chapter 2.5.1 Sediment transports* it can be seen that the sediment transport increases along the Delfland coast, this implies that the coast is erosive. If the transport increases over the years the coast will erode more, because the sediment transport gradient becomes steeper. Due to the resurfacing of groins the sediment transport along the coast will decrease, which implies less erosion than when groins are absent.

In Figure 69, Figure 70 and Figure 71 the transports in the three schematized cases are given for one condition compared to the test case results. In *Appendix H - Dissipation in profiles* the dissipation due to the waves is shown to indicate the location of the surf zone.

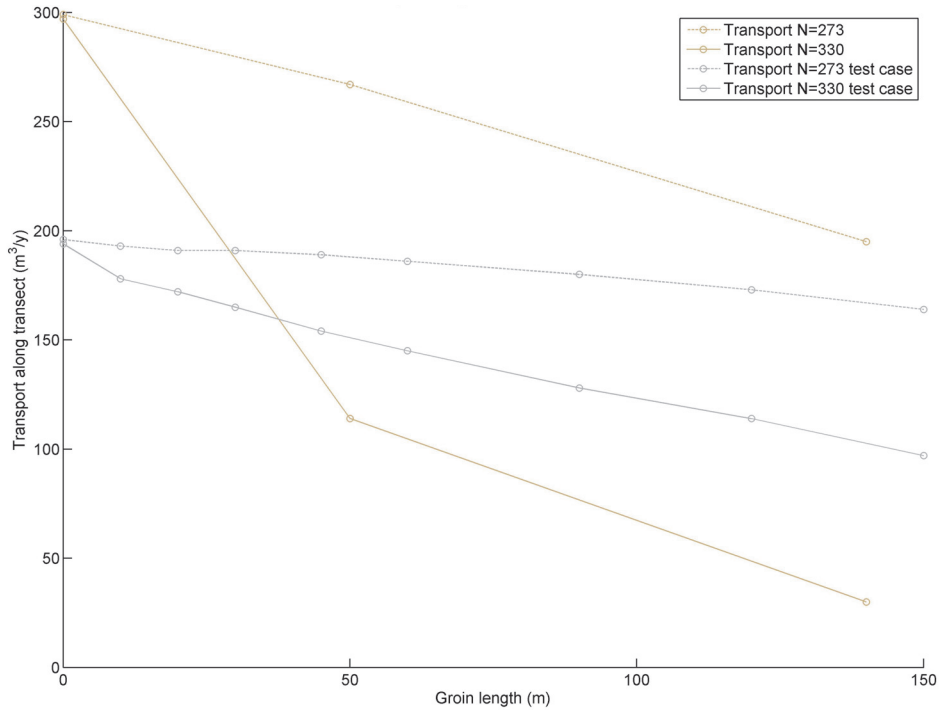

Figure 69 Transport along transects, condition 01 (Hs = 0.7m, Tp = 5.9s, Dir = 314°)

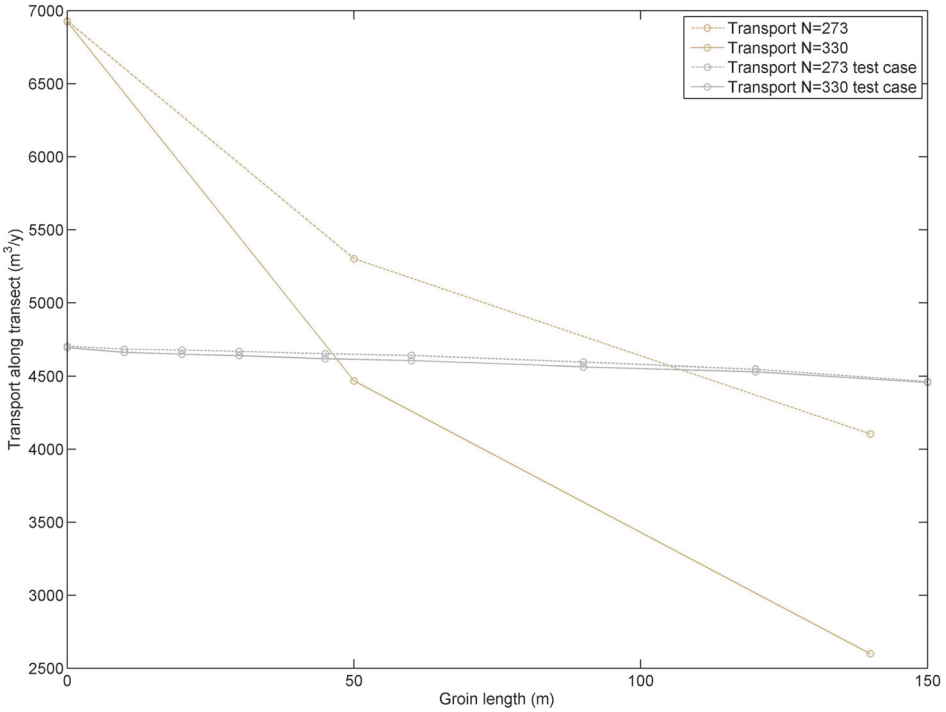

Figure 70 Transport along transects condition 06 (Hs = 1.9m, Tp = 7.6s, Dir = 340°)

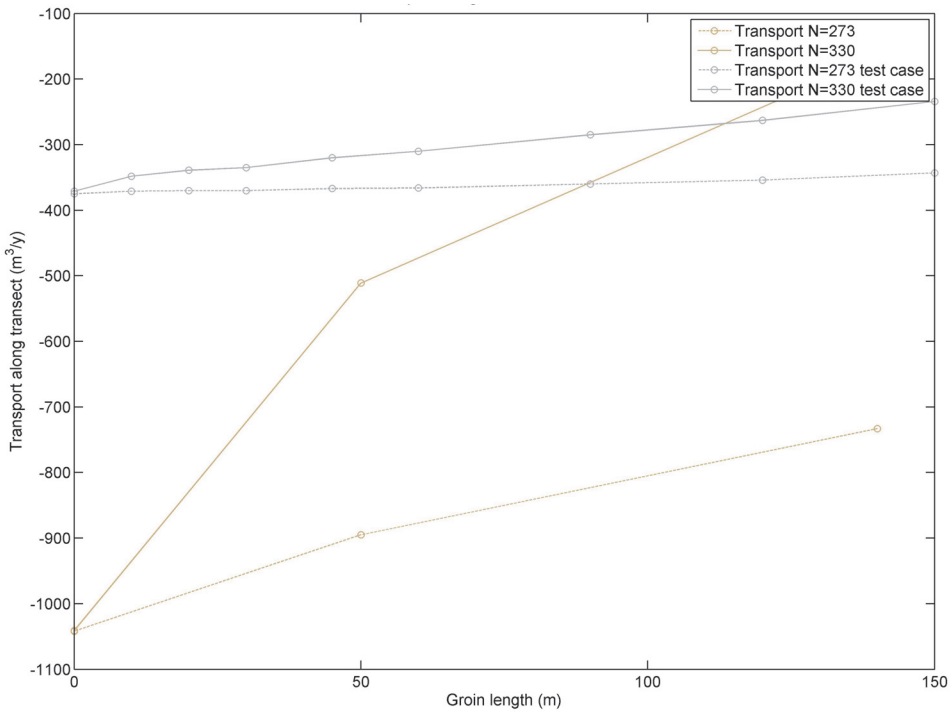

Figure 71 Transport along transects, condition 09 (Hs = 1.1m, Tp = 5.8s, Dir = 19°)

The transports decrease faster than in the test case. The cause for this can again be found in the bathymetry. The 2010 profile is steep, which results in fast wave breaking and higher transports. Because of the steepness the gravitational force on the sediment particles can play a larger role.

In the 2009 profile the depth at the tip of the groin is over 2 meters, in the test case this is only 1 meter. The current velocities, and thus the transport, at the tip of the groin will therefore be lower. The profile has a bar just in front of the groin however which will cause a part of the sediment transport to travel in front of the groin and increase the total transport.

The 1990 profile has a gentle slope with the depth at the tip of the groin at 2 meters. The test case depth is 1.5 meters at that point, this means that more waves will break in between the groins in the 1990 profile and thus have more effect under certain condition.

4.5.2 OFFSHORE DIRECTED TRANSPORTS

The yearly averaged offshore transports are also given in Figure 66 to Figure 68. Because the bathymetries are different, the offshore transport due to the groins must therefore be determined with a simulation in which the groins are absent. Due to the available computational power and time this is not done, it is recommended however to have a closer look at the offshore transport due to groins in the real schematized case. In **Table 2** the offshore transports are given between the groin tips averaged over the year with all the conditions included. In the 2010 situation no groins are present so this situation is not taken into account.

Situation	Offshore transport (m^3/year)
1990	421
2009	419

Table 6 Offshore transports

The offshore transports are high, which indicates a changing profile. This can be explained by the fact that the shallow foreshore is dynamic and dependant on the wave conditions that are occurring. This means that with high waves the inner bar will move offshore, and with lower waves the bar moves onshore. Because the morphology is left out in the model a higher sediment transport may be induced. The offshore sediment transports with high waves remain high because the profile does not adapt. The real offshore transports through the year are therefore hard to determine, further investigation needs to be done here.

An interesting effect that is seen in the offshore transports for only one condition, is that the onshore part of the sediment transport is very small. In Figure 72 this is shown for condition 01. This is most likely the effect of the offshore directed rip-current, described earlier in *chapter 4.3.3 Offshore directed currents*. The sediment is transported offshore and does not flow back after the groin. The importance of the occurrence of an offshore directed rip-current is again stressed and further research is recommended.

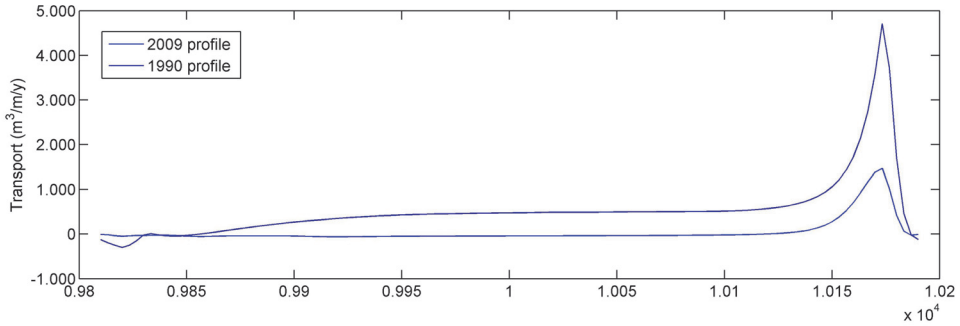

Figure 72 Offshore transport between groin tips, condition 01 (Hs = 0.7m, Tp = 5.9s, Dir = 314°)

CONCLUSIONS

The following conclusions can be drawn from the above:

- The sediment transport decreases with increasing groin length and is around 50% less in the 1990 situation with long groins compared to no groins in the 2010 situation.
- The bathymetry does affect the blocking of sediment transport by the groins.
- The bathymetry and bars in the profile are important for the effect that the groins have on sediment transport.
- The offshore sediment transport cannot be accurately determined in case the morphology is left out of the model.
- During certain conditions an offshore directed rip-current is present which causes offshore transport.

4.6 SENSITIVITY BATHYMETRY

To determine the influence of the bathymetry around a groin, simulations have been made with scour holes in front of the groins. In Figure 73 the results of the 1990 situation with a scour hole in front of the groin during condition 01 can be seen. The offshore directed currents are more contracted and stronger. This is interesting because the water is deeper and therefore could also induce lower current velocities. The higher and more contracted currents are most likely due to the effect of the breaking of the waves. A rip current on a beach is formed in the same way; the waves break on the bar and therefore induce a higher water level behind the bar, when on a certain position the bar is lower the waves break less and thus the setup is less. The water now flows offshore in this region. The scour hole in the situation with groins makes the bar less high and therefore the rip current offshore is even stronger. In *Appendix I - Offshore currents with scour condition 01* the offshore currents can be seen for a groin of 60 meters, where the same phenomenon can be observed.

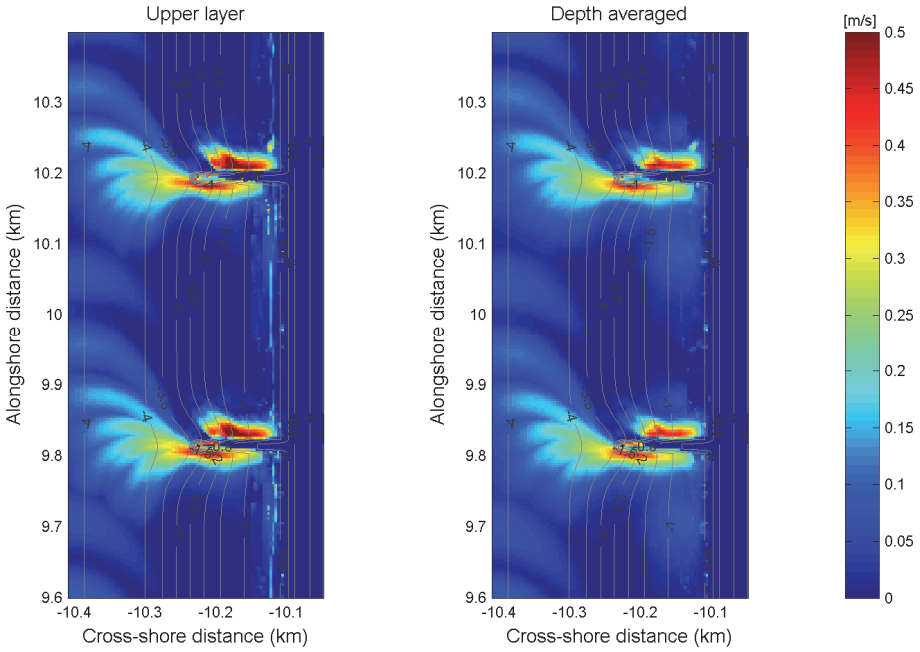

Figure 73 Maximum offshore directed current over a tidal cycle, with scour hole, condition 01 (Hs = 0.7m, Tp = 5.9s, Dir = 314°)

The alongshore maximum velocities also change. Depending on the condition and the occurrence of a rip-current, the velocities are different. In Figure 74 can be seen that the maximum alongshore velocities during condition 01 are smaller on the transect in between the groins (transect N=273), but higher on the transect over the groins. This is most likely due to the rip-current. In Figure 75 can be seen that for condition 09 the maximum velocities are lower everywhere. Due to the scour hole the water is deeper so the velocities decrease when no rip-current occurs. The velocities over the transect in between the groins is also lower. It is thought that the current velocity is more spread out over the surf zone

due to the scour hole, therefore the maximum is lower. It is recommended to have a closer look on the effect of scour holes on currents and sediment transport.

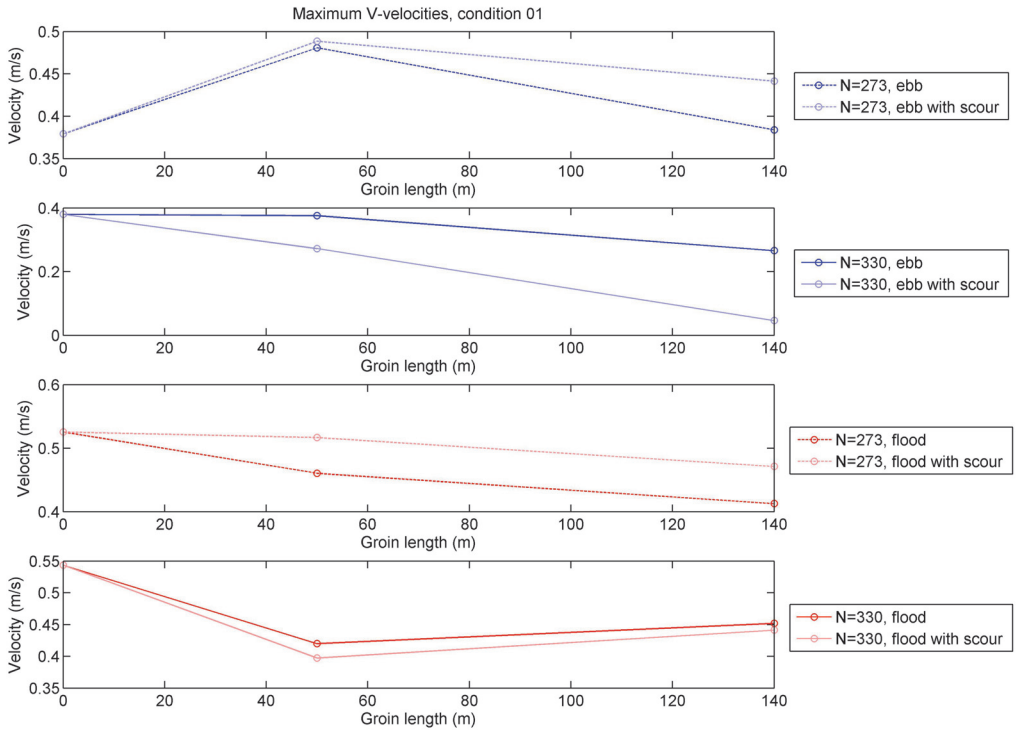

Figure 74 Maximum alongshore velocities with and without scour hole, condition 01 (Hs = 0.7m, Tp = 5.9s, Dir = 314°)

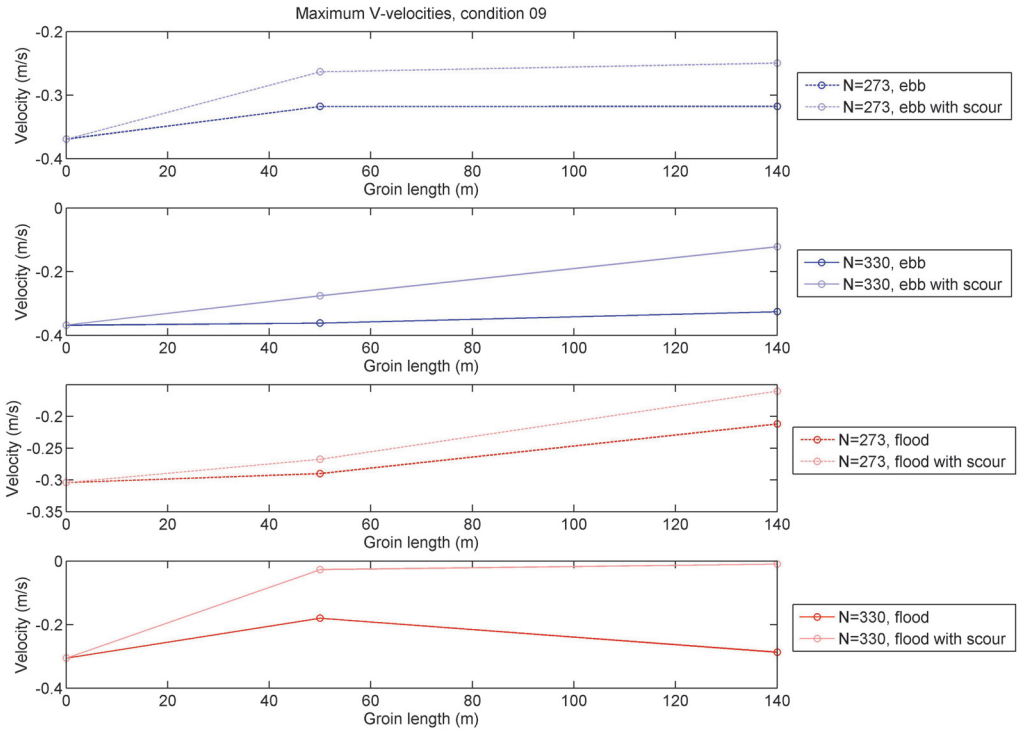

Figure 75 Maximum alongshore velocities with and without scour hole, condition 09 (Hs = 1.1m, Tp = 5.8s, Dir = 19°)

5 CONCLUSION

It can be concluded that the impact of resurfacing groins depends on two main aspects: the bathymetry and the groin length. From the test case, where the influence of groin lengths on a constant sloping foreshore were investigated, some conclusions can be drawn. The translation to a real case must be done with care however.

5.1 HYDRODYNAMICS

From the test case the following conclusions can be drawn regarding the hydrodynamics:

- In an alongshore uniform profile with a constant slope, the maximum alongshore velocities due to the groins begin to change significantly at a groin length of 50 to 60 meters.
- The maximum current speeds due to the groin in this situation are 10 to 15 % higher with a groin of 150 meter, then when no groin is present.
- The tide influences the maximum current speeds when the groin reaches far enough offshore. In this case the maximum current speeds are affected when the groin has a length of approximately 90m.
- The offshore directed currents increase with increasing groin length and the offshore directed current on the lee side of the groin does not extend beyond the surf zone.

When the test case is compared to the real schematized case the following conclusions can be drawn:

- The bathymetry plays a major role in maximum current speeds near the coast and near groins, because the conclusions from the test case do not apply for the real schematized situations.
- The magnitude of the offshore directed currents is dependent on the groin length.
- The eddy on the lee side of the groin (seen from the wave driven current direction) can induce strong rip currents that do not extend beyond the tip of the groin. The length of the groin plays a major role in the occurrence and the velocity of the eddy.

5.2 SEDIMENT TRANSPORT

From the test case the following conclusions can be drawn regarding the sediment transport:

- Sediment transport decreases quite constantly with increasing groin length up to 150 meter.
- An alongshore uniform profile around a groin is not realistic and will have a large impact on the longshore sediment transport gradients.
- In the alongshore uniform profile with a constant slope, the groin catches the majority of the sediment from the cross-shore sediment transport distribution at the same cross-shore distance as the groin.

- The offshore sediment transport due to groins is relatively small.

When the test case is compared to the real schematized case the following conclusions can be drawn:

- The sediment transport decreases with increasing groin length and is around 50% less in the 1990 situation with long groins compared to no groins in the 2010 situation, the decrease is however not as constant as is observed in the test case.
- The bathymetry does affect the blocking of sediment transport by the groins.
- Bars in the profile are important for the effect that the groins have on sediment transport.
- During certain conditions an offshore directed flume is present which causes offshore transport.
- The offshore sediment transport cannot be accurately determined in case the morphology is left out of the model.

From the simulation with simple scour holes the conclusion can be drawn that the bathymetry around the groin is important and can affect the currents greatly. A scour hole increases the rip current speed because of the effect it has on breaking waves. The waves break less because of the increased depth and therefore lower the set-up, which triggers a stronger offshore directed current.

5.3 REFLECTION ON THE DELFLAND COAST

From the above conclusions something can be said about the resurfacing of groins in front of Delfland.

Regarding the hydrodynamics

Because the maximum current speeds are highly dependent on the local bathymetry, it is not possible to give quantitative differences in maximum current speeds. It can be concluded however that the current speeds will be affected by the groins if they are sufficiently long. It is not to be expected that the groins induce major current velocity increases when they are less than 60 meters. The influence of the bathymetry should not be forgotten however.

The offshore currents are increasing when the groins resurface. When the groins are short, in the order of 50 meters, the offshore currents are present in front of the groin. With longer groins, in the order of 100 meters or longer, also a lee side eddy appears with a strong offshore directed current just behind the groin. This eddy does not extend beyond the tip of the groin. Scour holes most likely increase the offshore directed current speeds but further investigation is needed to give a better view on the exact influence.

It must be noticed that short groins can have influence on the occurrence and location of rip currents. The non erodible groin can be the cause of a rip current that is fixed to a certain position. The advantage is that the location of the rip current is known, the disadvantage is that the rip current is most likely stronger than without a groin.

Regarding the sediment transport

The alongshore sediment transports in the 2010 profile are much higher than in the 2009 and 1990 profile. The relatively steep decrease of the sediment transport between the profiles is most likely due to the steepness of the profile in 2010. This indicates that the initial erosion after the nourishment is high, the profile adapts and the transports decrease. When the groins resurface the transport will probably decrease quite constant with increasing relative groin length. This followed from the test case. Due to the decreasing sediment transport, the sediment transport gradient along the Delfland coast decreases and therefore the erosion will decrease. This affects the nourishment demand along the coast, which will decrease when the groins resurface. Again the importance of the effects due to the bathymetry is noted. This affects the effectivity of the blockage of sediment due to the groin.

6 RECOMMENDATIONS

6.1 MODELING

Regarding the modeling with Delft3D the following recommendation are made. It is recommended to further investigate:

- The functioning of the wavecon file to specify the wave conditions in Delft3D WAVE when used in combination with the roller model.
- The way in which the boundary conditions are applied and the effects or interference with other boundary conditions.
- The functioning of the sediment transport formula van Rijn 2004. This may not work well in the vicinity of groins in a 3D model due to the shallow water depth in combination with a non-erodible layer.

During the derivation of the nearshore wave climate use is made of the Building with Nature wave transformation tool. This did not lead to satisfactory results. The sediment transport due to the wave conditions derived with this tool, are directed south. This is highly doubtful since sediment transport studies indicate a northerly directed transport due to a significant amount of south westerly waves. The waves from this wave direction are underestimated in the results of the Building with Nature tool. It is recommended to have a closer look at this.

6.2 RESULTS

During the study interesting results have been found which were out of the scope of the study or not fully investigated due to time constraints.

It is recommended to:

- Investigate what is the influence of the bathymetry profile on sediment transport and current velocities.
    - What is the influence of the inner and the outer bar.
    - What is the influence of bottom slope.
    - What is the influence of the bars and the slope with respect to the groin length.

- Investigate the bathymetry around a groin and the influence on the current velocities.
    - What does a scour hole look like.
    - How does a scour hole influence the sediment transports and currents.
    - How does the waterline change and what are the influences.

- Have a closer look on the offshore directed currents and transports.
  - When does an offshore directed rip-current occur.
  - What happens with the offshore directed transports when an offshore directed rip-current occurs.
  - Investigate the offshore transports due to groins in the three schematized situations.
  - Better investigation on what the offshore transport due to groins is, regarding the influence of the groins on the wave pattern.

- Study the nourishment demand along the Delfland coast when groins resurface.
  - What is the influence of groins on the sediment transport gradients along the coast.

REFERENCES

Basco, D. R. (1983). "Surfzone currents." Coastal Engineering **7**(4): 331-355.

Beets, D. J., L. van der Valk, et al. (1992). "Holocene evolution of the coast of Holland." Marine Geology **103**(1-3): 423-443.

Berendsen, H.J.A. (2005). "The Rhine-Meuse delta at a glance." 8th International Conference on Fluvial Sedimentology, Delft, the Netherlands. Mid-conference excursion guide, August 10, 2005.

Bloteling, J. and P. Heinsius (± 1766). Kaart van de kustlijn van Ter Heijde tot Hoek van Holland door de landmeter Joh. Bloteling in de jaren 1606, 1611, 1665, 1712, 1737 en 1765**:** Getekend op de kaart van Johannes Bloteling uit 1738.

Bosboom, J. and M. J. F. Stive (2010a). Coastal Dynamics 1, part 1, VSSD.

Bosboom, J. and M. J. F. Stive (2010b). Coastal Dynamics 1, part 2, VSSD.

Deeben, J., E. Drenth, et al. (2005). De steentijd van Nederland, Stichting Archeologie.

DHV, Alterra, et al. (2007a). Waterbouwrapport versterking Delflandse kust. W3487-02.001/ WG-SE20061125.

DHV, Alterra, et al. (2007b). Duincompensatie Delflandse kust. W3487-02.001/ WG-SE20060985.

Dolk, F. J. A. (1939). Geschiedenis van het Hoogheemraadschap Delfland. 's Gravenhage, Martinus Nijhof.

Eisma, D. (1968). "Composition, origin and distribution of Dutch coastal sands between Hoek Van Holland and the island of Vlieland." Netherlands Journal of Sea Research **4**(2): 123-150, IN1, 151-267.

Elzelingen, J. M. W. and A. Groothoff (1912). Verhandeling over de kustverdediging van Delfland, Provinciale waterstaat van Zuid-Holland.

Hoogheemraadschap Delfland (1911). Zeewering van Delfland, Zeewaartse verlenging van strandhoofd 12,13 en 14. Bestek No 107.

Hoogheemraadschap Delfland (1922). Verlaging van strandhoofd No 14. Bestek No 156.

Hoogheemraadschap Delfland (1997). Legger Zeewering, Hoogheemraadschap van Delfland.

Longuet-Higgins, M. S. and R. w. Stewart (1964). "Radiation stresses in water waves; a physical discussion, with applications." Deep Sea Research and Oceanographic Abstracts **11**(4): 529-562.

MacMahan, J. H., E. B. Thornton, et al. (2006). "Rip current review." Coastal Engineering **53**(2-3): 191-208.

Mol, A. C. S. (2007). R&D Kustwaterbouw Reductie Golfrandvoorwaarden. OPTI Manual, WL|Delft Hydraulics Netherlands.

Pattiaratchi, C., D. Olsson, et al. (2009). "Wave-driven circulation patterns in the lee of groynes." Continental Shelf Research **29**(16): 1961-1974.

Raudkivi, A. J. and H. H. Dette (2002). "Reduction of sand demand for shore protection." Coastal Engineering **45**(3-4): 239-259.

Roelvink, J. A. (2001). Reference scenarios and design alternatives. Phase 1. Rapport Z3029, Mare, parcel 2, subproduct 3.

Steetzel, H. J. and J. H. de Vroeg (1999). Update and validation of the PonTos-model. Rapport A244/Z2259, Alkyon Hydraulic Consultancy & Research en WL|Delft Hydraulics, Netherlands.

Stive, M. J. F., H. J. de Vriend, et al. (1992). "Shore nourishment and the active zone: a time scale dependent view." Coastal Engineering: 2464 - 2473.

Stive, M. J. F. and W. D. Eysink (1989). Voorspelling ontwikkeling kustlijn 1990-2090, fase 3 (deelrapport 3.1): dynamisch model van het Nederlandse kustsysteem deelrapport. Rapport H0825, WL|Delft Hydraulics, Netherlands.

Sumer, B. M. and J. Fredsøe (1997). "Scour at the head of a vertical-wall breakwater." Coastal Engineering **29**(3-4): 201-230.

Tonnon, P. K., J. J. van der Werf, et al. (2009). Morfologische berekeningen MER zandmotor, Deltares.

van de Rest, P. (2004). Morfodynamica en hydrodynamica van de Hollandse kust. Graduation report, TU Delft, Netherlands.

van der Spek, A. J. F. and D. J. Beets (1992). "Mid-Holocene evolution of a tidal basin in the western Netherlands: a model for future changes in the northern Netherlands under conditions of accelerated sea-level rise?" Sedimentary Geology **80**(3-4): 185-197.

van Langenhuysen, J. and H. van Langenhuysen (1917). Verslag aan het college van Dijkgraaf en Hoogheemraden van Delfland. 's Gravenhage, Commissie van advies in zake Delfland's kustverdediging**:** Appendix A.

van Rijn, L. C. (1995). Sand Budget and coastline changes of the central coast of Holland between Den Helder and Hoek van Holland period 1964-2040. Project kustgenese, Delft Hydraulics.

van Rijn, L. C. (1997). "Sediment transport and budget of the central coastal zone of Holland." Coastal Engineering **32**(1): 61-90.

van Rijn, L. C. (2005). Principles of sedimentation and erosion engineering in rivers, estuaries and coastal seas, Aqua Publications.

APPENDICES

APPENDIX A - MAPS

MAP 1

Map of the groins in front of Delfland with their names, building year and spacing (van Langenhuysen and van Langenhuysen 1917). Please note the building years of the first 4 groins (numbers 1 to 4) are most probably different then stated on the map. Dolk states that the assumption that the groins were built in 1776 is wrong (Dolk 1939). Although he doesn't give a source for this statement, in the archives of the 'Hoogheemraadschap van Delfland' no payments can be found around that year for the execution of the building of the groins.

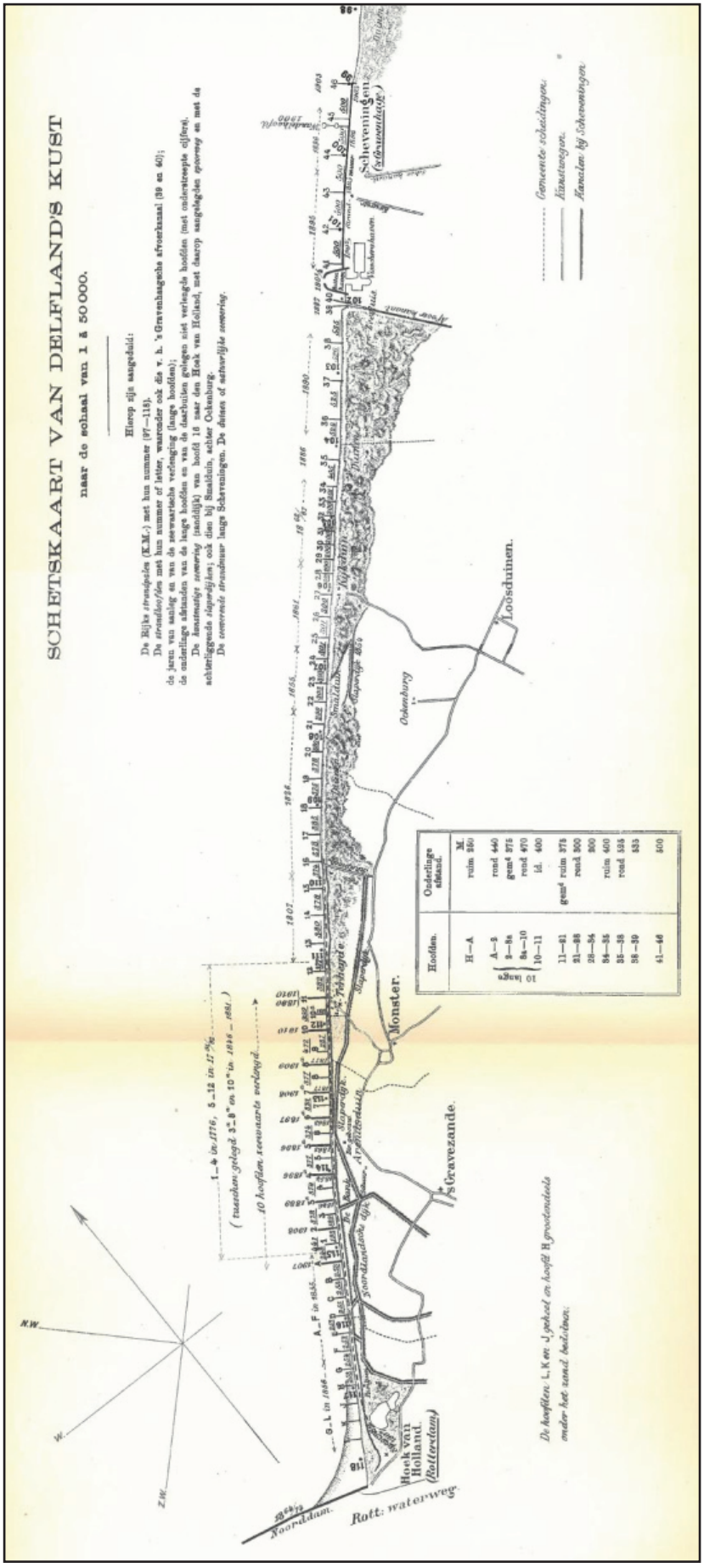

MAP 2

Map of (Bloteling and Heinsius ± 1766). The map shows the coastal retreat in the years 1606, 1611, 1665, 1712, 1737 and 1765 between Ter Heijde and Hoek van Holland. The lines are drawn on the map of Johannes Bloteling from 1738.

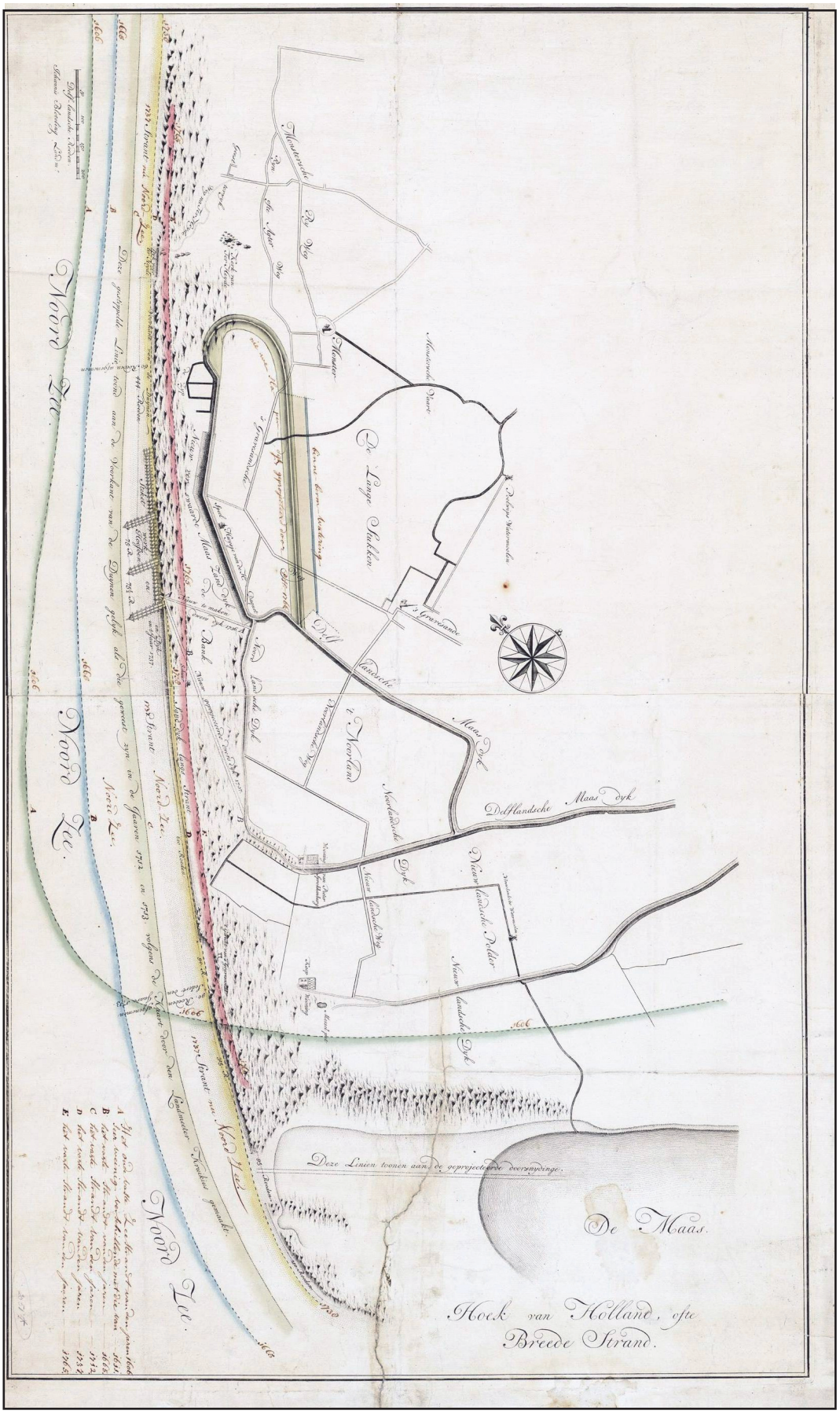

APPENDIX B - GROIN DATA

Groin data from 1776 – 1912 (Elzelingen and Groothoff 1912)

Groin	RSP	Year built	Length from RSP (m)		Length (m)	Distance (m)	Year extended	Extension (m)	Year extended	Extension (m)
			Seawards	Landwards						
L		1856								
K		1856								
I		1856								
H	116,997	1856	148	27	175					
G	116,744	1856	152	28	180	253				
F	116,490	1855	160	25	185	254				
E	116,237	1855	165	25	190	253				
D	115,977	1855	200	40	240	260	1880	36		
C	115,730	1855	197	55	252	247	1880	40,8		
B	115,476	1855	194	65	259	254	1880	48,5		
A	115,224	1855	287	71	358	252	1881	42,5	1908	±96
1	114,957	1791	186	45	231	267				
2	114,784	1791	284	60	344	173	1880	6	1908	98
3	114,595	1791	185	35	220	189	1880	10		
3a	114,406	1846	285	40	325	189	1881	18	1890	100
4	114,216	1791	184	45	229	190	1880	23		
4a	114,033	1854	283	53	336	183	1880	31,5	1897	100
5	113,841	1791	181	50	231	192	1880	30		
5a	113,656	1863	281	50	331	185	1880	95	1897	±100
6	113,467	1791	180	50	230	189	1881	24,5		
6a	113,283	1863	278	50	328	184	1881	88,1	1897	100
7	113,100	1791	178	50	228	183	1881	15		
7a	112,911	1877	277	56	333	189	1881	96,8	1908	±100
8	112,720	1791	176	50	226	191	1881	7		
8a	112,534	1877	278	50	328	186	1881	86,8	1909	±104
9	112,350	1791	173	40	213	184	1881	4,5		
10	112,063	1792	282	40	322	287	1910	112		
10a	111,862	1881	173	40	213	201				
11	111,664	1792	280	35	315	198	1890		1910	±110
12	111,282	1792	171	30	201	382				
13	110,905	1807	163	30	193	377				
14	110,525	1807	154	35	189	380				
15	110,150	1807	145	50	195	375				
16	109,775	1826-1827	141	45	186	375				
17	109,400	1826-1827	142	40	182	375				
18	109,010	1826-1827	140	40	180	390				
19	108,640	1826-1827	159	40	199	370				
20	108,260	1826-1827	160	35	195	380				
21	107,885	1826-1827	164	25	189	375				
22	107,585	1855	156	40	196	300				

23	107,280	1855	147	47	194	305				
24	106,980	1855	143	37	180	300				
25	106,680	1861-1862	133	35	168	300				
26	106,375	1861-1862	125	50	175	305				
27	106,075	1861-1862	117	50	167	300				
28	105,770	1861-1862	108	55	163	305				
29	105,570	1861-1862	105	60	165	200				
30	105,370	1863	103	53	156	200				
31	105,170	1864	101	64	165	200				
32	104,970	1865	99	81	180	200				
33	104,770	1866	97	87	184	200				
34	104,570	1867	95	80	175	200				
35	104,170	1886	91	140	231	400				
36	103,645	1890	97	150	247	525				
37	103,120	1890	97	134	231	525				
38	102,595	1890	97	105	202	525				
39	102,050	1887	101	86	187	545				
40	101,978	1887	102	86	188	72				
41	101,500	1895	124	80	204	478				
42	101,000	1895	146	80	226	500				
43	100,500	1895	185	62	247	500				
44	100,000	1896	193	24	217	500				
45	99,500	1896	200	23	223	500				
46	99,000	1902	190	25	215	500				
47										
48										
49										
50										

APPENDIX C - NOURISHMENTS

Place	Month	Year	Month	Year	Transect	Transect	Type	Volume
	start	*start*	*end*	*end*	*km*	*km*		*m3*
Hoek van Holland	1	1989	12	1989	118,00	118,75	Beach Nourishment	100000
Hoek van Holland	1	1988	12	1988	118,00	118,50	Beach Nourishment	200000
Hoek van Holland	1	1999	12	1999	117,75	118,50	Beach Nourishment	200680
Hoek van Holland	1	1997	12	1997	117,75	118,75	Beach Nourishment	200000
Hoek van Holland	1	1996	12	1996	117,75	118,75	Beach Nourishment	200000
Hoek van Holland	1	1995	12	1995	117,75	118,75	Beach Nourishment	200000
Hoek van Holland	1	1994	12	1994	117,75	118,75	Beach Nourishment	200000
Hoek van Holland	1	1992	12	1992	117,75	118,75	Beach Nourishment	560000
Hoek van Holland	1	1991	12	1991	117,75	118,75	Beach Nourishment	223000
Hoek van Holland	1	1990	12	1990	117,75	118,75	Beach Nourishment	183000
Hoek van Holland	1	2004	12	2004	117,50	118,50	Beach Nourishment	230000
Hoek van Holland	1	2003	12	2003	117,50	118,50	Beach Nourishment	213606
Hoek van Holland	1	2000	12	2000	117,50	118,50	Beach Nourishment	200000
Hoek van Holland	4	2007	5	2007	117,25	118,70	Beach Nourishment	744124
Hoek van Holland	1	1977	12	1977	115,70	118,75	Beach Nourishment	870000
Hoek van Holland	1	1976	12	1976	115,70	119,00	Beach Nourishment	1500000
Hoek van Holland	1	1971	12	1971	115,70	118,75	Beach Nourishment	18940000
s Gravenzande	3	1993	4	1993	114,00	118,75	Beach Nourishment	463000
Ter Heijde	8	1997	11	1997	113,15	114,85	Foreshore Nourishment	1028950
s Gravenzande-Hoek van Holland	7	2007	11	2007	113,00	118,00	Foreshore Nourishment	753277
Ter Heijde	5	1995	6	1995	112,21	114,50	Beach Nourishment	300000
Monster	10	2005	11	2005	108,60	113,00	Foreshore Nourishment	1014364
Kijkduin-Ter Heyde	4	2001	6	2001	108,00	112,00	Beach Nourishment	801178
Ter Heijde	1	2004	12	2004	107,73	113,19	Beach Nourishment	1150000
Ter Heijde	9	2003	11	2003	107,73	113,19	Beach Nourishment	1252797
Ter Heijde	5	1986	10	1986	107,73	115,61	Beach Nourishment	1900000
Ter Heijde	5	1986	10	1986	107,73	115,61	Landward dune reinforcement	1300000
Ter Heijde	1	1997	12	1997	107,50	112,50	Beach Nourishment	834000
Kijkduin-Ter Heyde	3	2001	11	2001	107,40	112,50	Foreshore Nourishment	3581899
Ter Heijde	6	1993	7	1993	106,23	112,21	Beach Nourishment	1143000
Scheveningen	1	1953	12	1953	100,50	101,50	Beach Nourishment	70000
Scheveningen	9	1969	10	1969	100,00	101,50	Beach Nourishment	45000
Scheveningen	1	2004	12	2004	99,30	101,10	Beach Nourishment	778500
Scheveningen fase 2	10	2010	3	2011	99,00	101,50	Beach Nourishment	959130
Scheveningen	1	1987	12	1987	99,00	101,00	Beach Nourishment	8000
Scheveningen	1	1982	12	1982	99,00	101,00	Beach Nourishment	15400
Scheveningen	1	1981	12	1981	99,00	101,00	Beach Nourishment	10000
Scheveningen fase 1	10	2009	3	2010	99,00	101,50	Beach Nourishment	1363913
Scheveningen	3	1985	4	1985	98,75	101,25	Beach Nourishment	250000
Scheveningen	3	1985	4	1985	98,75	101,25		80000
Scheveningen	4	1975	8	1975	98,50	101,50	Beach Nourishment	700000
Scheveningen	2	1991	5	1991	97,81	101,39	Beach Nourishment	1005699
Scheveningen	2	1999	6	1999	97,73	100,50	Foreshore Nourishment	1425780
Scheveningen	1	1996	12	1996	97,00	101,00	Beach Nourishment	800000

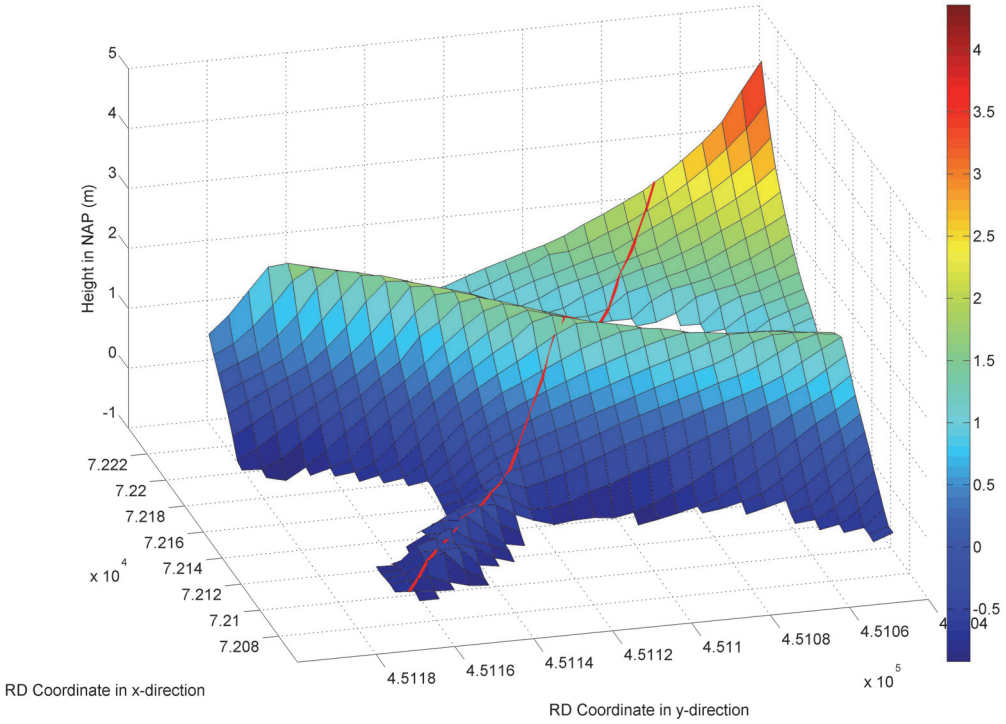

Groin 15.

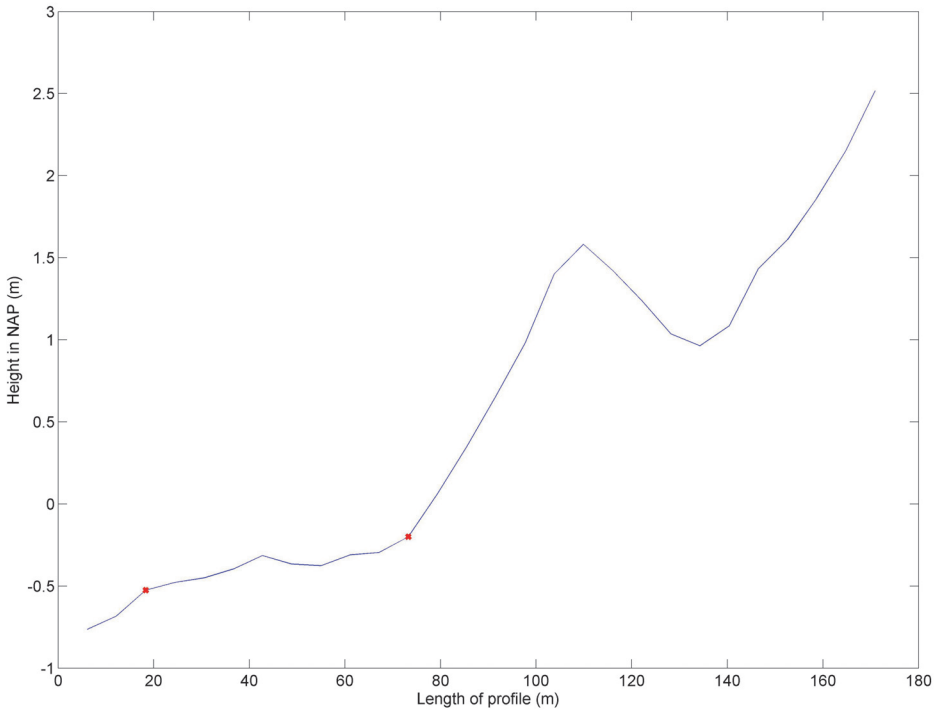

Groin 15 height, the red dots are the points from which the dimensions are determined.

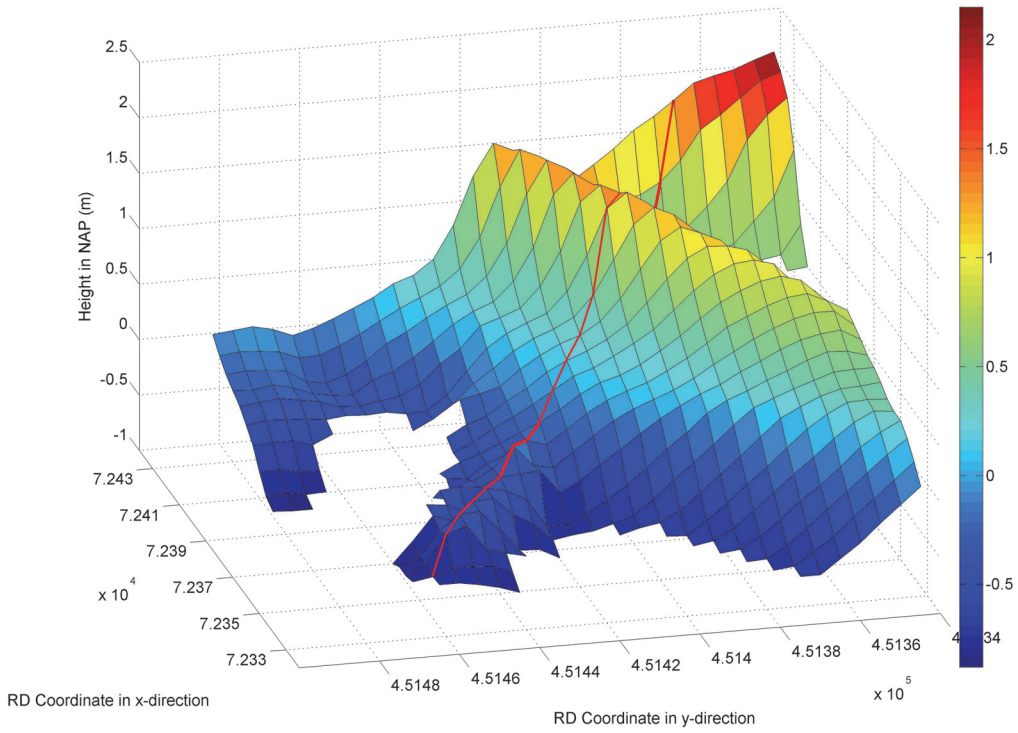

Groin 16.

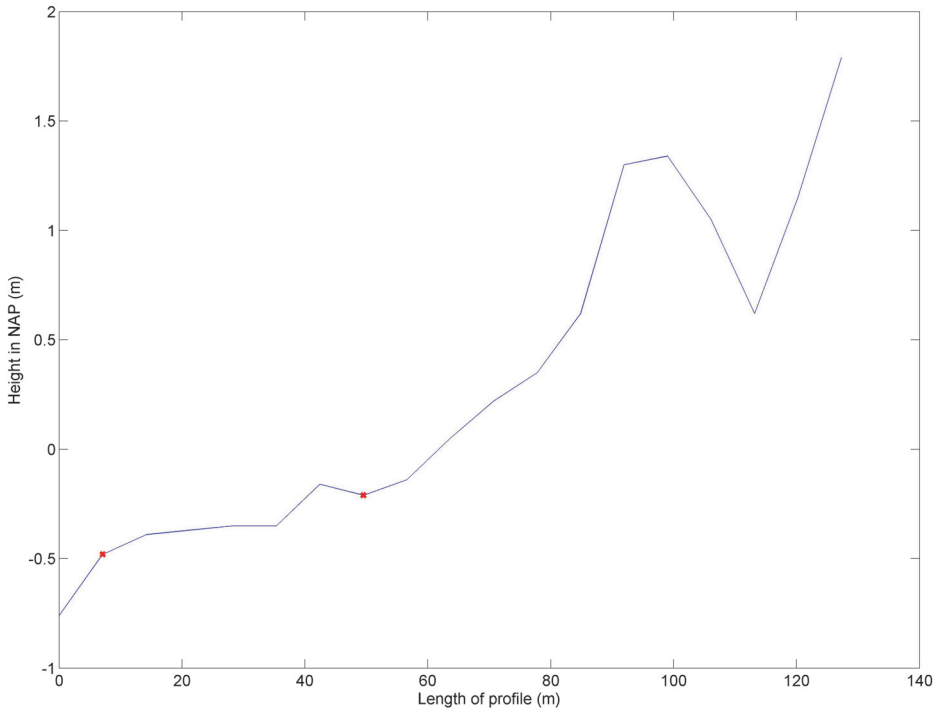

Groin 16 height, the red dots are the points from which the dimensions are determined.

These wave roses represent the wave conditions at the IJerlandse gat and Europlatform, the offshore stations from which the nearshore wave conditions are determined in the BwN tool.

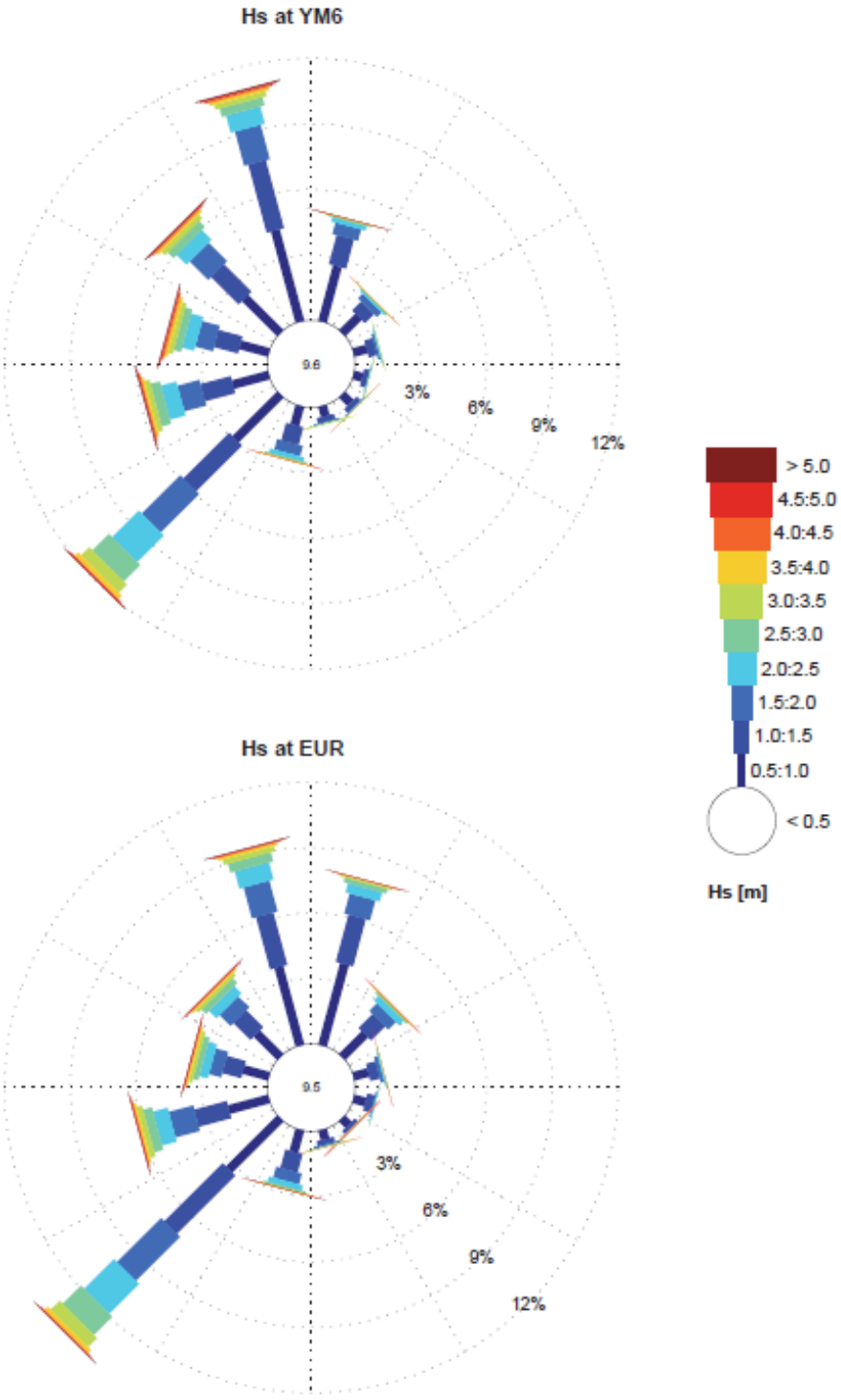

Wave conditions in the offshore measuring points IJmuiden and Europlatform

The wave climate nearshore is shown below. In this figure it is noticeable that the southwesterly waves that are clearly visible at the offshore measuring stations are absent in the nearshore wave climate. This is remarkable because many studies showed a northern directed sediment transport mainly due to the waves from the southwest. The black line represents the coast normal.

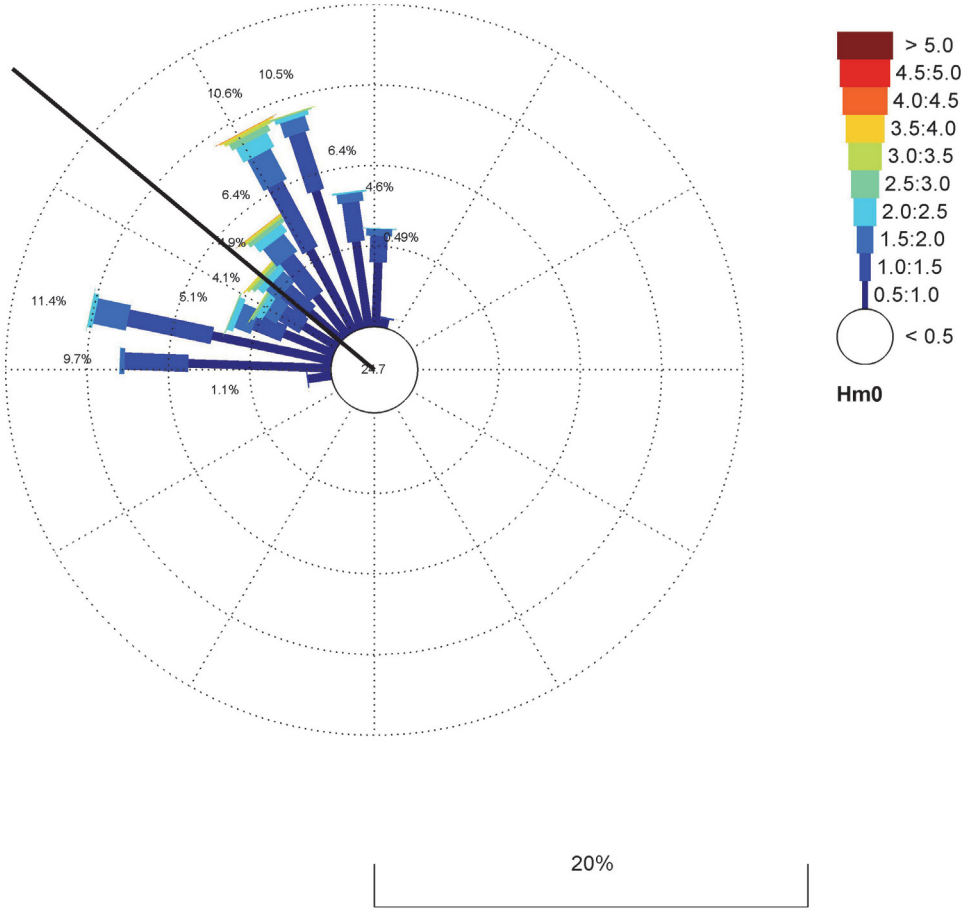

Wave rose representing the wave climate on the model boundary

APPENDIX F - MAXIMUM ALONGSHORE VELOCITIES CONDITION 06 AND 09

Maximum Alongshore velocities in transects N=273 and N=330.

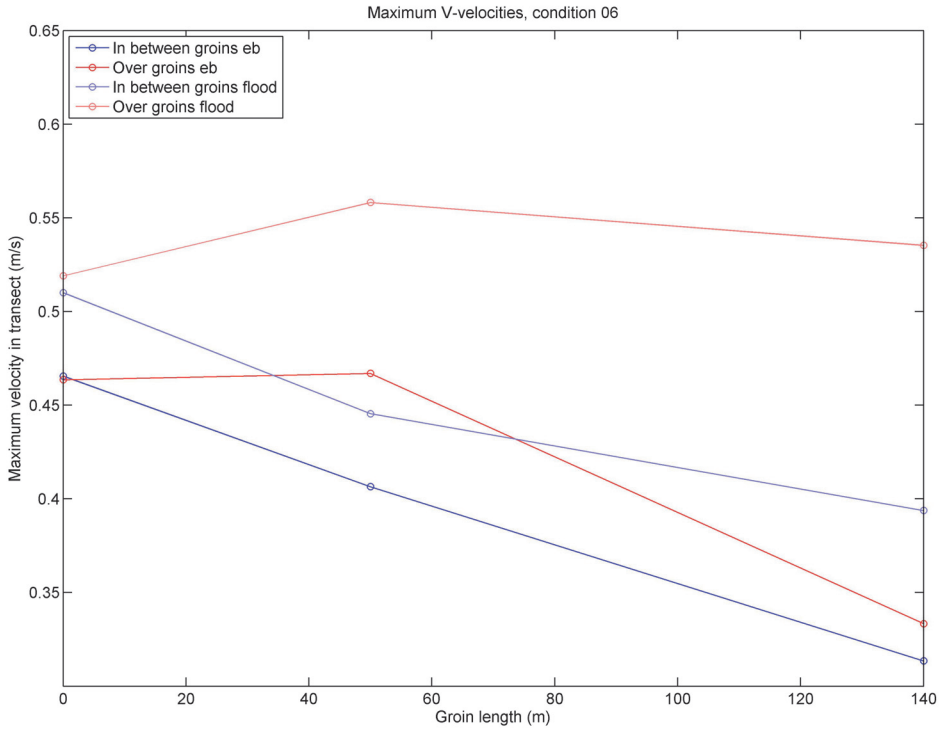

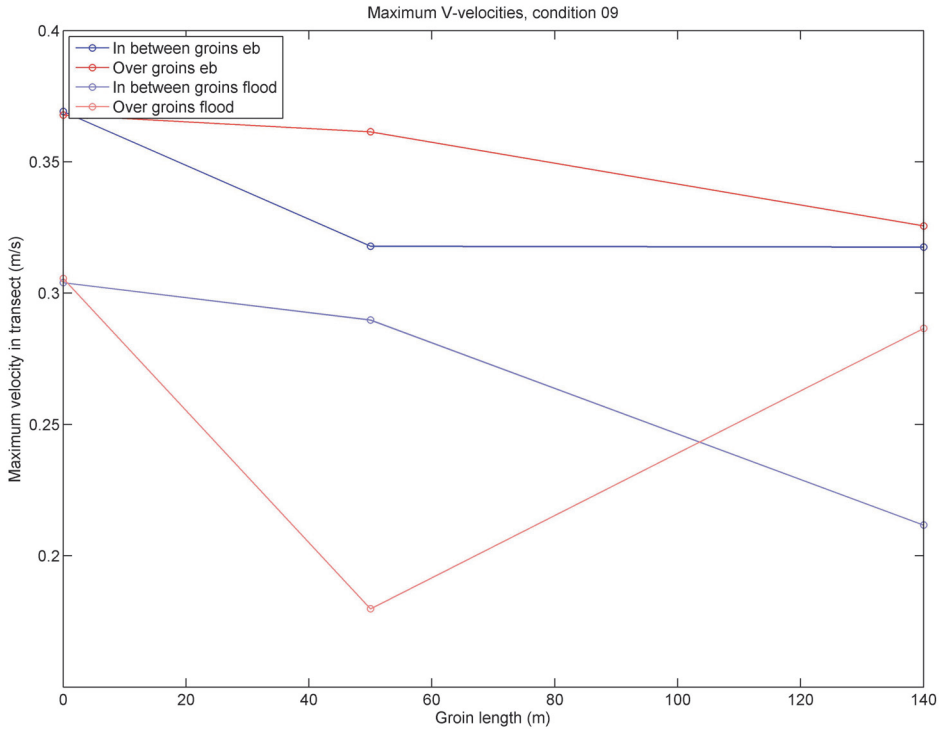

APPENDIX G - TEST CASE OFFSHORE TRANSPORTS CONDITION 06 AND 09

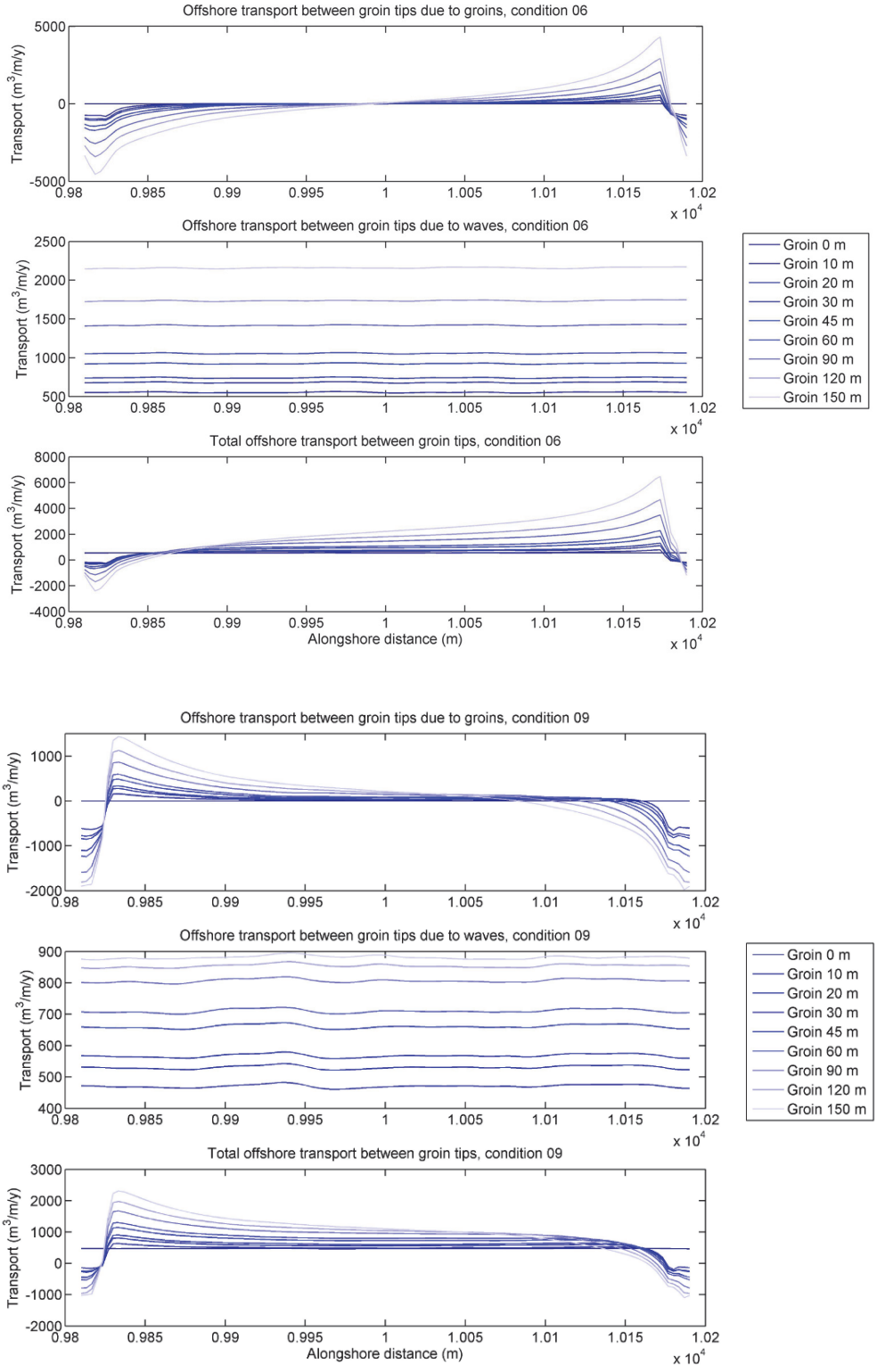

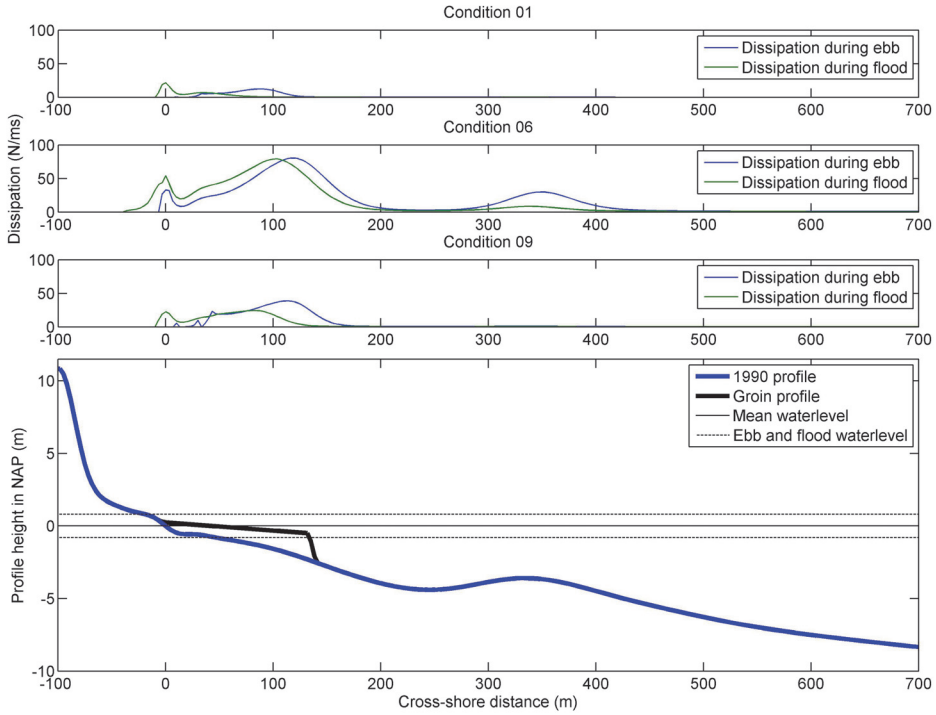

Dissipation in the 1990 profile

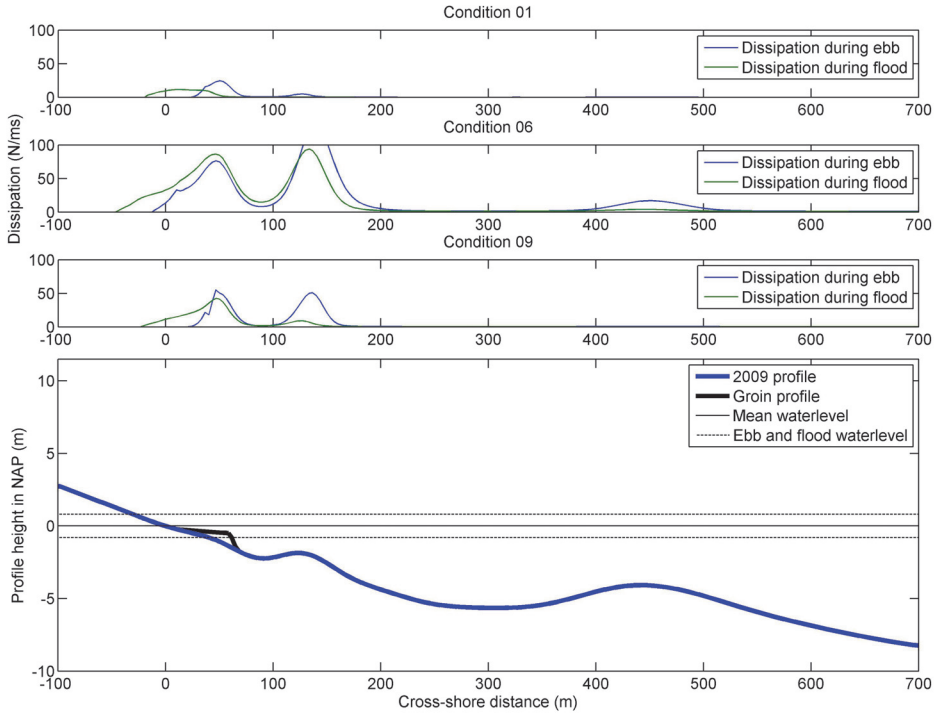

Dissipation in the 2009 profile

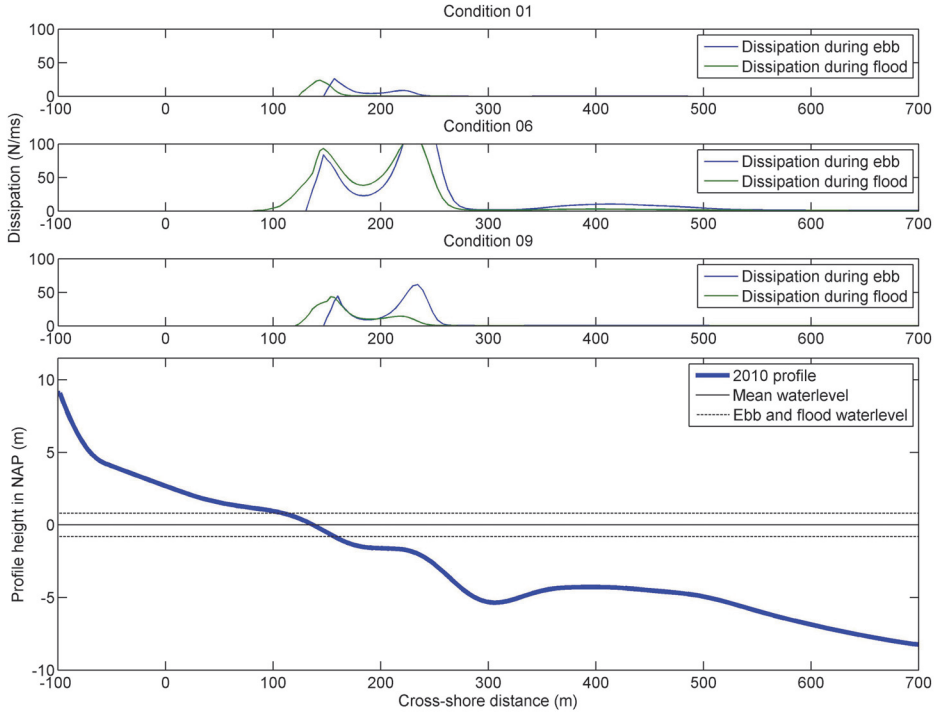

Dissipation in the 2010 profile

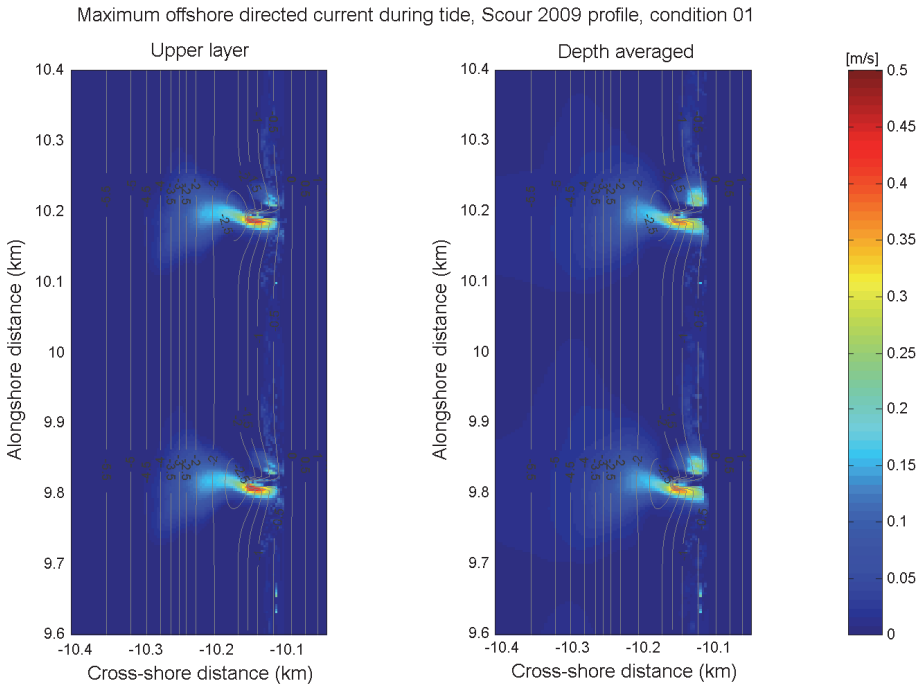
Maximum offshore directed current during tide, Scour 2009 profile, condition 01
Upper layer
Depth averaged
[m/s]
0.5
0.45
0.4
0.35
0.3
0.25
0.2
0.15
0.1
0.05
0
Alongshore distance (km)
Cross-shore distance (km)
10.4
10.3
10.2
10.1
10
9.9
9.8
9.7
9.6
-10.4
-10.3
-10.2
-10.1

Depth averaged current velocity and direction during max flood, 1990 condition 07

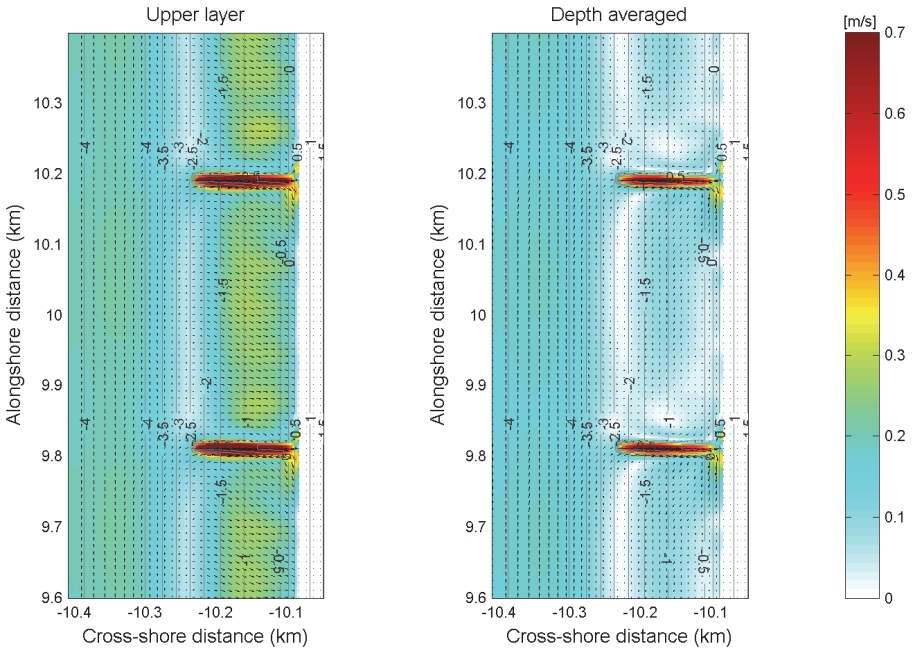

Depth averaged current velocity and direction during (LW) reversal, 1990 condition 07

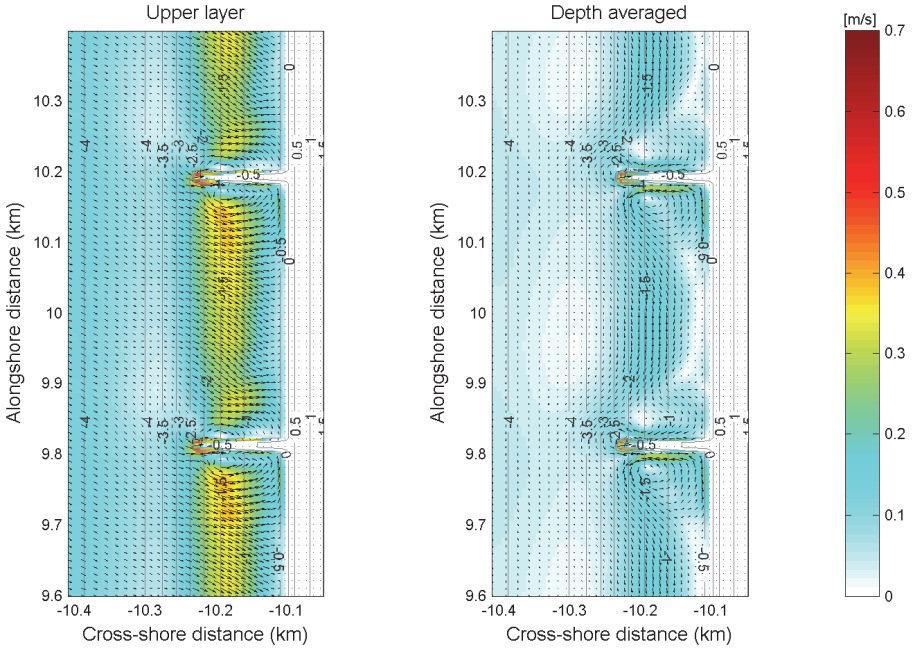

Depth averaged current velocity and direction during maximum eb-current, 1990 condition 07

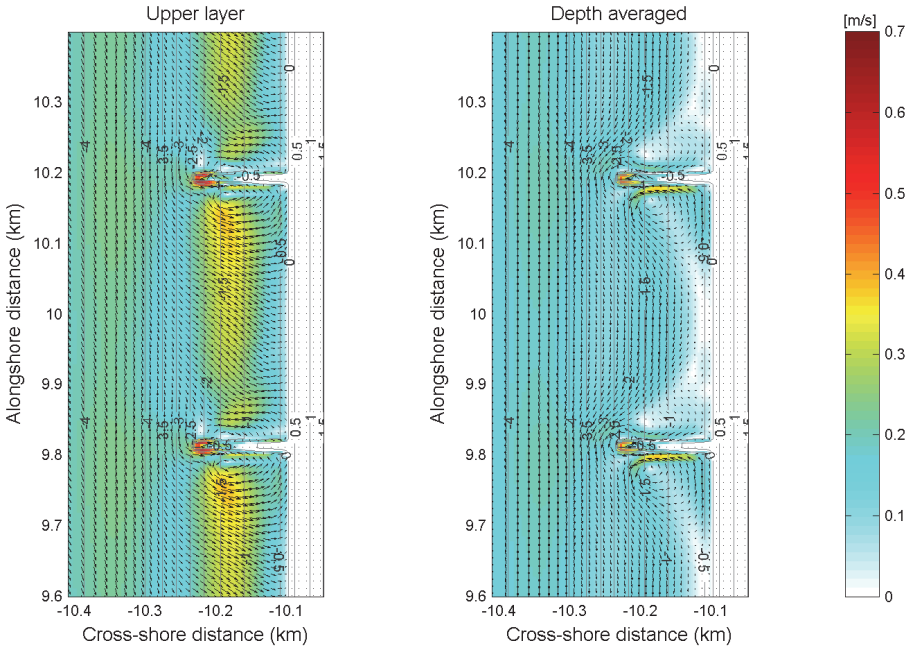

Depth averaged current velocity and direction during max flood, 2009 condition 07

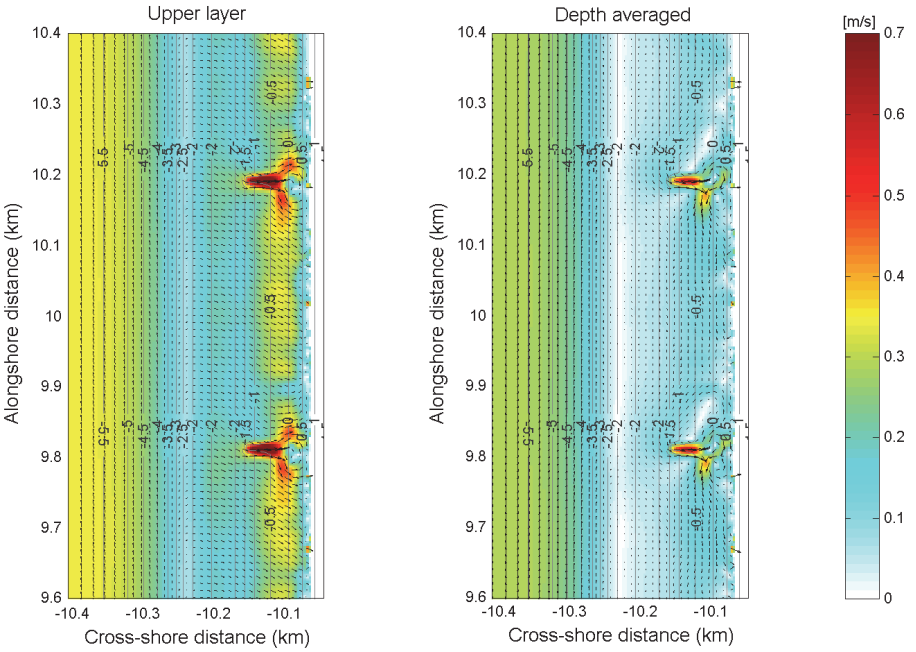

Depth averaged current velocity and direction during (LW) reversal, 2009 condition 07

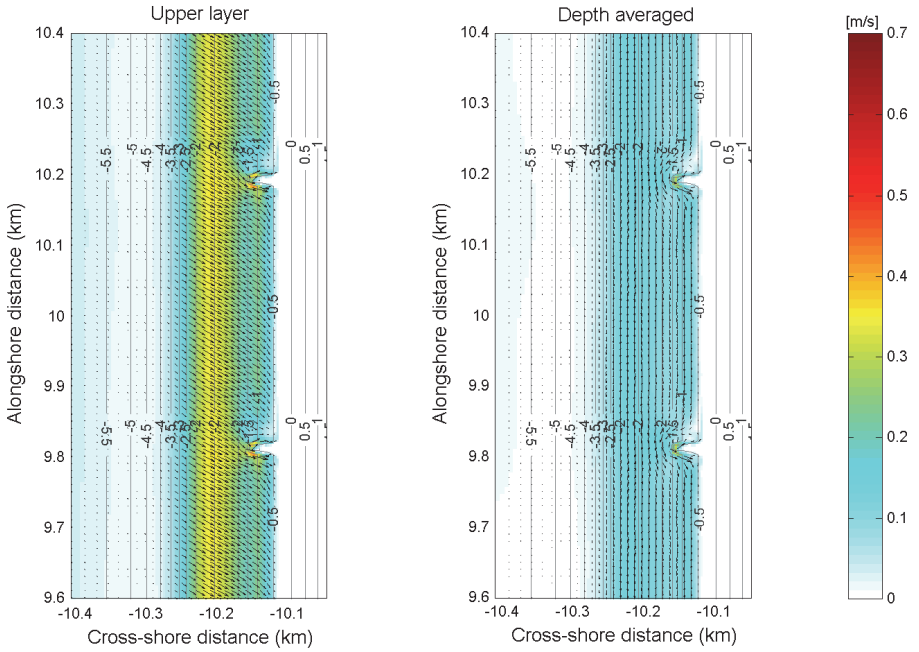

Depth averaged current velocity and direction during maximum eb-current, 2009 condition 07

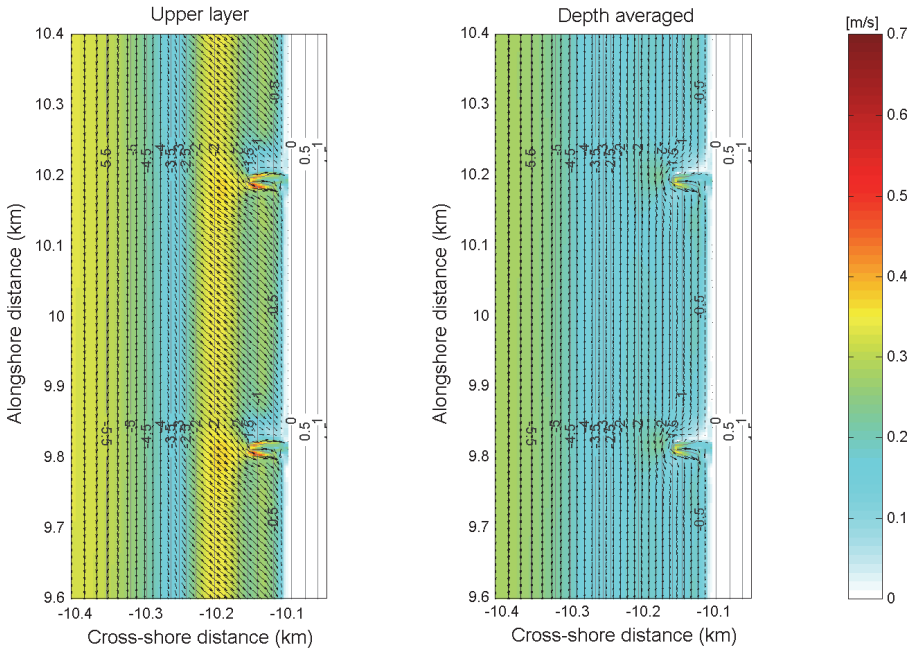

Depth averaged current velocity and direction during max flood, 2010 condition 07

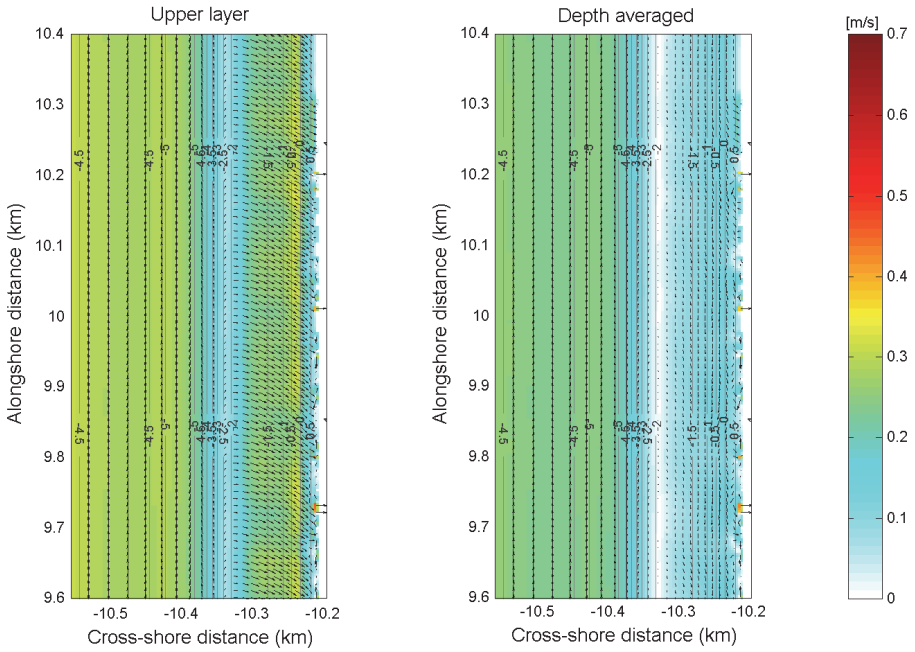

Depth averaged current velocity and direction during (LW) reversal, 2010 condition 07

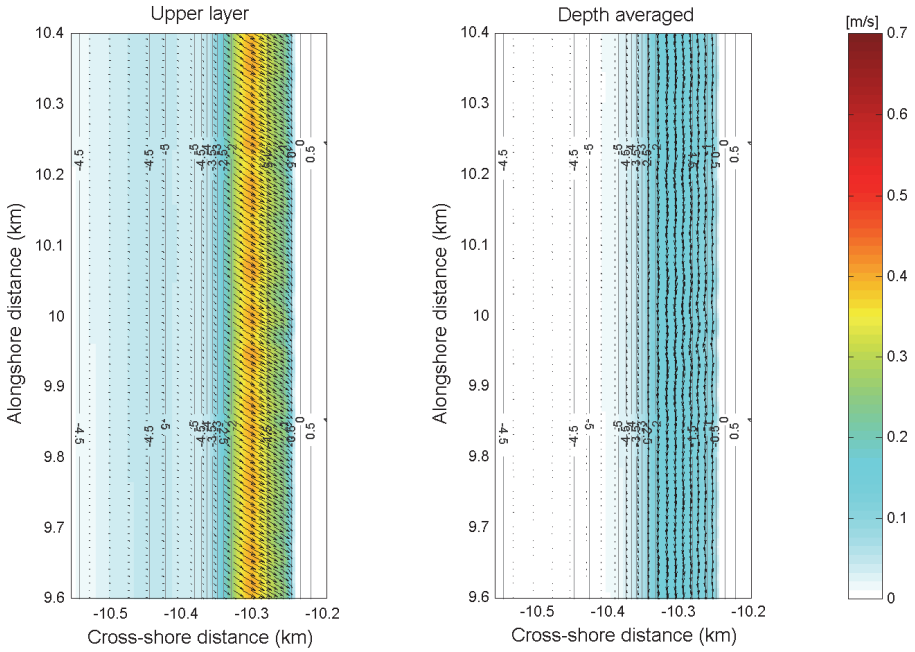

Depth averaged current velocity and direction during maximum eb-current, 2010 condition 07

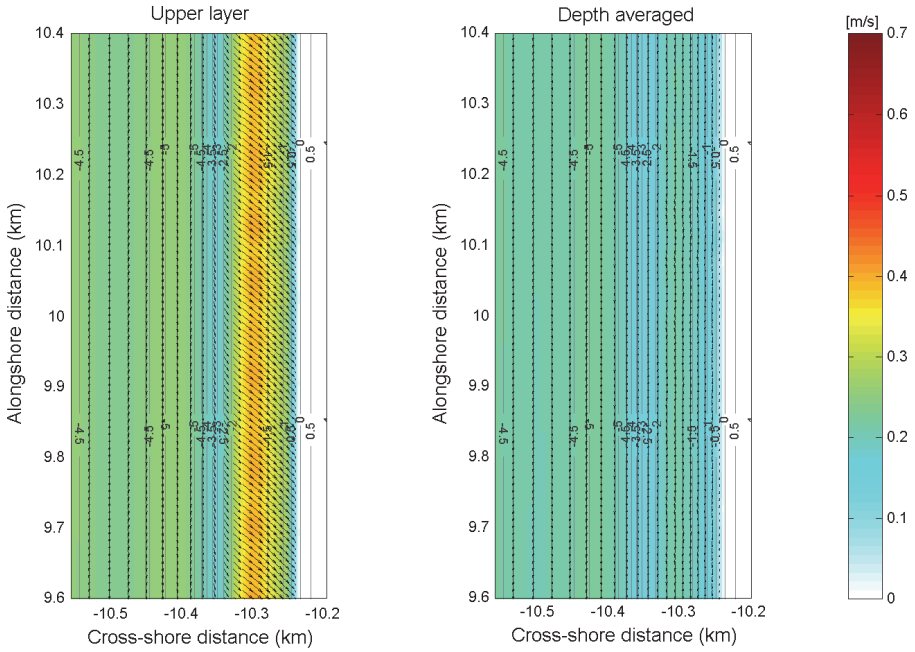

Depth averaged current velocity and direction during max flood, 1990 condition 09

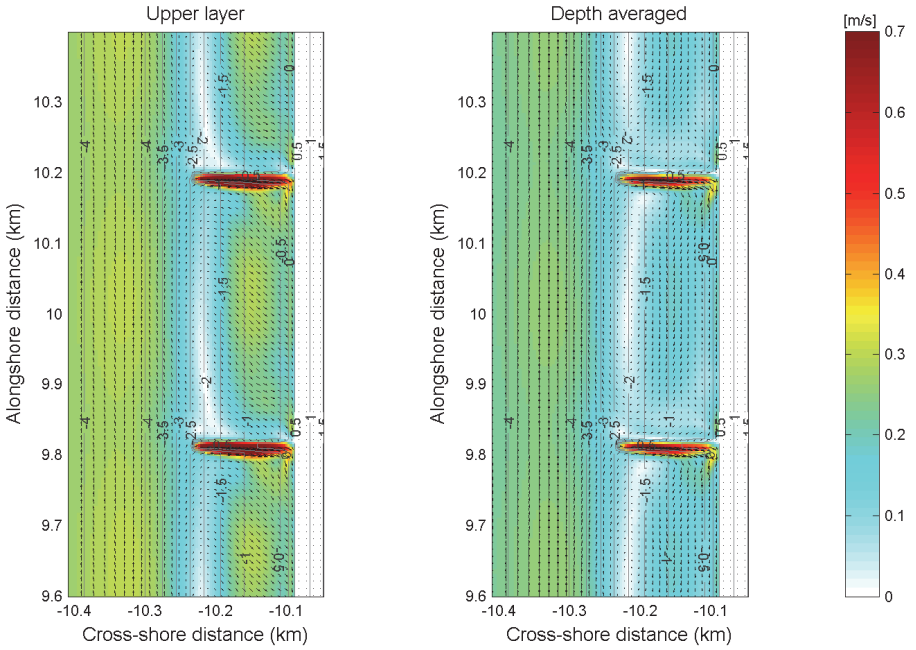

Depth averaged current velocity and direction during (LW) reversal, 1990 condition 09

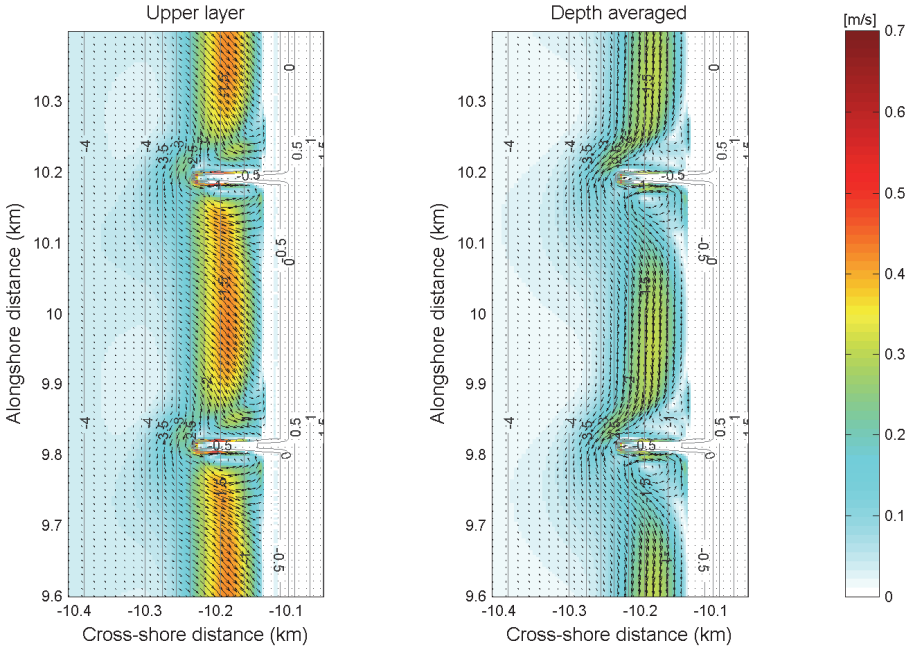

Depth averaged current velocity and direction during maximum eb-current, 1990 condition 09

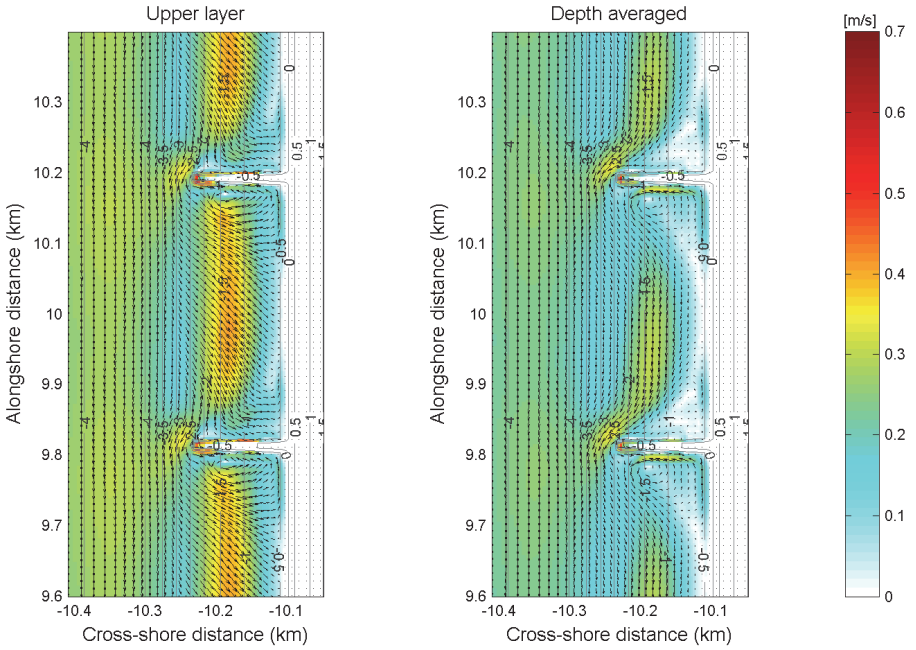

Depth averaged current velocity and direction during max flood, 2009 condition 09

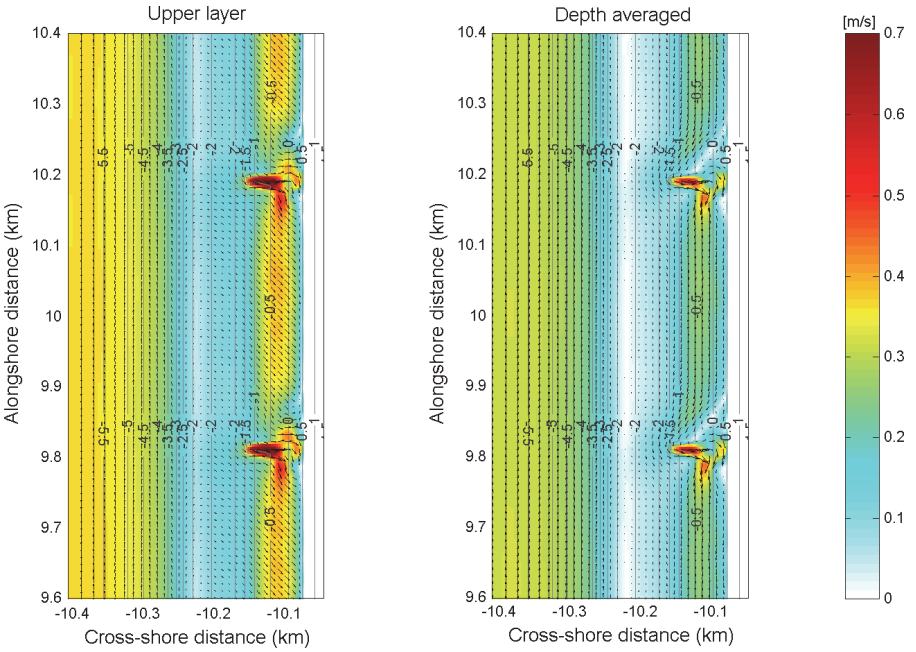

Depth averaged current velocity and direction during (LW) reversal, 2009 condition 09

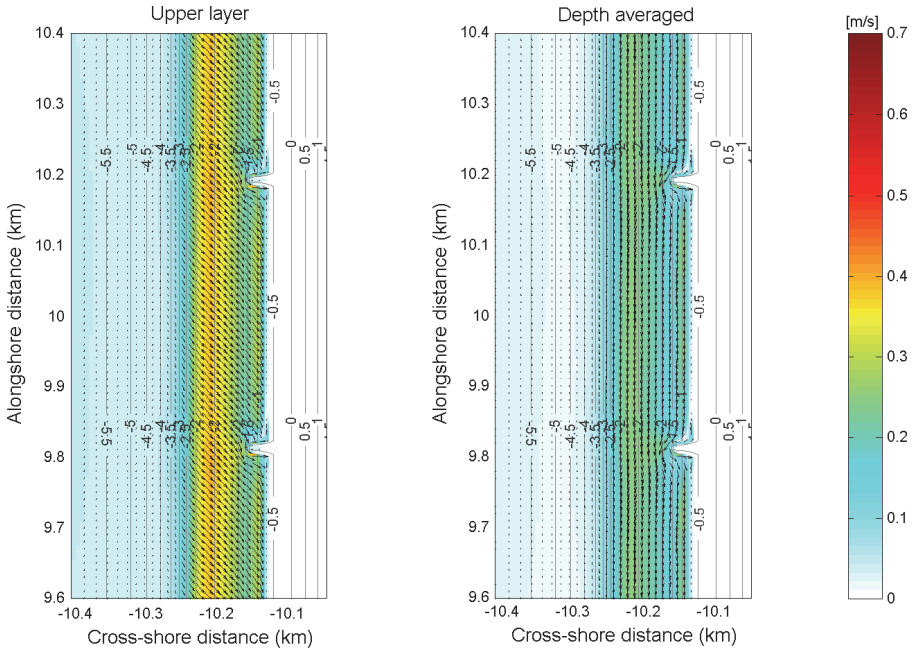

Depth averaged current velocity and direction during maximum eb-current, 2009 condition 09

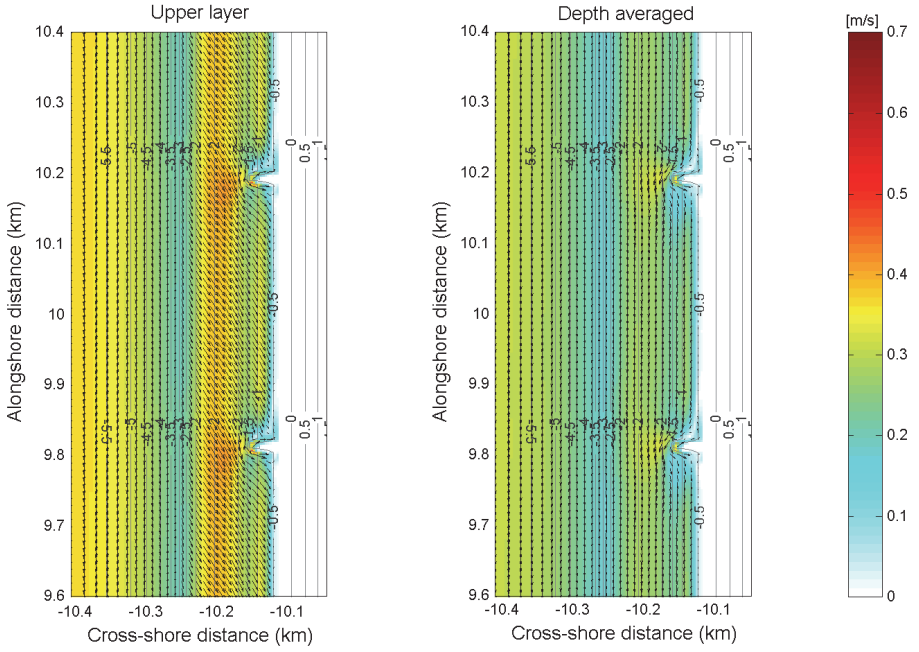

Depth averaged current velocity and direction during max flood, 2010 condition 09

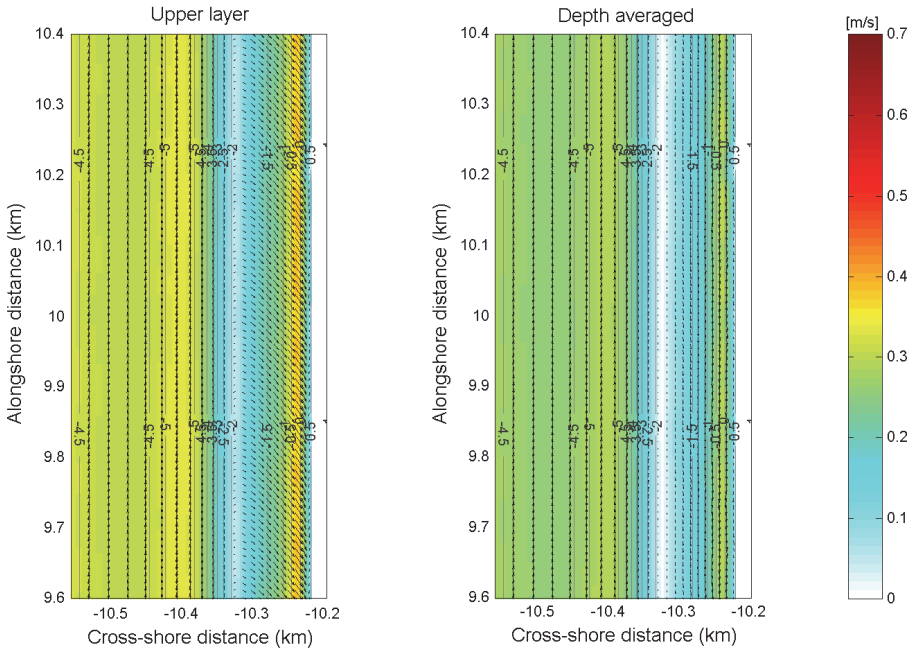

Depth averaged current velocity and direction during (LW) reversal, 2010 condition 09

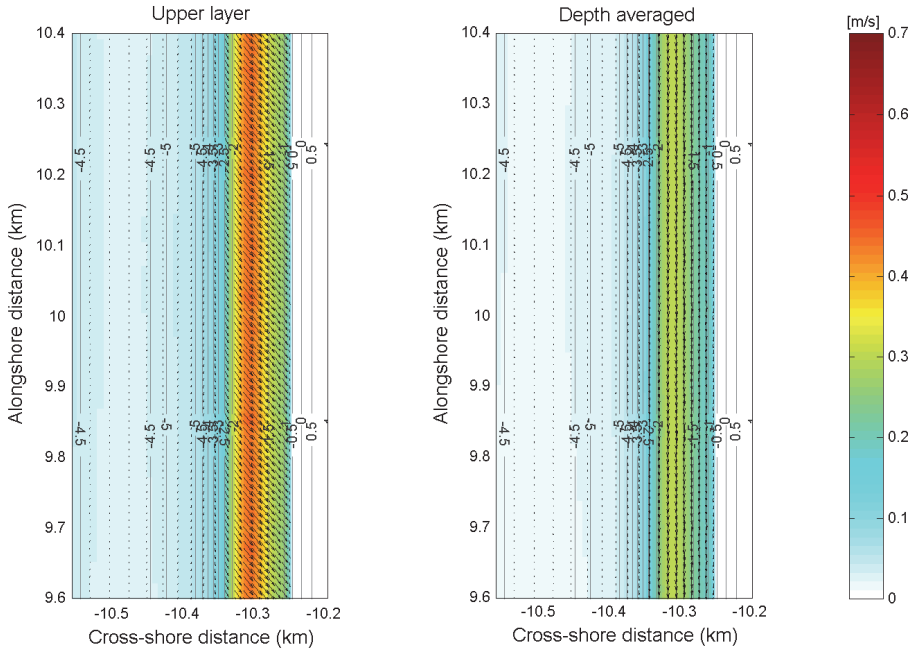

Depth averaged current velocity and direction during maximum eb-current, 2010 condition 09